STRUCTURAL BEHAVIOUR OF LIGHTWEIGHT CONCRETE STRENGTHENED WITH ENGINEERED CEMENTITIOUS COMPOSITES

By

© Tayseer Zakaria Mahmoud Mohamed Batran

A thesis submitted to

The School of Graduate Studies

in partial fulfillment of the requirements for the degree of

Master of Engineering

Faculty of Engineering and Applied Science – Civil Engineering

Memorial University of Newfoundland

February 2022

St. John’s, Newfoundland, Canada

Abstract

This thesis evaluated the feasibility of using engineered cementitious composite (ECC), to strengthen lightweight concrete (LWC) against various mechanical loads. Three experimental studies have been conducted on both plain small-scale and reinforced large-scale concrete specimens to accomplish the research objective. The first and second studies investigated the use of ECC to strengthen either the tension or compression zone of large-scale reinforced LWC beams tested in flexure and shear. The third study focused on the use of ECC in strengthening small-scale unreinforced beams and cylindrical specimens tested under drop-weight impact loads. The results of the first and second studies indicated that using ECC developed with polyvinyl alcohol fibers or steel fibers (ECCP or ECCS, respectively) is an effective technique to improve the flexural and shear behaviour of LWC beams with no significant increase in their self-weight. In both studies, strengthening the compression zone yielded higher ductility and energy absorption capacity. Meanwhile, better cracking control was observed when the tension zone was strengthened, thus assuring a better durability for structural members. In flexure, the highest improvement in the load-carrying capacity was obtained when the LWC beams strengthened at the tension zone, whereas strengthening the compression zone was more effective in improving the shear capacity. The results of the third study indicated that either ECCP or ECCS could achieve a good bonding with LWC substrate. The use of ECC along with LWC also offers novel hybrid composites with low-density and improved impact resistance, thus providing promising composites for strengthening lightweight structures exposed to high impact loading.

Acknowledgements

First of all, I would like to thank The Almighty ALLAH for giving me the strength, knowledge, and ability to accomplish my research study. Without his blessings, this achievement would not have been possible.

I want to express my sincere thanks and gratitude to my supervisor and co-researchers, Dr. Assem Hassan, Dr. Mohamed Ismail, and Dr. Basem AbdelAleem for their unlimited guidance, support, encouragement, valuable discussions, and great efforts throughout every single step in my master's program at Memorial University. I would also like to thank the Lab Technologists at Memorial, particularly Mr. Shawn Organ, Mr. Jamal Tinkov, and Mr. Matt Curtis for their help and technical support during my experimental program. I am gratefully acknowledging the financial assistance and the in-kind contributions provided by Dr. Assem Hassan, NSERC CRD, and the School of Graduate Studies at Memorial University.

I am extremely grateful to my beloved family. I am very grateful to my father (Zakaria Batran), mother (Fatama Abdelrahman), brothers (Ahmed and Ibrahim) and sisters (Samar, Rasha, and Doaa) for their endless support and encouragement throughout the course of my life.

My deepest appreciation and love to my husband Mohamed Ismail and my lovely daughter Lana Ismail, they mean the world to me. I am incredibly grateful to God for giving me such an amazing family.

Tayseer Batran

Disclaimer

It is worth noting that the published versions of each paper presented in Chapters 2, 3, and 4 have been slightly modified to satisfy the required thesis format.

Co-Authorship Statement

I, Tayseer Zakaria Mahmoud Mohamed Batran, hold the principal author status for all the manuscript chapters in this thesis. However, the manuscripts are co-authored by my supervisor (Dr. Assem A. A. Hassan) and my co-researcher (Dr. Mohamed K. Ismail and Dr. Basem H. AbdelAleem). The authors' contribution in each manuscript is detailed as follows:

- Paper 1 in chapter 2: Batran, T.Z.; Ismail, K.M.; and Hassan, A.A.A., "Flexural Behavior of Lightweight Self-Consolidating Concrete Beams Strengthened with Engineered Cementitious Composite," ACI Materials Journal, 2021, V. 118, No. 4, pp. 39-50.
- Paper 2 in chapter 3: Batran, T.Z.; AbdelAleem, B.H.; and Hassan, A.A.A., "Development of Lightweight Composite Beams with High Shear Capacity," ACI Materials Journal (*Accepted*).
- Paper 3 in chapter 4: Batran, T.Z.; Ismail, K.M.; and Hassan, A.A.A., "Behavior of Novel Hybrid Lightweight Composites Under Drop-Weight Impact Loading," Structures, V. 34, 2021, pp. 2789-2800

Tayseer Z. Batran (Master's student/Primary author): I was the primary author in the papers 1, 2, and 3 which are presented in chapters 2, 3, and 4, respectively. In all papers, I was responsible for defining the overall problem; proposing the scientific idea/methodology; designing and implementing the experimental program; collecting and analyzing the experimental results; writing the first draft of the paper; and finalizing the final draft of the paper according to supervisor and co-authors comments.

Dr. Mohamed K. Ismail (Co-researcher/Co-author): Dr. Ismail was the second author in papers 1 and 3 which are presented in chapters 2 and 4, respectively. He contributed to the idea, its formulation and development, and refinement of the presentation.

Dr. Basem H. AbdelAleem (Co-researcher/Co-author): Dr. AbdelAleem was the second author in paper 2 which is presented in chapter 3. He contributed to the idea, its formulation and development, and refinement of the presentation.

Dr. Assem A.A. Hassan (Supervisor/Co-author): Dr. Hassan was the third author in papers 1, 2, and 3 which are presented in chapter 2, 3, and 4, respectively. He contributed to the idea, its formulation and development, funding, and refinement of the presentation.

Tayseer Batran February 2022

Table of Contents

Abstract ii
Acknowledgements iii
Disclaimer iv
Co-Authorship Statement v
Table of Contents vii
List of Tables x
List of Figures xi
List of Symbols, Nomenclature or Abbreviations xiii
1. Introduction 1
1.1. Background and Overview 1
1.2. Research Objective and Significance 4
1.3. Scope of Research 5
1.4. Thesis Outline 6
1.5. Chapter References 7
2. Flexural behavior of lightweight self-consolidating concrete beams strengthened with ECC 14
2.1. Abstract 14
2.2. Introduction 15
2.3. Research Significance 17
2.4. Experimental Program 18
2.4.1. Material Properties and Concrete Mixtures 18
2.4.2. Test Specimens 23
2.4.3. Concrete Casting 26
2.4.4. Test Setup 27
2.5. Discussion of Test Results 28
2.5.1. Properties of LWSCC and ECC Mixtures 28
2.5.2. Cracking and Failure Mode 30
2.5.2.1. Control Beams (LWSCC, ECCP, and ECCS) 30
2.5.2.2. Comparison of Beams Strengthened at The Compression Zone and The Control LWSCC Beam 32

2.5.2.3. Comparison of Beams Strengthened at The Tension Zone and The Control LWSCC Beam 32
2.5.2.4. Evaluation of Cracking Based on Durability Aspect 33
2.5.3. Load-Deflection Behavior 35
2.5.3.1. General 35
2.5.3.2. Control Beams (LWSCC, ECCP and ECCS) 35
2.5.3.3. Comparison of Beams Strengthened at The Compression Zone and The Control LWSCC Beam 37
2.5.3.4. Comparison of Beams Strengthened at The Tension Zone and The Control LWSCC Beam 37
2.5.4. First Crack and Ultimate Load 38
2.5.5. Theoretical predictions of the beams' capacity 39
2.5.6. Ductility and Energy Absorption Capacity 43
2.6. Conclusions 46
2.7. References 48
3. Development of lightweight composite beams with high shear capacity 54
3.1. Abstract 54
3.2. Introduction 55
3.3. Research Significance 58
3.4. Experimental Program 59
3.4.1. Material Properties 59
3.4.2. Concrete Specimens 64
3.4.3. Casting and Specimen Preparation 65
3.4.4. Four-Point Loading Test Setup and Loading Procedure 66
3.5. Discussion of Test Results 70
3.5.1. Failure Mode and Cracking Behavior 70
3.5.2. Load-Deflection Curves 74
3.5.3. Post Diagonal Cracking Resistance 77
3.5.4. Post Cracking Shear Ductility and Energy Absorption 79
3.5.5. Theoretical Prediction of Shear Strength According to Design Codes 81
3.6. Conclusions 88
3.7. References 90

4. Behavior of novel hybrid lightweight concrete composites under drop-weight impact loading 97
4.1. Abstract 97
4.2. Introduction 98
4.3. Research Significance 100
4.4. Experimental Program 101
4.4.1. Material Properties and Concrete Mixtures 101
4.4.2. Mechanical Properties Tests For LWC, ECCP, and ECCS Mixtures 105
4.4.3. Bond Strength Test For LWC-ECCP/ECCS Interface 105
4.4.4. Impact Resistance Tests 106
4.4.4.1. Impact Test Procedures 106
4.4.4.2. Impact Test Program 108
4.5. Discussion of Test Results 111
4.5.1. Mechanical Properties of LWC, ECCP And ECCS 111
4.5.2. Bond Strength for LWC-ECCP/ECCS Interface 112
4.5.3. Static Flexural Strength 113
4.5.4. Impact Resistance of Cylindrical Slices 116
4.5.5. Impact Resistance of Small-Scale Beams 119
4.6. Conclusions 123
4.7. References 125
5. Summary and recommendation 131
5.1. Summary 131
5.2. Limitations of Research 136
5.3. Recommendation For Future Research 136
Bibliography 138

List of Tables

Table 2-1 Mix design of the developed mixtures 21
Table 2-2 Fresh and mechanical properties of the developed mixtures..... 26
Table 2-3 Results of all tested beams tested in flexure..... 34
Table 3-1 Compositions of all developed mixtures 60
Table 3-2 Results of all tested beams 68
Table 4-1 Mixtures used in this study..... 104
Table 4-2 Results of flexure and impact tests 118

List of Figures

Figure 2-1 Geometry, reinforcement details, and test setup of the tested beams 25
Figure 2-2 Cracking pattern at failure of the tested beams 31
Figure 2-3 Load-deflection curves for all tested beams 36
Figure 2-4 Design assumptions for tested beams 41
Figure 2-5 Experimental-to-theoretical ultimate moment capacity 43
Figure 2-6 Results of all tested beams (a) ductility ratio, (b) energy absorption capacity 44
Figure 3-1 Grading curves for the aggregates used 63
Figure 3-2 Geometry and configuration of fibers used 63
Figure 3-3 Beam dimensions, reinforcement details for (a) LWC/NWC/ ECC; (b) composite beams with ECC layer, Test setup for (c) LWC/NWC; (d) full depth ECC (ECCS, ECCP); (e) composite beams with ECC layer in tension side; (f) composite beams with ECC layer in compression side 69
Figure 3-4 Cracking pattern of all tested beams 73
Figure 3-5 Experimental load-midspan deflection responses: (a) reference beams (LWC, NWC, ECCP, and ECCS); (b) reference beam and composite beams with ECC layer in the compression side (LWC, NWC, ECCP-C, and ECCS-C); (c) reference beam and composite beams with ECC layer in the tension side (LWC, NWC, ECCP-T, and ECCS-T) 75
Figure 3-6 Experimental-to-theoretical ultimate shear ratios for all tested beams: (a) theoretical prediction of ultimate shear capacity for LWC, NWC, and composite beams with ECC layer in the compression side; (b) theoretical prediction of ultimate shear capacity for ECC reference beams and composite beams with ECC layer in the tension side 85
Figure 3-7 Shear force distribution mechanism for (a) composite beams with ECC layer in the tension side; (b) ECC reference beams 87
Figure 4-1 Gradation curves of the silica sand and lightweight aggregates used 103
Figure 4-2 PVA and SFs fibers used 104
Figure 4-3 Configurations of the motorized-impact tests used 107
Figure 4-4 (a) Configurations of cast composites (b) preparation before casting the top layer 110
Figure 4-5 Strength-to-weight ratio of the developed mixtures 111
Figure 4-6 Splitting and flexural strength ratio of the developed mixtures 112
Figure 4-7 LWC-ECCP/ECCS interface bond strength 113
Figure 4-8 Load-midspan deflection of tested beams 114
Figure 4-9 Typical cracking pattern of ECCP and ECCS at failure 115
Figure 4-10 Results of impact resistance of cylindrical specimens (a) N1 of the single-layer specimens, (b) N2 of the single-layer specimens, (c) N1 of the two-layer hybrid composites, and (d) N2 of the two-layer hybrid composites 119

Figure 4-11 Typical failure crack patterns in the tested two-layer hybrid composites (cylindrical specimens and beams) 122
Figure 4-12 Results of impact resistance of beams (a) N1 of the single-layer specimens, (b) N2 of the single-layer specimens, (c) N1 of the two-layer hybrid composites, and (d) N2 of the two-layer hybrid composites..... 123

List of Symbols, Nomenclature or Abbreviations

ACI	is the American Concrete Institute
A_s	is the area of tension reinforcement
A'_s	is the area of compression reinforcement
ASTM	is the American Society for Testing and Materials
b	is the width of beam
b_v	is the effective web width of beam
BC	is the binder content
BS	is the British Standard Institute
C.A.	is the lightweight coarse aggregate
CSA	is the Canadian Standards Association
d	is the distance from extreme compression fiber to centroid of tension reinforcement
DC	is the ductility coefficient
Ddc	is the deflection corresponding to first diagonal crack load
d_f	is the fiber diameter
D_f	is the fiber bond factor
Du	is the deflection corresponding to ultimate load
d_v	is the beam effective shear depth
ECC	is the engineered cementitious composite
ECCP	is the ECC with polyvinyl alcohol fibers
ECCS	is the ECC with steel fibers

EFNARC is the European Federation for Specialist Construction Chemicals and Concrete Systems

ESCA is the expanded slate coarse aggregate

ESFA is the expanded slate fine aggregate

EC2 is the Eurocode

FA is the fly ash

F_{be} is the bond efficiency of the fiber

f_c' is the concrete compressive strength

f_y is the yield strength of reinforcing bar

f_s is the stress of compression reinforcement

g is the acceleration due to gravity

h is the drop height

HRWRA is the high range water reducer admixtures

K is the size effect factor

l_f is the fiber length

LWC is the Lightweight Concrete

LWSCC is the lightweight self-consolidating concrete

LVDT is the linear variable differential transformer

m is the mass of the drop hammer

M_n is the nominal moment capacity of beam

M^{theo} is the theoretical design moment of beam

MK is the metakaolin

N	is the number of drops
N_1	is the number of drops required to cause the first crack
N_2	is the number of drops required to cause the failure crack
NWC	is the normal weight concrete
IE	is the ultimate impact resistance
PDSR	is the post diagonal shear resistance
PVA	is the polyvinyl alcohol fibers
S	is the lightweight sand / silica sand
SCC	is the self-consolidating concrete
SCMs	is the supplementary cementing materials
SFs	is the steel fibers
STS	is the splitting tensile strength
S/W	is the strength-to-weight ratio
S_z	is the crack spacing parameter
T_{50}	is the time to reach a diameter of 500 mm in the slump flow test
V_{exp}	is the experimental shear capacity of beam
v_f	is the fiber volume fraction
V_f	is the shear resistance provided by fibers
V_{theo}	is the theoretical shear capacity of beam
W/B	is the water to binder ratio
σ_0	is the tensile strength of non-fibered
σ_f	is the tensile strength of fibered ECC

σ_t	is the tensile stress of fibrous concrete
σ_{t1}	is the tensile stress of fibrous concrete proposed by the Henager and Doherty model
σ_{t2}	is the experimental tensile stress of fibrous concrete
ρ_f	is the percent by volume of steel fibers
λ	is the lightweight concrete modification factor
ρ_c	is the dry density of concrete
ρ_w, ρ_s	is the longitudinal reinforcement ratio
τ	is the fiber matrix interfacial bond stress

1. Introduction

1.1. Background and Overview

Lightweight concrete (LWC) is a special class of building materials that offers various advantages for the construction industry. LWC is produced by composing cementitious materials, water, coarse and/or fine lightweight aggregates. Examples of structural lightweight aggregates include expanded slag, shale, clay, and slate. According to the ACI 318 (2019) and CSA (2004) standards, concrete can be classified as LWC when its density reaches a value of less than 1850 kg/m^3, while normal-weight concretes have a density in a range of 2100~2500 kg/m^3. Therefore, structures made with LWC typically have lower dead loads, which usually represent a considerable portion of design loads. The reduction in design loads helps to reach more economical structural systems—in turn consume less volumes of building materials (e.g., concrete and steel) (Real et al., 2016a; Sadek et al., 2020a). The economic benefits of LWC can be more significant in certain applications such as in precast structures (e.g., buildings, bridges, stadiums), where the reduced self-weight of precast elements leads to lower haulage costs and faster construction rate (Kayali, 2008; Jafari and Mahini, 2017). LWC can also be used to achieve a design requirement and/or improve a structural response. For example, the use of LWC in high-rise buildings decreases the mass of structures, which in turn reduces the forces imposed by earthquakes (Vandanapu and Krishnamurthy, 2018). In addition, LWC is used in the construction of offshore gravity and floating concrete platforms to improve their buoyancy (Hoff, 1996; Sadek, 2020). LWC also possess other excellent physical characteristics such as low thermal conductivity, high fire resistance, and high sound insulation (Ünal et al., 2007;

Real et al., 2016a and 2016b; Go et al., 2012; Díaz and Rabanal, 2010). In addition to all aforementioned advantages, developing LWC with high self-compactability properties (i.e., high flowbility, filling ability, passing ability, and segregation resistance) expands its construction feasibility. Such features allow mixtures to easily spread and consolidate under its own weight without mechanical vibration, fill complex formwork and heavy reinforcement areas, thus offering faster construction rate and less labor requirements (Lachemi et al., 2009). Despite the several advantages of LWC, the low strength and high brittleness of lightweight aggregates (due to their porous structure) still represent a major problem that may significantly limit the performance of LWC to maintain high endurance against mechanical loads (e.g., static, dynamic, and impulsive loads) (Abouhussien et al., 2015; Hassan et al., 2015; Atmaca et al., 2017; Sadek et al., 2020b). Therefore, most of design guidelines suggest modification factors in their design models when lightweight concrete is used. According to the ACI-318 and CSA (2004), the reduction factors in the tensile and shear strength of LWC can be taken up to 0.75 (i.e., 25% reduction) compared to that of normal weight concrete produced at the same compressive strength. The proposed reduction factors are assumed to consider the effect of low strength, limited interlock mechanism, and high brittleness of lightweight aggregates on performance of LWC structures. This indicates that at same concrete class (i.e., same compressive strength), structures made from LWC typically have lower capacity compared to that made from normal-weight concrete. This highlights a growing need to overcome the drawbacks of traditional LWC and find new alternatives to construct high-performance lightweight structures. One of these alternatives is developing a new hybrid lightweight composite by combining LWC with one of high-performance cement-based materials.

Engineered cementitious composite (ECC) is one of high-performance cement-based materials that was originally invented by Victor Li based on micromechanics theory (Li, 1993). ECC is produced using a high volume of cementitious materials (i.e., Portland cement, fly ash, silica fume, metakaolin etc.), silica sand as a fine aggregate, and a moderate volume of fibers. Compared to other traditional concretes, ECC uniquely exhibit an excellent mechanical performance under either compression or tension. In particular, the high ductility, strain hardening behavior, and cracking resistance are considered as the main superior characteristics of ECC over other concrete composites. ECC can, for example, exhibit tensile strain up to 2%~6%, which is 200~600 times as much as the strains exhibited by conventional concretes (Li, 1998; Kong et al., 2003). Such high strain capacity is attributed to the strain hardening behavior of ECC, which allows composite to undergo large inelastic deformations associating with a formation of multiple macro cracks (Li, 1998; Sahmaran and Li, 2010; Ranade et al., 2014; Ismail et al., 2018a). The inclusion of fibers also helps ECC to endure high uniaxial tensile stress that can reach 6 MPa (Said and Razak, 2015; Ismail et al., 2018a and 2018b). In addition, ECC can withstand compressive stress above 70 MPa and exhibit a compressive strain of up to 0.65% (Li, 2002; Said and Razak, 2015; Ismail et al., 2019). The material testing also proved that ECC has high resistance against fatigue, impact energy, freezing and thawing cycles, salt scaling, chloride, and sulfate attack (Zhang and Li, 2002; Suthiwarapirak et al., 2004; Jun and Mechtcherine, 2010; Meng et al., 2018; Ismail et al., 2019; Şahmaran and Li, 2007; Şahmaran et al., 2009; Şahmaran et al., 2007). At structural level, limited studies attempted to evaluate the use of ECC in large-scale members such as beams, columns, and beam-column joints. The results obtained from these studies indicated that ECC can remarkably

improve the overall structural behavior in terms of cracking, load-carrying capacity, shear strength, ductility, and energy dissipation capacity (Yuan et al., 2012; Kang et al., 2017; Ismail et al., 2018a; Ismail and Hassan, 2021a). Despite the excellent characteristics of ECC, the high production cost of ECC hinders its use in the construction process. However, ECC can be strongly recommended for strengthening and rehabilitation applications where ECC can be used in specific locations or with limited volume (Ismail and Hassan, 2021b). And since ECC can be produced with a relative low density— makes it an ideal alternative (*i*) to be used efficiently in strengthening existing LWC structures with no significant additional loads; and (*ii*) to be combined with LWC in one lightweight hybrid composite for constructing high-performance lightweight structures.

1.2. Research Objective and Significance

LWC is a unique class of concrete which can present significant economic benefits to the construction industry. However, the LWC typically has low tensile and shear strength, ductility, energy absorption capacity, and impact resistance, which limit its applicability for multiple applications, especially those are exposed to harsh loads (e.g., earthquake, impulsive load etc.). Strengthening LWC with one of the high-performance cement-based materials, in particular ECC, can be an efficient strategy to reach superior structural performance. In addition, the relative low density of ECC can maintain the economic benefits of LWC, i.e., strengthening without significant additional load. Despite the possible benefits that can be achieved by using ECC in strengthening LWC, the mechanical and structural performance of LWC-ECC composite is not well investigated in the available literature. Contributing to fill this gap of knowledge, this study was conducted at

both material and structural level to experimentally evaluate the structural feasibility of using ECC in strengthening LWC. At material level, the use of LWC and ECC together to develop cost-effective, lightweight composites with superior performance under drop-weight impact loading, was evaluated. Meanwhile, at structural level, the ECC was used to strengthen large-scale reinforced concrete beams tested in either flexure or shear. The conducted studies also included ECC developed with two types of fibers in order to assess how the fiber type can affect the efficiency of ECC in strengthening. The use of ECC in strengthening and rehabilitation applications can be also the best option due to its relative high production cost, which hinders the ECC to be widely used in the construction industry as a main building material. The outcomes obtained from the conducted investigations can greatly help to reach cost-effective, high-performance lightweight structures.

1.3. Scope of Research

This research included three successive experimental studies, detailed as follows:

1. The first study evaluated the flexure behavior of large-scale reinforced self-consolidating LWC beams strengthened with ECC. The beams were strengthened at either the compression or tension zone using ECC with polyvinyl alcohol fibers (ECCP) or steel fibers (ECCS). The performance of strengthened beams was compared to that of control beams which were fully cast with LWC or ECCP or ECCS.
2. The second study investigated the use of ECCP and ECCS in strengthening LWC beams in shear. Similar to the first study, the beams were strengthened at either

compression or tension zone and compared to that were fully cast with LWC, ECCP, ECCS, and normal weight concrete (NWC).

3. The third study assessed the feasibility of combining LWC and either ECCP or ECCS in one composite, aiming to develop a novel, cost effective lightweight composite with high impact resistance. For this purpose, cylindrical specimens and small-scale beams were cast with two layers: a LWC layer and either an ECCP or an ECCS layer. The layers were varied in terms of depth and arrangement. Additional cylindrical specimens and beams were fully cast with LWC, ECCP, and ECCS for comparison. All specimens were tested under drop-weight impact loading. The interface bond strength between LWC and either ECCP or ECCS was also assessed.

1.4. Thesis Outline

This thesis consists of five chapters described as follows:

Chapter 1 includes background, objective, significance, and the scope of the research.

Chapter 2 includes an experimental investigation for the flexural behavior of large-scale LWC beams strengthened with ECC (ECCP and ECCS).

Chapter 3 includes an experimental investigation for the shear behavior of large-scale LWC beams strengthened with ECC (ECCP and ECCS).

Chapter 4 includes an experimental investigation for the feasibility of combining LWC and either ECCP or ECCS to develop novel, efficient hybrid composites with superior impact resistance.

Chapter 5 demonstrates the conclusions, summary, and recommendations out of the conducted studies.

1.5. Chapter References

Abouhussien, A. A.; Hassan, A. A. A.; and Ismail, M. K., "Properties of Semi-Lightweight Self-Consolidating Concrete Containing Lightweight Slag Aggregate," Construction and Building Materials, V. 35, 2015, pp. 63-73.

ACI (American Concrete Institute), "Building Code Requirements for Structural Concrete (ACI 318-95) and Commentary (ACI 318 R-95)," Committee 318, Farmington Hills, MI, 2019.

Atmaca, N.; Abbas, M. L.; and Atmaca, A., "Effects of Nano-Silica on the Gas Permeability, Durability and Mechanical Properties of High-Strength Lightweight Concrete," Construction and Building Materials, V. 147, 2017, pp. 17–26.

Canadian Standards Association Committee A23.3, "Design of Concrete Structures," CSA A23.3-04, Canadian Standards Association, Rexdale, Ontario, Canada, 2004.

Del Coz Díaz, J. J.; Alvarez Rabanal, F. P.; García Nieto, P. J.; and Serrano Lopez, M. A., "Sound Transmission Loss Analysis Through a Multilayer Lightweight Concrete Hollow Brick Wall by FEM And Experimental Validation," Building and Environment, V. 45, No. 11, 2010, pp. 2373-2386.

Go, C. G.; Tang, J. R.; Chi, J. H.; Chen, C. T.; and Huang Y. L., "Fire-Resistance Property Of Reinforced Lightweight Aggregate Concrete Wall," Construction and Building Materials, V. 30, 2012, pp. 725-733.

Hassan, A. A. A.; Ismail, M. K.; and Mayo, J., "Mechanical Properties Of Self-Consolidating Concrete Containing Lightweight Recycled Aggregate In Different Mixture Compositions," Journal of Building Engineering, V. 4, 2015, pp. 113-126.

Hoff, G. C., "Fire Resistance of High-Strength Concretes for Offshore Concrete Platforms," Special Publication, V. 163, 1996, pp. 53-88.

Ismail, M. K.; Abdelaleem, B. H.; and Hassan, A. A. A., "Effect of Fiber Type on The Behavior of Cementitious Composite Beam-Column Joints Under Reversed Cyclic Loading," Construction and Building Materials, V. 186, 2018a, pp. 969-977.

Ismail, M. K.; Hassan, A. A. A.; and Lachemi, M., "Performance of Self-Consolidating Engineered Cementitious Composite Under Drop-Weight Impact Loading," Journal of Materials in Civil Engineering, V. 31, No. 3, 2019, 04018400.

Ismail, M. K.; and Hassan A. A. A., "Influence of Fibre Type on the Shear Behaviour of Engineered Cementitious Composite Beams," Magazine of Concrete Research, V. 73, No. 9, 2021a, pp. 464-475.

Ismail, M. K.; and Hassan A. A. A., "Structural performance of large-scale concrete beams reinforced with cementitious composite containing different fibers," Structures, V. 31, 2021b, pp. 1207-1215.

Ismail, M. K.; Sherir, M. A. A.; Siad, H.; Hassan, A. A. A.; and Lachemi, M., "Properties of Self-Consolidating Engineered Cementitious Composite Modified with Rubber," Journal of Materials in Civil Engineering, ASCE, V. 30, No. 4, 2018b, p. 04018031. doi: 10.1061/(ASCE)MT.1943-5533.0002219

Jafari, S.; and Mahini, S. S., "Lightweight concrete design using gene expression programing," Construction and Building Materials, V. 139, 2017, pp. 93–100.

Jun, P.; and Mechtcherine, V., "Behaviour of Strain-Hardening Cement-Based Composites (SHCC) Under Monotonic and Cyclic Tensile Loading: Part 1–Experimental Investigations," Cement Concrete Composites, V. 32, 2010, pp. 801–809.

Juradin, S.; Baloević, G.; and Harapin, A., "Experimental Testing of The Effects of Fine Particles on The Properties of The Self-Compacting Lightweight Concrete," Advances in Materials Science and Engineering, V. 1, 2012.

Kang, S. B.; Tan, K. H.; Zhou, X. H.; and Yang, B., "Experimental Investigation on Shear Strength of Engineered Cementitious Composites," Engineering Structures, V. 143, 2017, pp. 141-151.

Kayali, O., "Fly Ash Lightweight Aggregates in High Performance Concrete," Construction and Building Materials, V. 22, 2008, pp. 2393-2399.

Kong H. J.; Bike, S. G.; and Li V. C., “Development of A Self-Consolidating Engineered Cementitious Composite Employing Electrosteric Dispersion/Stabilization,” Cement and Concrete Composites, V. 25, 2003, pp. 301–309.

Lachemi, M.; Bae, S.; Hossain, K. M. A.; and Sahmaran, M., “Steel-Concrete Bond Strength of Lightweight Self-Consolidating Concrete,” Materials and Structures, V. 42, 2009, pp. 1015-1023.

Li, V. C., “From Micromechanics to Structural Engineering – The Design of Cementitious Composites for Civil Engineering Applications,” Journal of Structural Mechanics and Earthquake Engineering, JSCE, V. 10, No. 2, 1993, pp. 37-48.

Li, V. C., “Engineered Cementitious Composites (ECC) - Tailored Composites Through Micromechanical Modeling,” in Fiber Reinforced Concrete: Present and the Future, N. Banthia, A. Bentur, and A. Mufti, Eds., Canadian Society of Civil Engineers, Montreal, 1998, pp. 64-97.

Li, V. C., “Advances in ECC research. Material Science to Application — A Tribute to Surendra P Shah,” ACI Bookstore, 2002, pp. 373–400.

Meng, D.; Lee, C.; and Zhang, Y., “Flexural Fatigue Properties of A Polyvinyl Alcohol-Engineered Cementitious Composite,” Magazine of Concrete Research, V. 71, No. 21, 2019, pp. 1130-1141

Ranade, R.; Zhang, J.; Lynch, J. P.; and Li, V. C. “Influence of Micro-Cracking on The Composite Resistivity of Engineered Cementitious Composites,” Cement and Concrete Research, V. 58, 2014, pp. 1-12.

Real, S.; Bogas, J. A.; Gomes, M. D. G.; and Ferrer, B., “Thermal Conductivity of Structural Lightweight Aggregate Concrete,” Magazine of Concrete Research, V. 68, No. 15, 2016a, pp. 798–808.

Real, S.; Gomes, M. G.; Rodrigues, A. M.; and Bogas, J. A., “Contribution of Structural Lightweight Aggregate Concrete to The Reduction of Thermal Bridging Effect in Buildings,” Construction and Building Materials, V. 121, 2016b, pp. 460-470.

Sadek, M. M.; Ismail, M. K.; and Hassan, A. A. A., “Stability of Lightweight Self-Consolidating Concrete Containing Coarse and Fine Expanded Slate Aggregates,” ACI Materials Journal, V. 117, No. 3, 2020a, pp. 133-134.

Sadek, M. M.; Ismail, M. K.; and Hassan, A. A. A., “Impact Resistance and Mechanical Properties of Optimized SCC Developed with Coarse and Fine Lightweight Expanded Slate Aggregate,” Journal of Materials in Civil Engineering, V. 32, No. 11, 2020b, 04020324.

Sadek, M. M. “Properties of Self-Consolidating Concrete Containing Expanded Slate Lightweight Aggregate,” Master Thesis, Memorial University of Newfoundland, Canada, October 2020.

Şahmaran, M.; Lachemi, M.; and Li, V. C. “Assessing the Durability of Engineered Cementitious Composites under Freezing and Thawing Cycles,” Journal of ASTM International, V. 6, No. 7, 2009, pp. 1-13.

Şahmaran, M.; Li, V. C.; and Li, M., “Transport properties of engineered cementitious composites under chloride exposure,” ACI Materials Journal, V. 104, No. 6, 2007, pp. 604-611.

Şahmaran, M.; and Li, V. C. “De-icing salt scaling resistance of mechanically loaded engineered cementitious composites,” Cement and Concrete Research, V. 37, No. 7, 2007, pp. 1035–1046.

Sahmaran, M.; and Li, V. C. “Engineered Cementitious Composites: Can Composites Be Accepted As Crack-Free Concrete?.” Transportation Research Record, 2010, V. 2164, No. 1, pp. 1–8.

Said, S.H.; and Razak, H.A., “The effect of synthetic polyethylene fiber on the strain hardening behavior of engineered cementitious composite (ECC),” Materials & Design, V. 86, 2015, pp. 447-457.

Suthiwarapirak, P.; Matsumoto, T.; and Kanda, T., “Multiple Cracking and Fiber Bridging Characteristics of Engineered Cementitious Composites under Fatigue Flexure,” Journal of Materials in Civil, V. 16, No. 5, 2004, pp. 433-443.

Ünal, O.; Uygunoğlu, T.; and Yildiz, A., "Investigation of Properties of Low-Strength Lightweight Concrete for Thermal Insulation," Building and Environment, V. 42, No. 2, 2007, pp. 584- 590.

Vandanapu, S. N.; and Krishnamurthy, M., "Seismic performance of lightweight concrete structures." Advances in Civil Engineering, V. 2018, 2018, pp. 1-6.

Yuan, F.; Pan, J.; Xu, Z.; and Leung, C. K. Y., "A Comparison of Engineered Cementitious Composites Versus Normal Concrete In Beam–Column Joints Under Reversed Cyclic Loading," Materials and Structures, V. 46, No. 1-2, 2012, pp. 145–159.

Zhang, J.; and Li, V. C. "Monotonic and Fatigue Performance in Bending of Fiber-Reinforced Engineered Cementitious Composite in Overlay System," Cement Concrete Research, V. 32, 2002, pp. 415–423.

2. Flexural behavior of lightweight self-consolidating concrete beams strengthened with ECC

2.1. Abstract

This study investigated the structural behavior of lightweight self-consolidating concrete (LWSCC) beams strengthened with engineered cementitious composite (ECC). Four LWSCC beams were strengthened at either the compression or tension zone using two types of ECC developed with polyvinyl alcohol (PVA) fibers or steel fibers (SFs). Three beams were also cast in full depth with LWSCC, ECC with PVA, and ECC with SFs, for comparison. The performance of all tested beams was evaluated based on load-deflection response, cracking behavior, failure mode, first crack load, ultimate load, ductility, and energy absorption capacity. The flexural ultimate capacity of the tested beams was also estimated theoretically and compared to the experimental results. The results indicated that adding ECC layer at the compression zone of the beam helped the LWSCC beams to sustain a higher ultimate loading, accompanied with obvious increases in the ductility and energy absorption capacity. Higher increases in the flexural capacity were exhibited by the beams strengthened with the ECC layer at the tension zone. Placing the ECC layer at the tension zone also contributed to controlling the formation of cracks, ensuring better durability for structural members. Using ECC with SFs yielded higher flexural capacity in beams compared to using ECC with PVA fibers. The study also indicated that the flexural capacity of single-layer and/or hybrid composite beams was conservatively estimated by the ACI ultimate strength design method and the Henager and Doherty model. More improvements in the Henager and Doherty model's estimates were observed when the tensile stress of fibrous concrete was obtained experimentally.

2.2. Introduction

Lightweight self-consolidating concrete (LWSCC) is a special type of concrete that has distinct advantages in both fresh and hardened states. In the fresh state, LWSCC has the desirable self-compactability properties, in which the mixture can easily flow and consolidate under its own weight without external vibration (Hassan et al., 2015; Omar et al., 2020). This can offer a faster production rate with less labour and high-quality finishes. In the hardened state, LWSCC possesses the economic benefits of lightweight concrete, which help to reach a more economic design and achieve significant savings in construction costs (Omar et al., 2020; Sadek et al., 2020a). Such properties render LWSCC as a promising candidate for constructing many reinforced concrete structures. The first application of the LWSCC was in Japan in 1992, where it was used for casting the main girder of a cable-stayed bridge (Okamura and Ouchi, 2003). Then, the use of LWSCC was expanded to the construction of various structures such as high-rise buildings, bridges, offshore platforms, pre-stressed beams, and precast elements (e.g., thin walls, panels, benches) (Papanicolaou and Kaffetzakis, 2011; Shi and Yang, 2005; Yao and Gerwick, 2006; Hubertova and Hela, 2007; Sadek et al., 2020b).

Lightweight concrete structures may suffer various levels of damage due to harsh environmental conditions and excessive mechanical loading (Kim et al., 2007). The damages can be, for example, cover spalling, severe cracking, excessive deflections, corrosion of steel reinforcement, and degradation of concrete durability (Muthya et al., 2018; Deng et al., 2018). These damages can negatively affect the stability and integrity of structures, leading to a catastrophic failure in severe cases. To avoid reaching such failures and restore the design capacity of deteriorating structures, rehabilitation is necessary. The proper rehabilitation technique is typically chosen based on the damage type and level. For example, when concrete

is damaged, it must be removed and replaced with new repair material. Therefore, developing high-performance, cost-effective repair materials, is an important factor in achieving efficient rehabilitation.

In recent years, the rehabilitation of civil infrastructures generally demands materials with excellent properties such as high strength, ductility, energy absorption capacity and durability. Such properties can be offered by high-performance fiber-reinforced cement-based composites such as engineered cementitious composite (ECC), which is characterized by a superior performance under both compressive and tensile loading. Under tensile loading, ECC can reach a uniaxial tensile strength of 3–6 MPa with a strain capacity in the range of 3%–5% (Li et al., 2002; Ismail et al., 2018b). The behavior of ECC in tension is typically accompanied by strain-hardening behavior and a formation of multiple micro-cracks with widths that are often below 100 μm (Sahmaran and Li, 2010). Similarly, under compressive loading, the ECC can attain a compressive strength up to 80 MPa and a strain capacity in the range of 0.4%–0.65% (Li, 2002; Said and Razak, 2015). The high strain capacity and strengths of ECC allow this composite to have a superior performance under fatigue and impact loading (Suthiwarapirak et al., 2004; Ismail et al., 2019). The small- and large-scale testing also proved that ECC has a high resistance to shear force because it contains a moderate volume of fibers such as polyvinyl alcohol (PVA), polypropylene, polyethylene, and steel fibers (SFs) (Kang et al., 2017; Ismail and Hassan, 2021). Other studies have indicated that replacing normal concrete with ECC in beam-column joints improved their cyclic behavior in terms of cracking load, ultimate load, ductility, and energy dissipation capacity (Yuan et al., 2018; Ismail et al., 2018a). In addition to its superior mechanical properties, ECC proved to maintain excellent

mechanical properties and high durability even after exposure to freezing and thawing cycles, salt scaling, chloride, and sulfate attack (Şahmaran and Li, 2007; Şahmaran et al., 2009; Liu et al., 2017). This typically contributes to diminishing the deterioration rate and improving the serviceability of strengthened structures.

The aforementioned properties of ECC indicate high potentials for this composite to be used in structural strengthening applications. However, there is a lack of research focused on this area, especially when LWSCC is strengthened. Therefore, this study was conducted to evaluate the flexural behavior of LWSCC beams strengthened with ECC at either the compression or tension zone. Two types of ECC were used for strengthening: ECC with PVA (ECCP) and ECC with SFs (ECCS). In this investigation, seven reinforced beams were tested under four-point flexural loading. The tested beams are detailed as follows: three full-depth control beams (LWSCC, ECCP, and ECCS), two LWSCC beams strengthened with ECCP or ECCS at compression zone, and two LWSCC beams strengthened with ECCP or ECCS at tension zone. The performance of all tested beams was assessed by examining the load-deflection response, cracking behavior, failure mode, first crack load, ultimate load, ductility, and energy absorption capacity. The ultimate flexural capacity of each tested beam was compared to the theoretically estimated values.

2.3. Research Significance

In recent years, the use of ECC has been attracting great attention from researchers attempting to present a novel construction material with promising potential for multiple applications. The excellent workability, mechanical properties, and durability of ECC reported by many conducted studies show this composite to be a strong candidate for rehabilitation and

strengthening applications. Employing the superior properties of the ECC in strengthening structural elements made with LWSCC, can be considered as an effective rehabilitation technique to extend the service life and maintain the economic benefits of the LWSCC. However, the ECC concrete composite behavior is not well demonstrated in the available literature, especially when LWSCC is retrofitted. For this reason, this study was conducted to assess the flexural behavior of LWSCC beams strengthened with ECC at either the compression or tension zone, aiming to evaluate their compatibility and the possible structural benefits when used together. The present study also included ECC developed with two types of fibers in order to evaluate how the fiber type can change the efficiency of ECC in strengthening. The authors believe that the experimental results discussed in the present study can help to investigate the feasibility of using ECCP and ECCS in strengthening LWSCC beams. Further investigations are also needed to confirm outcomes of this study.

2.4. Experimental Program

2.4.1. Material Properties and Concrete Mixtures

Three mixtures, namely LWSCC, ECCP, and ECCS, were developed to cast the single layer or hybrid composite beams tested in this study. **Table 2-1** lists the proportions of each developed mixture. The development of the mixtures used is detailed as follows:

(a) The LWSCC mixture was developed with expanded slate lightweight coarse and fine aggregates with a maximum aggregate size of 12.5 mm (0.49 in.) and 4.75 mm (0.19 in.), specific gravity of 1.53 and 1.8, respectively, and water absorption of 7.1% and 10%, respectively. The density of the developed LWSCC mixture was 1727 kg/m^3 (107.8 lb/ft^3), which is classified as a lightweight concrete according to the ACI (2019) and CSA (2004) codes. At such low density, developing LWSCC with self-compactability properties and good strength (suitable for structural applications) had several challenges:

- The high risk of segregation as a result of the low density of both fine and coarse lightweight aggregates.
- The high-water absorption and low mechanical properties as a result of the high porosity of both fine and coarse lightweight aggregates.

Based on a preliminary trial mix stage, these challenges were overcome through different steps, as follows:

- Both fine and coarse lightweight aggregates were used in a saturated surface dry condition in order to eliminate the negative impact of the aggregates' high absorption.

- A 550 kg/m^3 (34.3 lb/ft3) ternary binder material content at a relatively low water-to-binder (w/b) ratio of 0.4 was used. The total weight of binder content consisted of 40% ordinary Portland cement Type I (ASTM C150), 40% class F fly ash (ASTM C618), and 20% class N metakaolin (ASTM C618). These proportions were found (from the trial mix stage) achieve a cementitious paste with a high strength and sufficient viscosity, which allows for adequate particle suspension (i.e., less risk of segregation) and compensates for the low strength of aggregates.

Table 2-1 Mix design of the developed mixtures

Mixture	BC	C/BC	SCM (Type)	FA/BC	MK/BC	S/BC	C.A./BC	W/BC	fibers (%)	Fiber type	Dry density (kg/m^3)
LWSCC	1	0.40	FA+M	0.40	0.20	0.94	0.8	0.40	-	-	1727
ECCP	1	0.45	FA+M	0.35	0.20	0.36	-	0.27	2	PVA	2091
ECCS	1	0.45	FA+M	0.35	0.20	0.36	-	0.27	2	SF	2222

Note: BC = binder content; C = cement; SCMs = supplementary cementing materials; FA = fly ash; MK = metakaolin; S = sand; C.A. = coarse aggregate; W/BC = water-to-binder (i.e., cement + SCMs); PVA = polyvinyl alcohol fiber; SF = steel fiber; 1 kg/m^3 = 0.062428 lb/ft^3.

(b) The ECCP and ECCS mixtures were also produced with a ternary binder material system, consisting of 45% ordinary Portland cement Type I (ASTM C150), 35% class F fly ash (ASTM C618), and 20% class N metakaolin (ASTM C618). Silica sand with a maximum aggregate size of 400 µm (0.016 in.) and specific gravity of 2.65 was used as a fine aggregate, and no coarse aggregate was incorporated as per ECC's design specifications (Li, 1993; Li, 1998). In terms of fibers, the ECCP and ECCS mixtures were reinforced with 8 mm (0.32 in.) PVA fibers and 35 mm (1.38 in.) hooked-ends SFs, respectively. As per the manufacturers' data sheets, the PVA fibers had an 8 mm (0.32 in.) length, 210 aspect ratio, 38 µm (0.0015 in.) diameter, 1600 MPa (23.2 ksi) tensile strength, 40 GPa (5801.5 ksi) Young's modulus, and 1300 kg/m^3 (81.2 lb/ft^3) density. The SFs had a 35 mm (1.38 in.) length, 65 aspect ratio, 0.55 mm (0.02 in.) diameter, 1050 MPa (152.3 ksi) tensile strength, 210 GPa (30457.9 ksi) Young's modulus, and 7850 kg/m^3 (490.1 lb/ft^3) density. It should be noted that the metakaolin (a high pozzolanic reactive material) was incorporated in the development of ECC mixtures to achieve ECC with a compressive strength above 70 MPa (10152.6 psi). Metakaolin was also used to adjust the viscosity of the cementitious paste, allowing for better distribution and suspension for fibers, which had a varied density (i.e., low density for PVA fibers and high density for SFs).

2.4.2. Test Specimens

In order to evaluate the flexural behavior of LWSCC strengthened with ECC, seven RC beams were cast and tested. All beams had typical dimensions and steel reinforcements as shown in **Figure 2-1**. The beams were constructed with a total length of 2160 mm (85.04 in.), having a square cross-section with a height/width of 250 mm (9.8 in.) and effective depth of 197.5 mm (7.8 in.). Each beam was reinforced with three 25 mm (0.98 in.) deformed steel bars placed at the tension zone (tension reinforcement ratio = 3.04%) and two 10 mm (0.39 in.) deformed steel bars placed at the compression zone. All beams were designed to fail in ductile flexural mode. To avoid shear failure, two leg stirrups with a 10 mm (0.39 in.) diameter deformed steel bar were placed at a spacing of 100 mm (3.9 in.) along the whole length of the beams. The concrete cover was 30 mm (1.3 in.) thick on all sides. The seven beams are detailed as follows:

- The first three beams were fully cast with LWSCC, ECCP, and ECCS, respectively. These beams were used as control specimens for the strengthened beams (see **Figure 2-1**).
- The fourth and fifth beams were cast with two layers: the bottom layer was LWSCC with a depth of 165 mm (6.5 in.) and the top layer was ECCP or ECCS with a depth of 85 mm (3.4 in.). These beams were used to evaluate the behavior of LWSCC strengthened with ECCs at the compression zone. These beams were designated as ECCP-C and ECCS-C, respectively, in which ECCP or ECCS referred to the mixture name and the letter “C” referred to strengthening the compression zone (see **Figure 2-1**).

- The sixth and seventh beams were cast with two layers: the bottom layer was ECCP or ECCS with a depth of 85 mm (3.4 in.), while the top layer was LWSCC with a depth of 165 mm (6.5 in.). These beams were tested to assess the behavior of LWSCC strengthened with ECCs at the tension zone. These beams were designated as ECCP-T and ECCS-T, respectively, in which ECCP or ECCS referred to the mixture name and the letter "T" referred to strengthening the tension zone (see **Figure 2-1**).

The depth of the ECC layer (ECCP or ECCS) was chosen to ensure a sufficient depth for concrete around the longitudinal steel bars placed at the compression or tension sides. This was assumed to be achieved at a depth equal to the concrete cover (30 mm (1.2 in.)) below and on top of the longitudinal steel bars (at either compression or tension sides). Accordingly, the depth of the ECC layer was selected as 85 mm (3.4 in.), and this depth was kept constant at both the tension and compression zones, for comparison.

The provided shear stirrups were mainly responsible for achieving sufficient bond between the ECC layer and LWSCC. However, in order to further increase this bond and avoid a shear interface failure, the surface of the interface between the two layers was roughened (i.e. scratched and grooved) before pouring the new layer. It should be noted that in beams with insufficient stirrups, other techniques such as shear connectors or planting dowels can be used to ensure sufficient bond between the two layers.

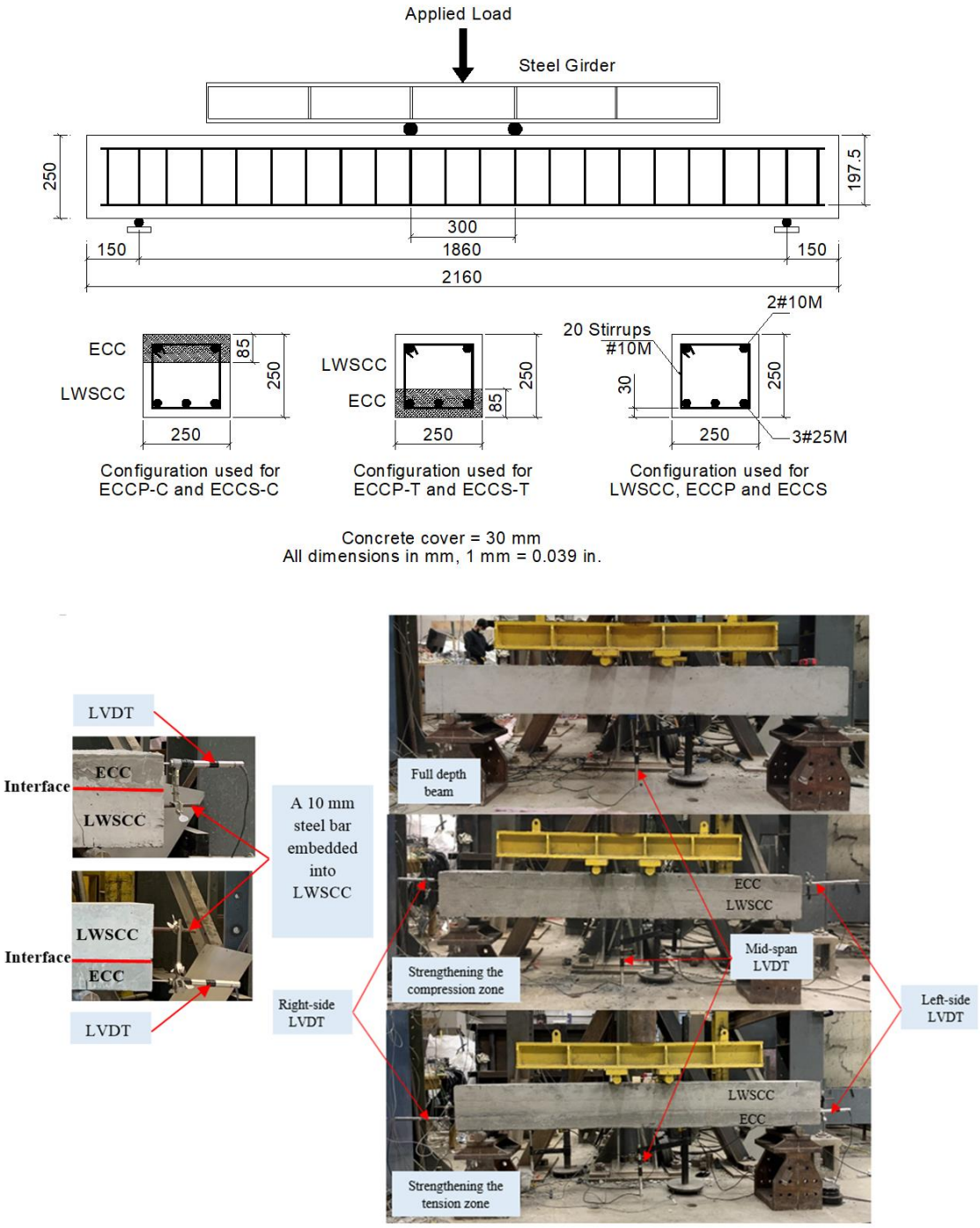

Figure 2-1 Geometry, reinforcement details, and test setup of the tested beams

2.4.3. Concrete Casting

The LWSCC and ECCP were developed with self-compactability properties. According to the EFNARC (2005), the flowability of LWSCC and ECCP was evaluated using slump flow and V-funnel tests, while the passing ability was assessed by the L-box. Once the fresh properties were tested, the mixtures were poured and consolidated into the formwork under its own weight with no external vibration. On the other hand, it was not possible to achieve a full self-compactability performance for the ECCS due to the existence of SFs with high rigidity and heavy density. However, the ECCS was developed with high workability (**Table 2-2**), evaluated using the slump test (ASTM C143).

Table 2-2 Fresh and mechanical properties of the developed mixtures

Mixture	Slump flow		V-funnel time (sec)	L-box	f_c' MPa	STS MPa
	Diameter (mm)	T_{50} (sec)				
LWSCC	700	2.91	11.51	0.82	42.5	2.6
ECCP	800	2.11	9.88	0.94	77.5	8.8
Mixture	Slump (mm)				f_c' MPa	STS MPa
ECCS	200				82.5	10.5

Note: 1 mm = 0.039 in.; and 1 MPa = 0.145 ksi.

For the control beams (LWSCC, ECCP, and ECCS), the mixtures were gradually cast until the formwork was fully filled with a depth of 250 mm (9.8 in.). In the strengthened beams (ECCP-C, ECCS-C, ECCP-T, and ECCS-T), the casting started with the LWSCC to simulate the typical strengthening condition as the LWSCC is the existing layer and the ECC (strengthening layer) is the new layer. After pouring the LWSCC layer, the beam was left until the initial setting and then the top concrete surface was scratched and grooved (i.e. improving the surface roughness) for better bonding with the ECC layer. After 24

hours, high air pressure was applied to the hardened concrete surface to clean any impurities, and then the ECC layer was poured. From each mixture layer, six cylinders were taken to test the compressive and splitting tensile strength (STS) as per procedures given by the ASTM C39 and C496, respectively. The formwork was removed for the beams and cylinders 24 hours after completing the casting, and then all specimens were air-cured for 28 days.

2.4.4. Test Setup

Four-point flexural test was conducted for all beams as seen in **Figure 2-1**. Each beam was simply supported by two round bars at a loading span of 1860 mm (73.2 in.). The loading was applied using a 500-kN (112.4 kips) hydraulic jack acting on a steel girder, and then the load was distributed onto two points kept 300 mm (11.8 in.) apart. In the initial loading stage, the load was gradually applied to easily monitor any crack activity at the beam's midspan, i.e. distance between the two loading points (maximum pure moment region). Once the first crack was visually detected, the load was applied in steps with a constant increment of 45 kN (10.1 kips). After each step, the cracks were detected and mapped out, then their widths were measured using a microscope with 60x magnification. During the loading, the deflection of each tested beam was measured using a linear variable differential transformer (LVDT) vertically placed at the midspan point and touching the beam's bottom surface. Another two LVDTs were horizontally attached, one at each beam's end, in order to measure any lateral movement/slip between ECC and LWSCC layers (as shown in **Figure 2-1**). Strain gauges were attached to the longitudinal steel bars placed at the tension zone to record their strains.

2.5. Discussion of Test Results

2.5.1. Properties of LWSCC and ECC Mixtures

The fresh and mechanical properties of the LWSCC and ECCs used in this study are shown in **Table 2-2**. According to the EFNARC (2005) classification, the fresh properties tests showed that the flowability and passing ability of the LWSCC mixture can be classified as SF2/VS2/PA2, as it had a slump flow diameter of 700 mm (27.6 in.), T_{50} of 2.91 sec, V-funnel time of 11.51 sec, and L-box ratio of 0.82. In the hardened state, the LWSCC exhibited a compressive strength and STS of 42.5 MPa (6.16 ksi) and 2.6 MPa (0.36 ksi), respectively. Based on the fresh and mechanical properties measured, this mixture can be suitable for several structural applications, e.g., walls, columns, slabs, etc.

The ECCP could be developed as SF3/VS2/PA2 class (as per EFNARC (2005)), in which the slump flow diameter, T_{50}, V-funnel time, and L-box ratio were 800 mm (31.5 in.), 2.11 sec, 9.88 sec, and 0.94, respectively. On the other hand, the ECCS mixture could not be produced with self-compactability properties. This was attributed to the high friction and blockage caused by SFs (rigid fibers), which limited the flowability and passing ability of ECC. In addition, in the trial mixtures stage, the significantly heavier density of the SFs compared to the ECC mortar tended to cause a segregation when attempting to develop ECCS with self-compactability properties. For this reason, the ECCS was developed as vibrated concrete with a high slump of 200 mm (7.9 in.). In the hardened state, the ECCP and ECCS had a compressive strength of 77.5 MPa (11.2 ksi) and 82.5 MPa (12 ksi), respectively, and an STS of 8.8 MPa (1.3 ksi) and 10.5 MPa (1.5 ksi), respectively. Although both ECCs had the same mixture composition, the mechanical properties were affected by the fiber type. As seen from the results, the ECC reinforced with SFs exhibited

compressive strength and STS of about 6.5% and 19.3%, respectively, higher than the ECC reinforced with PVA fibers. The higher compressive strength of ECCS could be attributed to the higher modulus of the SFs (compared to the PVA fibers), which helped to produce ECC with overall higher stiffness, which increased the ability of composite to carry higher compressive loading. Also, the hooked ends of the SFs most likely increased their pull-out strength, which in turn improved their bridging mechanism and allowed for transferring higher levels of stress across cracks. Despite the better mechanical performance of the SFs, the PVA fibers can offer some advantages as follows:

- Unlike the SFs, the ECC with PVA fibers could be developed with lower density (as seen in **Table 2-1**) and self-compactability properties, which are suitable for many structural applications.
- The relatively low density and micro size of PVA fibers render them as a strong candidate for rehabilitation applications where a thin cementitious layer with a rich content of fibers can be placed.
- The use of PVA can be more useful in specific types of concrete such as shotcrete, in which the flexibility of PVA fibers allows for higher fluidity throughout concrete spraying equipment, i.e. less damage to equipment and faster placing rate (Jovičić et al., 2009).
- The PVA fibers also have a better durability due to their non-corrosive nature, which extends their applications to different harsh environment conditions.

2.5.2. Cracking and Failure Mode

The cracking characteristics and failure mode of each tested beam are shown in **Figure 2-2**.

2.5.2.1. Control Beams (LWSCC, ECCP, and ECCS)

With increasing the applied load, the tensile stress reached the maximum tensile strength of the bottom layer of concrete, leading to the development of the first crack. The first crack was typically detected at the maximum moment region at a width of 0.02 mm (0.0008 in). Beyond the formation of the first crack, more vertical cracks developed along the bottom side of the beam. With the load progress, vertical cracks within the shear spans (i.e. the distance between point load and support) started to diagonally propagate toward the loading zone at the compression zone. Additional increase in the applied load led to further increase in the number of cracks and their widths. Once the steel reinforcement yielded, the width of more than one crack in the area of maximum moment region was obviously increased. Then a localized widening occurred in a major crack, followed by a crushing in the top fibers of concrete (i.e. ductile flexural mode). Because of the much higher strain capacity of ECCs compared to the LWSCC, the compressive zone of ECCP and ECCS beams exhibited less damage even at the higher ultimate load. Unlike the LWSCC beam, the failure cracking pattern of both the ECCP and ECCS beams exhibited higher number of cracks with narrower widths. This was attributed to the stitching action of fibers which controls crack widths and prevents localized widening, thus allowing ECC to diffuse wide cracks into multiple fine cracks. The LWSCC, ECCP and ECCS beams failed after a formation of 24, 34 and 37 cracks, respectively.

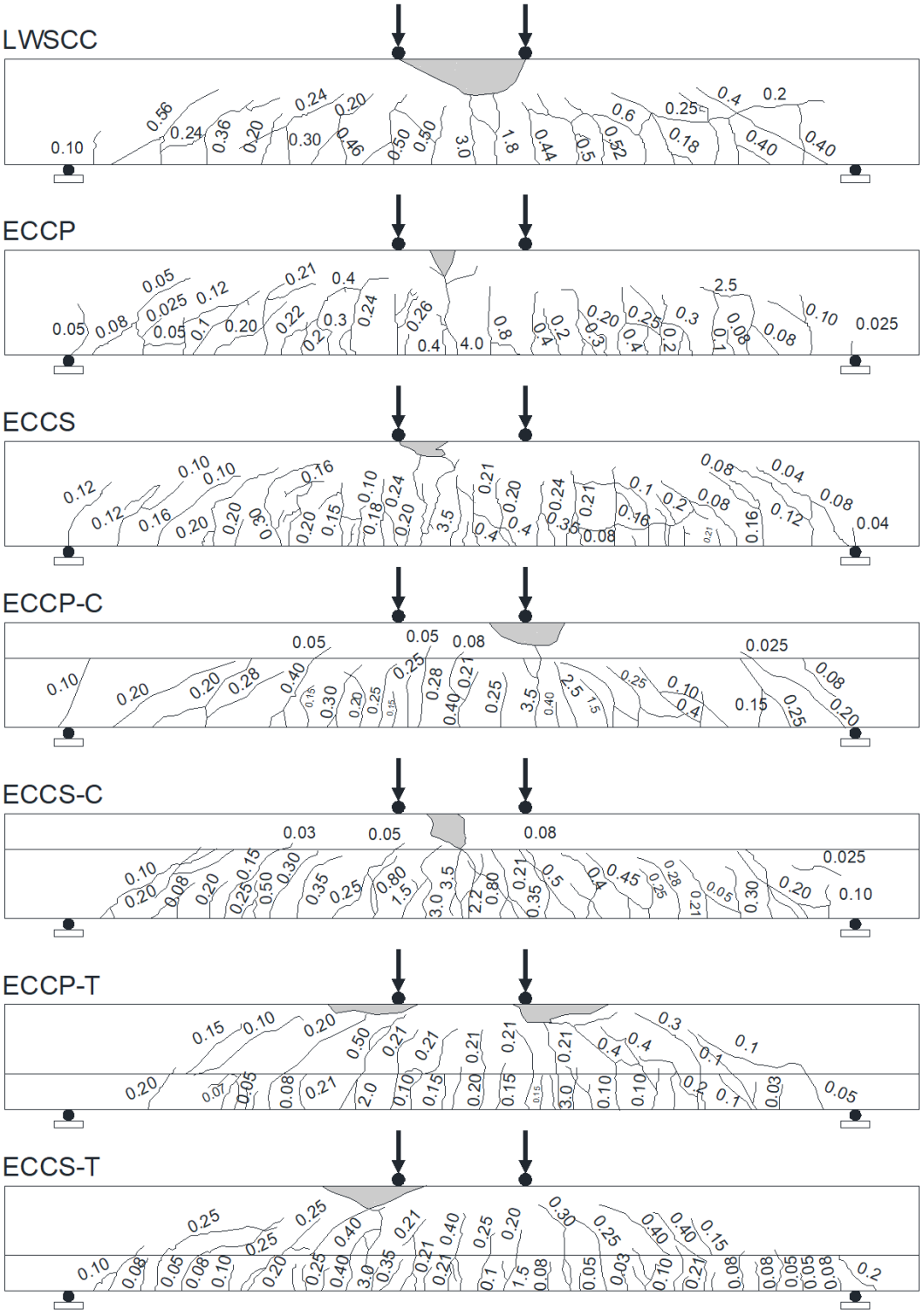

Conversion: 1 mm = 0.039 in.

Figure 2-2 Cracking pattern at failure of the tested beams

2.5.2.2. Comparison of Beams Strengthened at The Compression Zone and The Control LWSCC Beam

For ECCP-C and ECCS-C beams (which had ECC layers on the compression side), during the loading process, the cracks were initiated at the bottom LWSCC layer at the maximum moment region similar to the control LWSCC beam. Then, the developed cracks propagated toward the ECC layer. Once the cracks reached the LWSCC-ECC interface, some of cracks started to propagate horizontally at the interface, while other cracks could penetrate the ECC layer with tiny widths of less than 0.1 mm (0.004 in.). Finally, after the yielding of the tensile steel reinforcement, the beams failed in a ductile flexural mode as the ECCP and ECCS layers at the compression zone were crushed. Compared to the control LWSCC beam, the existence of the ECC layer at the compression zone allowed the beams to sustain higher loading and undergo larger deformation, which consequently was accompanied by higher cracking at the bottom LWSCC layer, as seen in **Figure 2-2**. At the ultimate load, there were 27 and 30 cracks located on the LWSCC layer.

2.5.2.3. Comparison of Beams Strengthened at The Tension Zone and The Control LWSCC Beam

In the ECCP-T and ECCS-T beams, strengthening the LWSCC beam with a layer of ECC at the tension zone helped to improve the cracking behavior compared to the LWSCC beam (with no strengthening). The layer of ECC showed better resistance to cracking as the initiation of cracks was delayed. The first crack occurrence was followed by a formation of more fine vertical cracks in the ECC layer along the beams' span. As the load increased, additional cracks were initiated from the ECC-LWSCC interface. These cracks propagated first upward in the LWSCC layer, and then, with higher loads, began to extend downward

in ECC layer with narrower widths and slower rate. This could be attributed to the existence of fibers in ECC, unlike the LWSCC, which delayed the propagation of cracks and allowed for developing multiple cracks with controlled width. In both the ECCP-T and ECCS-T, the tensile steel reinforcement reached to the yielding, and then a crushing in the concrete occurred underneath the loading points, after developing 30 and 37 cracks within the ECCP and ECCS layers, respectively. Once the concrete was crushed, significant diagonal cracks developed within the LWSCC layer. These diagonal cracks were induced as a result of the low shear strength of LWSCC due to the well-known weak interlock mechanism of lightweight aggregates.

It is worth noting that despite the cracking activity that occurred around or at the LWSCC-ECC interface in all strengthened beams, at either the compression or tension zone, no sign of delamination between the LWSCC and ECC layers was observed during the loading process. This was also confirmed by the two side-LVDTs attached to the strengthened beams, as they did not record any lateral movement. This pointed out that using the shear stirrups, in addition to the high surface roughness, can be an effective means of achieving sufficient bonding at the ECC-LWSCC interface in either tension or compression strengthening techniques.

2.5.2.4. Evaluation of Cracking Based on Durability Aspect

The cracking characteristics, particularly the maximum crack width is an important factor affecting the long-term durability of concrete structures. To ensure adequate protection for steel reinforcement, the maximum allowable crack width should not exceed 0.3 mm (0.012 in.) to 0.33 mm (0.013 in.) under service conditions for exterior-exposed structures (ACI 318 (2009), CSA (2004), BS 8110 (1997), ACI 224R (2001), and CEB-FIP (1992)). The

service condition in this study was assumed at 50% of the designed maximum capacity. As seen in **Table 2-3**, the maximum crack width at service condition in the control LWSCC and beams strengthened at the compression zone (ECCP-C and ECCS-C) ranged from 0.35 mm (0.014 in.) to 0.40 mm (0.016 in.), which exceeded the critical value proposed by the codes and guidelines. This was attributed to the low tensile strength of the bottom side layer (LWSCC layer with no fibers), which allowed for cracking localization. On the other hand, when the ECCP or ECCS layer was placed at the tension side (LWSCC layer at the top), narrower cracks were detected due to the stitching action of fibers that acts as a crack arrestor. The maximum crack width measured in the ECCP-T and ECCS-T beams was 0.20 mm (0.008 in.) and 0.22 mm (0.009 in.), respectively, (i.e. less than the permissible values). This indicates that ECC can contribute to enhancing the durability of concrete structures, especially those located in corrosive environments.

Table 2-3 Results of all tested beams tested in flexure

Beam	First crack load (kN)	Maximum crack width at service load	Failure Load (kN)	Failure Mode
LWSCC	14.2	0.40	275.0	Flexural
ECCP	27.6	0.18	349.8	Flexural
ECCS	23.1	0.24	358.7	Flexural
ECCP-C	14.5	0.35	301.9	Flexural
ECCS-C	15.1	0.40	308.0	Flexural
ECCP-T	28.3	0.20	313.7	Flexural
ECCS-T	26.2	0.22	330.4	Flexural

Note: 1 kN = 0.225 kips

2.5.3. Load-Deflection Behavior

2.5.3.1. General

The load-deflection response measured for all tested beams are presented in **Figure 2-3**. In the pre-cracking stage, all beams had a linear load-deflection response with a high slope, which indicates a high stiffness. Beyond the first crack load (post-cracking stage), the load-deflection curve maintained a linear manner but with continuous reduction in the slope (i.e. decreased stiffness) due to the formation of cracks. With further increase in the applied load, the steel reinforcement reached to the yielding, which significantly reduced the beams' stiffness. After that, the load-deflection curve deviated from linearity as the beams underwent a large deformation against a slight increase in the applied load. Once each beam reached the maximum capacity, a drop in the carried load was observed, followed by the start of the post-peak stage.

2.5.3.2. Control Beams (LWSCC, ECCP and ECCS)

Prior to the ultimate load, the load-deflection curves showed that the ECCP and ECCS beams had a higher stiffness than the LWSCC beam. This could be attributed to the higher strength of ECCs, in addition to the existence of PVA fibers or SFs in ECC, which delayed and restricted the formation of cracks, i.e., the less cracking the higher the stiffness. The LWSCC beam reached the ultimate load at a deflection of 12.5 mm (0.49 in.) and then experienced a high reduction rate in the carried load. Meanwhile, the ECCP and ECCS beams had a deflection value corresponding to the ultimate load of 15.7 mm (0.62 in.) and 14.4 mm (0.57 in.), respectively. In the post-peak stage, the ECCP and ECCS beams could sustain around 80% of the ultimate load, even after reaching a deflection of 70~80 mm

(2.76~3.15 in.). This indicates a better post-peak ductility, damage tolerance, and structural integrity for ECC beams over the LWSCC beam.

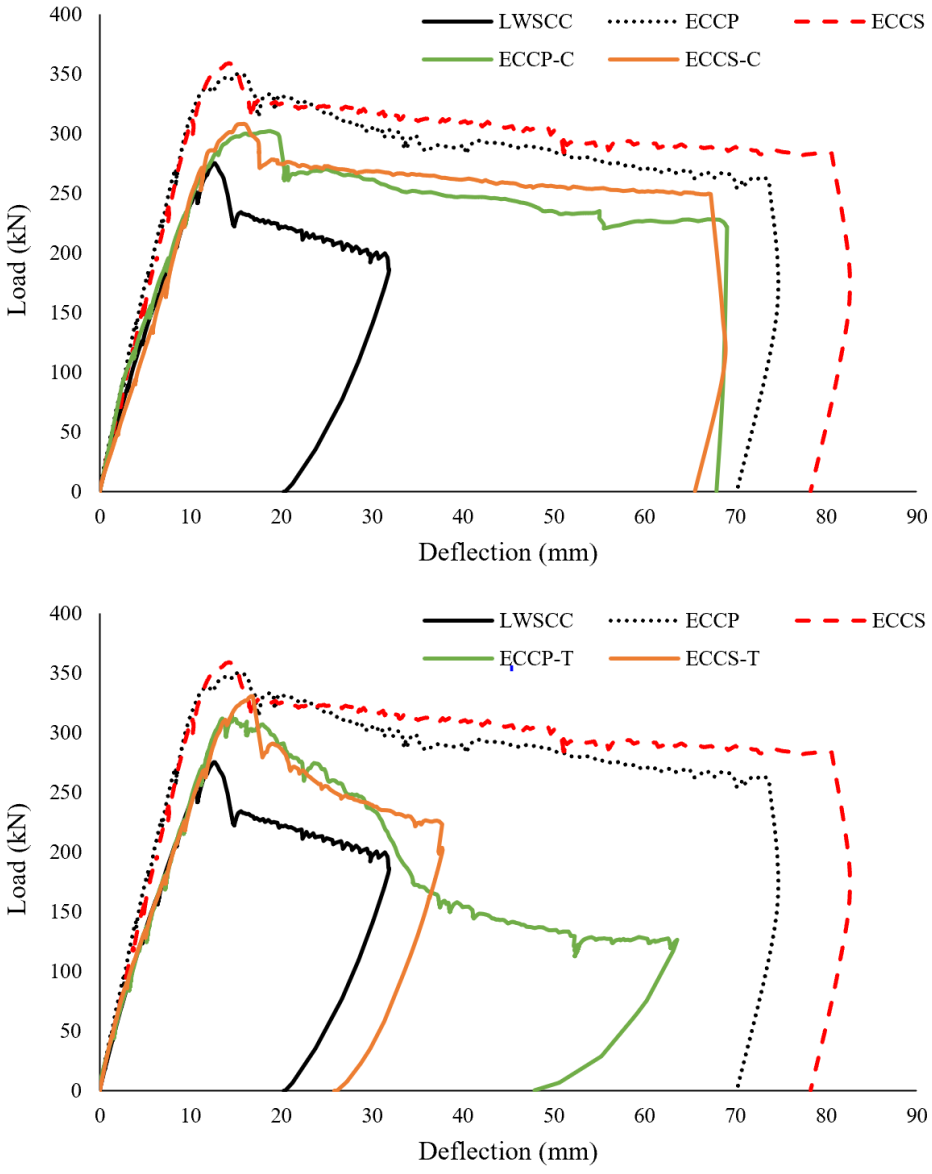

Conversion: 1 mm = 0.039 in.; 1 kN = 0.225 kips

Figure 2-3 Load-deflection curves for all tested beams

2.5.3.3. Comparison of Beams Strengthened at The Compression Zone and The Control LWSCC Beam

The incorporation of either ECCP or ECCS at the compression zone did not obviously affect the beam's stiffness as the ECCP-C, ECCS-C, and LWSCC beams had a comparable stiffness. However, strengthening the LWSCC with ECC significantly contributed to improving the structural performance of the beam, especially at the post-peak stage. This was attributed to the higher strain capacity and damage tolerance of the ECCs, which allowed beams to experience large deformation with no catastrophic failure or sharp drop in the sustained load. The maximum load-carrying capacity of ECCP-C and ECCS-C beams was reached at a deflection of 18.8 mm (0.74 in.) and 14.9 mm (0.59 in.), respectively, which were 1.50 and 1.20 times as much as the deflection exhibited by the control LWSCC beam. In addition, around 75%~80% of the ultimate load was maintained by the ECCP-C and ECCS-C beams up to a deflection of 60~70 mm (2.36~2.76 in.).

2.5.3.4. Comparison of Beams Strengthened at The Tension Zone and The Control LWSCC Beam

Using ECCP and ECCS in strengthening the tension zone of the LWSCC beam could improve the deformability before and after the ultimate load. However, the LWSCC beam strengthened with ECCP or ECCS at the tension zone showed less deformation capacity than the beam strengthened with ECCP or ECCS at the compression zone. This could be attributed to the fact that the compression zone of the ECCP-T and ECCS-T beams was cast from the LWSCC, which typically has a relatively low strain capacity and experiences high damage at failure (compared to ECC). This, in turn, limited the beam's ability to experience large deformation and/or sustain significant load at the post-peak stage. Despite

the fact that ECCP-T and ECCS-T (beams strengthened at the tension zone) showed less deformation capacity than beams strengthened at the compression zone, ECCP-T and ECCS-T beams still showed higher deformation capacity than the control LWSCC beam by 42.4% and 34.4%, respectively (at ultimate load).

2.5.4. First Crack and Ultimate Load

Table 2-3 shows the first crack load of each tested beam. From the results, it can be seen that the LWSCC beam had the first crack at a load of 14.2 kN (3.2 kips). Better cracking resistance was observed in the ECCP and ECCS beams, in which the first crack load was induced at a load of 27.6 kN (6.2 kips) and 23.1 kN (5.2 kips), respectively. These results indicated a better cracking resistance for the ECCP over the ECCS. This may be related to the micro size and low density of PVA, which typically leads to a high number of fibers dispersed in the ECC's paste compared to the SFs at same fiber percentage. This most likely allows more fibers to be perpendicularly oriented to crack propagation, further delaying the formation of macro-cracks.

By comparing beams strengthened at the compression zone (ECCP-C and ECCS-C) with the LWSCC beam, it can be observed that the first crack load was not significantly changed due to strengthening. This is because in these beams the tension zone (i.e. bottom side) was made from the LWSCC; consequently, a comparable first crack load was obtained. On the other hand, when ECC was used in strengthening the tension zone, the tensile strength and cracking resistance of the beam increased, leading to an increase in the first crack load. The ECCP-T and ECCS-T beams exhibited a first crack load of 1.99 and 1.85 times greater than that exhibited by the control LWSCC beam.

Table 2-3 also shows the ultimate loads, which were taken as the maximum load value sustained by each tested beam. Although the PVA fibers showed better performance compared to SFs at the pre-cracking stage, the two ECC beams with either PVA fibers or SFs (ECCP and ECCS, respectively) sustained comparable ultimate loads. The difference in the ECC beams' ultimate load did not exceed 2.6%. This could be attributed to the fact that the inclusion of SFs increased the compressive strength of ECC, as well as increased the pull-out strength of SFs (due to hooked ends), which helped the fibers to transfer higher stress across cracks. These effects balanced the high dispersion of the PVA fibers (as mentioned before), leading to a comparable performance for both fibers at the ultimate stage.

Strengthening the LWSCC with ECCP and ECCS led to improving the load-carrying capacity by 9.8% and 12%, respectively. This was due to increasing the strength of the compression concrete block as a result of replacing the relatively low-strength LWSCC (i.e. 42.5 MPa (6.2 kips)) with a layer of high-strength ECC (i.e. 77.5~82.5 MPa (11.2~12 kips)). Better results were obtained when ECC, with its high tensile strength and cracking resistance, was used for strengthening the tension zone of the LWSCC beam. The ultimate loads of the ECCP-T and ECCS-T beams were boosted by 14.2% and 20.2%, respectively, compared to the control LWSCC beam.

2.5.5. Theoretical predictions of the beams' capacity

The model developed by Henager and Doherty (1976) was used to estimate the theoretical design moments (M^{theo}) for the unstrengthened and strengthened beams. This model is similar to the ACI ultimate design method but takes the contribution of fibers into account.

Figure 2-4 shows a schematic for the internal forces, stress, and strain distributions in the cross-section. It should be noted that as per the ACI (2019) and Henager and Doherty's model (1976), the nominal moment capacity of all tested beams was computed when the strain in the extreme compression fiber in concrete reached a limit of 0.003. The equation for the nominal moment (M_n) of a doubly reinforced steel fibrous concrete beam is:

$$M_n = A_s f_y \left(d - \frac{a}{2}\right) + A'_s f_s \left(\frac{a}{2} - d'\right) + \sigma_t b (h - e) \left(\frac{h}{2} + \frac{e}{2} - \frac{a}{2}\right) \quad (2\text{-}1)$$

$$\sigma_{t1} = 0.00772 \, l/d_f \, \rho_f \, F_{be} \quad (2\text{-}2)$$

$$\sigma_{t2} = \sigma_f - \sigma_0 \quad (2\text{-}3)$$

where A_s = area of tension reinforcement; A'_s = area of compression reinforcement; f_y = yield strength of reinforcing bar; f_s = stress of compression reinforcement; d = distance from extreme compression fiber to centroid of tension reinforcement; b = width of beam; a = depth of rectangular stress block; c = distance from extreme compression fiber to neutral axis found; e = distance from extreme compression fiber to top of tensile stress block of fibrous concrete; σ_t = tensile stress in fibrous concrete, which is equal to either σ_{t1} or σ_{t2}; σ_{t1} = tensile stress in fibrous concrete proposed by the Henager and Doherty model; l = fiber length; d_f = fiber diameter; ρ_f = percent by volume of steel fibers; F_{be} = bond efficiency of the fiber which varies from 1.0 to 1.2 depending upon fiber characteristics; σ_{t2} = tensile stress in fibrous concrete obtained experimentally in this study; σ_f = tensile strength of fibered ECC; σ_0 = tensile strength of non-fibered ECC (ECC's cementitious paste).

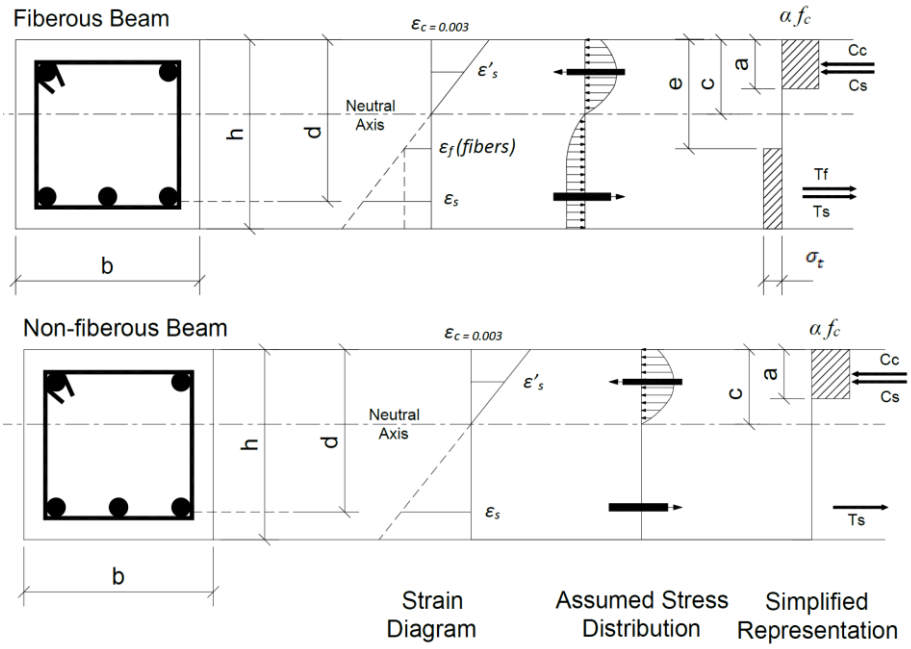

Figure 2-4 Design assumptions for tested beams

Eq. 2-1 (Henager and Doherty's model (1976)) was used to estimate the M_n for the ECCP, ECCS, ECCP-T, and ECCS-T beams, where the tension zone incorporated a fibrous concrete. It should be noted that this equation considers the fibers' contribution through the term σ_t (either σ_{t1} or σ_{t2}) given in **Eq. 2-2**; however, since the ECCs in this investigation were developed with two types of fibers (steel and polymeric fibers), general use of the proposed equations may produce inaccurate estimations. For this reason, and to check the validation of σ_t for different fiber types, σ_{t2} was also obtained experimentally (in addition to σ_{t1} proposed in the Henager-Doherty equation). Three small-scale prisms cast for each of the ECCP, ECCS and their non-fibrous mortar counterparts (i.e., their mortar with no fibers) were tested in flexure according to ASTM C78. The value of σ_{t2} was calculated as the difference between the experimental flexural strength of the ECCP/ECCS and the flexural strength of their non-fibrous mortar counterparts. The σ_{t1} was calculated

as 3.2 MPa (0.46 ksi) and 1.2 MPa (0.17 ksi) for the PVA fibers and SFs, respectively, while σ_{t2} was experimentally found to be 2.9 MPa (0.42 ksi) and 4.6 MPa (0.67 ksi) for PVA and SFs, respectively.

Figure 2-5a shows the experimental-to-theoretical moment (M^{exp}/M^{theo}) ratios calculated for all tested beams. Unlike SFs, PVA fibers showed no significant difference between the σ_{t1} and σ_{t2}. Therefore, the ratios of M^{exp}/M^{theo} calculated using σ_{t1} for beams with PVA fibers were comparable to M^{exp}/M^{theo} calculated using σ_{t2}. As seen in **Figure 2-5a**, the M^{exp}/M^{theo} ratios of the ECCP and ECCP-T beams were 1.09 and 1.13, respectively, at σ_{t1} = 3.2 MPa (0.46 ksi) and 1.10 and 1.09, respectively, at σ_{t2} = 2.9 MPa (0.42 ksi).

The results also indicated that the accuracy of **Eq. 2-1** was generally improved when the experimental σ_{t2} was used. As seen in **Figure 2-5a**, the M^{exp}/M^{theo} ratios of the ECCS and ECCS-T beams were 1.14 and 1.15, respectively, when the experimental σ_{t2} was used, while they were 1.21 and 1.25, respectively, when the theoretical σ_{t1} was used.

For the LWSCC, ECCP-C, and ECCS-C beams, where the tension zone mostly contained non-fibrous LWSCC, the term of fibers' contribution should be removed, and then **Eq. 2-1** will be similar to the ACI[21] ultimate strength design method, **Eq. 2-4**.

$$M_n = A_s f_y \left(d - \frac{a}{2}\right) + A_s' f_s \left(\frac{a}{2} - d'\right) \quad (2\text{-}4)$$

From **Figure 2-5b**, it can be seen that the flexural capacity of the LWSCC, ECCP-C, and ECCS-C beams was conservatively estimated using **Eq. 2-4**, in which the M^{exp}/M^{theo} ratios were 1.07, 1.09, and 1.11, respectively.

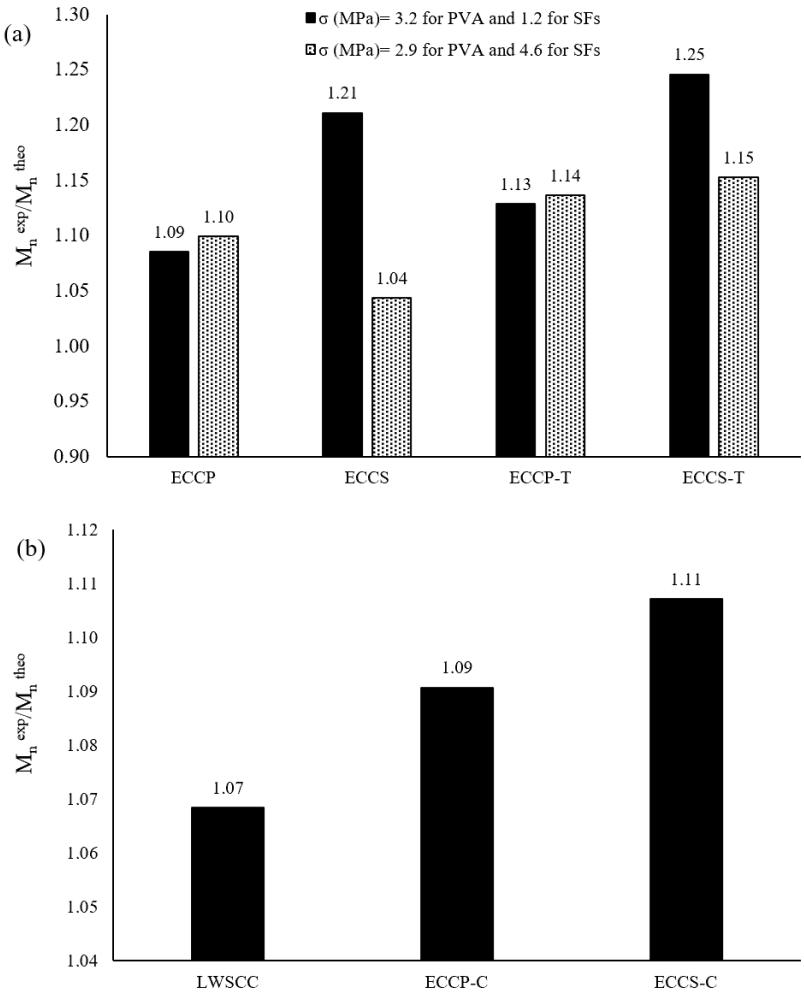

Conversion: 1 MPa = 0.145 ksi

Figure 2-5 Experimental-to-theoretical ultimate moment capacity

2.5.6. Ductility and Energy Absorption Capacity

The ductility was used to evaluate the inelastic deformation capability of structural members. This can be expressed in different terms such as deflection, curvature, and rotational ductility. In this study, the ductility of the tested beams was evaluated based on deflection ductility. This measurement was obtained by calculating the ratio between the ultimate deflection (Δu) and the deflection corresponding to yielding (Δy). The Δu was

defined as the deflection value corresponding to 85% of the maximum load located on the descending curve (post-peak stage). The deformability and load capacity of structural members were also assessed by another term called energy absorption capacity. This term was obtained by measuring the area under the experimental load-deflection curve up to failure; i.e. failure was defined when deflection reached to the Δu. **Figure 2-6** shows the ductility ratios and energy absorption capacity of all tested beams.

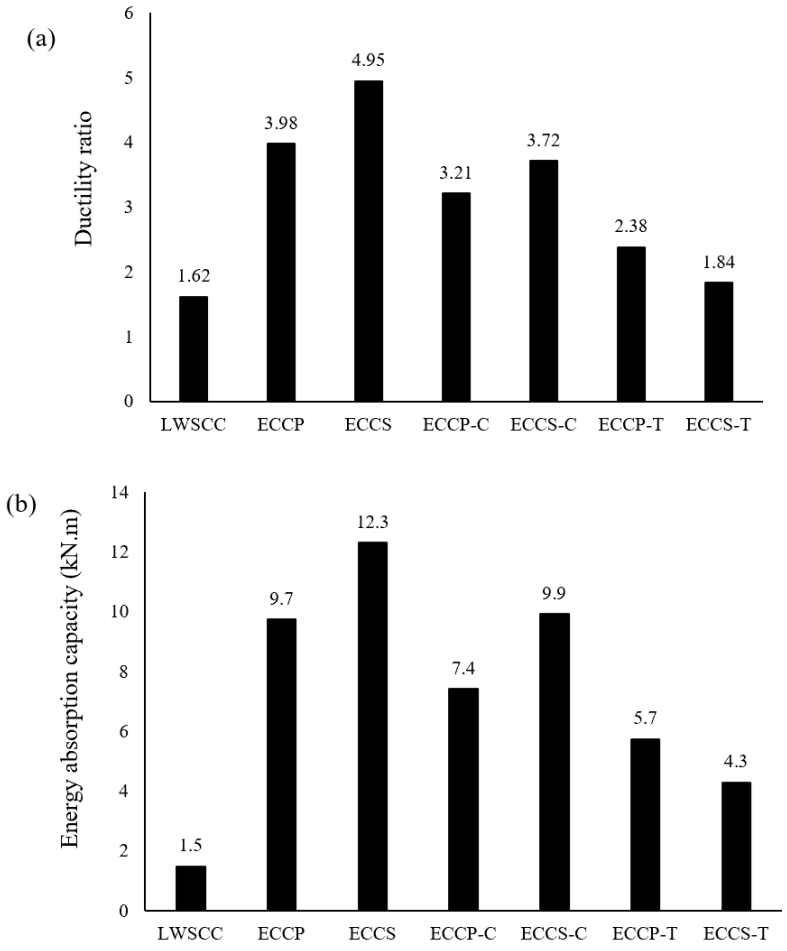

Conversion: 1 kN.m = 0.0088 kip.in.

Figure 2-6 Results of all tested beams (a) ductility ratio, (b) energy absorption capacity

As seen from the Figure, the LWSCC beam exhibited a ductility ratio of 1.62 and energy absorption capacity of 1.5 kN.m (13.3 kip.in). A significantly higher ductility and energy absorption capacity were observed in the ECCP and ECCS as the incorporation of fibers allowed the beams to endure high loading and experience large inelastic deflection. The ductility and energy absorption capacity of the ECCP beam were 3.98 kN.m (35.2 kip.in) and 9.7 kN.m (85.9 kip.in), respectively, while they were 4.95 kN.m (43.8 kip.in) and 12.3 kN.m (108.9 kip.in), respectively, for the ECCS beam.

Adding ECC layer at the compression zone greatly increased the ductility and energy absorption capacity as a result of improving both the sustained load and deformation capacity. The ECCP-C and ECCS-C beams showed a ductility ratio of 3.21 and 3.72, respectively, which were 1.98 and 2.3 times, respectively, as much as that of the control LWSCC beam. In addition, the improvement in the energy absorption capacity of the ECCP-C and ECCS-C beams reached up to 4.9 and 6.6 times, respectively, higher than that absorbed by the control LWSCC beam. These results indicate that the ECC has a promising potential for either full constructing or strengthening structural members exposed to loading accompanied by a substantial inelastic deformation, such as impact and seismic loading.

Although the use of ECC in strengthening the tension zone led to an increase in the beam's load capacity, lower improvements in the ductility and energy absorption capacity were obtained compared to beams strengthened in the compression zone. This was related to the low strain capacity of the top LWSCC layer, which limited the inelastic deformability of the hybrid composite beam. The ductility of the ECCP-T and ECCS-T beams were 2.38 and 1.84, respectively, which were 0.74 and 0.50 times, respectively, as much as that of

the ECCP-C and ECCS-C beams, respectively. The energy absorption capacity of these beams also reached a value of 5.7 kN.m (50.5 kip.in) and 4.3 kN.m (38.1 kip.in), respectively. These values were 0.77 and 0.43 times, respectively, greater than that absorbed by the ECCP-T and ECCS-T beams, respectively. But the ductility ratio and energy absorption capacity of the ECCP-T and ECCS-T beams were still obviously higher than those exhibited by the LWSCC beam.

2.6. Conclusions

This study investigated the flexural performance of LWSCC beams strengthened with ECC at either the compression or tension zone. Two types of fibers were used in the mixture to study the efficiency of ECC as a strengthening material. The study also compared the behavior of beams fully cast with ECCs and LWSCC. The flexural behavior of the unstrengthened and strengthened beams was evaluated by examining their load-deflection response, cracking behavior, failure mode, first crack and ultimate load, ductility, and energy absorption capacity. The performance of analysis method developed by Henager and Doherty was evaluated to estimate the flexural capacity of fibrous beams compared to the experimental results. The following conclusions can be drawn:

1. ECC developed with SFs proved to have better compressive strength, STS, and flexural performance compared to ECC developed with PVA fibers. However, unlike SFs, the use of PVA fibers allowed ECC to be produced with slightly lower density and self-compactability properties.
2. LWSCC beams strengthened with ECC at either the compression or tension zone exhibited better flexural behavior in terms of first crack load, ultimate load,

ductility, and energy absorption capacity compared to the non-strengthened fully cast LWSCC beam. These results indicate superior performance for using ECC as a strengthening material.

3. LWSCC beams strengthened with ECC at the tension zone exhibited higher first crack load and ultimate load compared to LWSCC beams strengthened with ECC at the compression zone. However, strengthening the beam with ECC at the compression zone exhibited higher ductility and energy absorption capacity.
4. When ECC layer was placed at the tension zone of the beam, the use of PVA fibers in the ECC showed more advantage over SFs in delaying the initiation of the first crack. However, using SFs in ECC at the tension zone yielded higher contribution to increasing the overall ultimate load-carrying capacity compared to using PVA fibers in ECC.
5. The use of ECC (with either PVA or SFs) at the tension zone delayed the propagation of cracks and allowed for developing multiple cracks with controlled width, which can help to provide a better protection for the tension steel reinforcement. Unlike the LWSCC beam, at the service load condition, using ECC at the tension zone of the beam limited the cracks' width to below the permissible limits given by the CSA, ACI 318, BS 8110, ACI 224R, and CEB-FIP for exterior-exposed structures.
6. In all beams strengthened with ECC layer, no sign of slip at the LWSCC-ECC interface was recorded, which indicates that the presence of the shear reinforcement and the roughened interface surface were sufficient to achieve adequate bonding between the ECC and LWSCC layers.

7. The ACI ultimate strength design method as well as the analysis developed by Henager and Doherty showed a conservative capability for estimating the flexural capacity of all tested beams. For beams with fibers, the accuracy of the estimations given by the Henager and Doherty model improved when the term of the tensile stress of fibrous concrete was obtained experimentally rather than by calculating it based on the model's equation.

2.7. References

ACI (American Concrete Institute), "Building Code Requirements for Structural Concrete (ACI 318-95) and Commentary (ACI 318 R-95)," Committee 318, Farmington Hills, MI, 2019.

ACI (American Concrete Institute), "Control of Cracking in Concrete Structures (224 R-90)," Committee 224, Farmington Hills, MI, 2001.

British Standard Institute, "Structural Use of Concrete. Part 1: Code of Practice for Design and Construction," BS 8110, London, UK, 1997.

Canadian Standards Association Committee A23.3, "Design of Concrete Structures," CSA A23.3-04, Canadian Standards Association, Rexdale, Ontario, Canada, 2004.

CEB-FIP, "CEB-FIP Model Code 1990," Thomas Telford, London, UK, 1992.

EFNARC. (2005). "The European Guidelines for Self-Compacting Concrete Specification, Production and Use." English ed. Norfolk, UK: European Federation for Specialist Construction Chemicals and Concrete Systems.

Deng, M.; Ma, F.; Ye, W.; and Li, F. “Flexural Behavior of Reinforced Concrete Beams Strengthened by HDC and RPC,” Construction and Building Materials, V. 188, 2018, pp. 995–1006.

Hassan, A. A. A.; Ismail, M. K.; and Mayo J., “Mechanical Properties of Self-Consolidating Concrete Containing Lightweight Recycled Aggregate in Different Mixture Compositions,” Journal of Building Engineering, V. 4, 2015, p. 113–126.

Henager, C. H.; and Doherty, T. J., “Analysis of Reinforced Fibrous Concrete Beams,” Proceedings, ASCE, V. 12, ST-l, 1976, pp. 177-188.

Hubertova, M.; and Hela R., “The Effect of Metakaolin and Silica Fume on the Properties of Lightweight Self-Consolidating Concrete,” ACI, Farmington Hills, MI, USA, ACI special publication 243, 2007, pp. 35–48.

Ismail, M. K.; Abdelaleem, B. H.; and Hassan, A. A. A., “Effect of Fiber Type on The Behavior of Cementitious Composite Beam-Column Joints Under Reversed Cyclic Loading,” Construction and Building Materials, V. 186, 2018a, pp. 969–977.

Ismail, M. K.; and Hassan A. A. A., “Influence of Fibre Type on the Shear Behaviour of Engineered Cementitious Composite Beams,” Magazine of Concrete Research, V. 73, No. 9, 2021, pp. 464-475.

Ismail, M. K.; Hassan, A. A. A.; and Lachemi, M., "Performance of Self-Consolidating Engineered Cementitious Composite Under Drop-Weight Impact Loading," Journal of Materials in Civil Engineering, V. 31, No. 3, 2019, 04018400.

Ismail, M. K.; Sherir, M. A. A.; Siad, H.; Hassan, A. A. A.; and Lachemi, M., "Properties of Self-Consolidating Engineered Cementitious Composite Modified with Rubber," Journal of Materials in Civil Engineering, V. 30, No. 4, 2018b, https://ascelibrary.org/doi/abs/10.1061/%28ASCE%29MT.1943-5533.0002219.

Jovičić, V.; Šušteršič, J.; and Vukelič, Ž. "The Application of Fibre Reinforced Shotcrete as Primary Support for A Tunnel in Flysch," Tunnelling and Underground Space Technology, V. 24, No. 6, 2009, pp. 723-730.

Kang, S. B.; Tan, K. H.; Zhou, X. H.; and Yang, B., "Experimental Investigation on Shear Strength of Engineered Cementitious Composites," Engineering Structures, V. 143, 2017, pp. 141-151.

Kim, J. H. J.; Lim, Y. M.; Won, J. P.; Park, H. G.; and Lee K. M. "Shear capacity and failure behavior of DFRCC repaired RC beams at tensile region," Engineering Structures, V. 29, 2007, pp. 121–131.

Li, V.C., "Advances in ECC Research," Material Science to Application—A Tribute to Surendra P Shah, ACI Bookstore, 2002, pp. 373–400.

Li, V. C., "From Micromechanics to Structural Engineering – The Design of Cementitious Composites for Civil Engineering Applications," Journal of

Structural Mechanics and Earthquake Engineering, JSCE, V. 10, No., 1993, pp. 37-48.

Li, V. C., "Engineered Cementitious Composites (ECC) - Tailored Composites Through Micromechanical Modeling." in Fiber Reinforced Concrete: Present and the Future, N. Banthia, A. Bentur, and A. Mufti, Eds., Canadian Society of Civil Engineers, Montreal, 1998, pp. 64-97.

Li, V. C.; Wu, C.; Wang, S.; Ogawa, A.; and Saito, T., "Interface Tailoring for Strain-Hardening Polyvinyl Alcohol-Engineered Cementitious Composites (PVA-ECC)," ACI Materials Journal, V. 99, No. 5, 2002, pp. 463–72.

Liu, H.; Zhang, Q.; Li, V.; Su, H.; and Gu, C. "Durability Study on Engineered Cementitious Composites (ECC) Under Sulfate And Chloride Environment," Construction and Building Materials, Volume 133, 2017, pp. 171-181.

Murthya, A. R.; Karihaloob, B. L.; Ranic, P. V.; and Priyad, D. S. "Fatigue Behaviour of Damaged RC Beams Strengthened with Ultra-High Performance Fibre Reinforced Concrete," International Journal of Fatigue, V. 116, 2018, pp. 659-668.

Omar, A. T.; Ismail, M. K.; and Hassan, A. A. A., "Use of Polymeric Fibers in the Development of Semilightweight Self-Consolidating Concrete Containing Expanded Slate," Journal of Materials in Civil Engineering, V. 32, No. 5, 2020, 04020067.

Okamura, H.; and Ouchi, M., "Self-Compacting Concrete," Journal of Advanced Concrete Technology, V. 1, No. 1, 2003, pp. 5–15.

Papanicolaou, C. G.; and Kaffetzakis, M. I., "Lightweight Aggregate Self-Compacting: State-of-Pumice Application," Journal of Advanced Concrete Technology, V. 9, No. 1, 2011, pp. 15–29.

Sadek, M. M.; Ismail, M. K.; and Hassan, A. A. A., "Stability of Lightweight Self-Consolidating Concrete Containing Coarse and Fine Expanded Slate Aggregates," ACI Materials Journal, V. 117, No. 3, 2020a, pp. 133-134.

Sadek, M. M.; Ismail, M. K.; and Hassan, A. A. A., "Impact Resistance and Mechanical Properties of Optimized SCC Developed with Coarse and Fine Lightweight Expanded Slate Aggregate," Journal of Materials in Civil Engineering, V. 32, No. 11, 2020b, 04020324.

Şahmaran, M.; Lachemi, M.; and Li, V. C. "Assessing the Durability of Engineered Cementitious Composites under Freezing and Thawing Cycles," Journal of ASTM International, V. 6, No. 7, 2009, pp. 1-13.

Şahmaran, M.; and Li, V. C. "De-icing salt scaling resistance of mechanically loaded engineered cementitious composites," Cement and Concrete Research, V. 37, No. 7, 2007, pp. 1035–1046.

Sahmaran, M.; and Li, V. C. "Engineered Cementitious Composites: Can Composites Be Accepted As Crack-Free Concrete?." Transportation Research Record, 2010, V. 2164, No. 1, pp. 1–8.

Said, S. H., Razak, H. A., “The Effect of Synthetic Polyethylene Fiber on the Strain Hardening Behavior of Engineered Cementitious Composite (ECC),” Materials & Design, V. 86, 2015, pp. 447–457.

Shi, C.; and Yang, X., “Design and Application of Self-Consolidating Lightweight Concrete,” Proceedings of China 1st International Symposium on Design, Performance and Use of Self-Consolidating Concrete, RILEM Publication SARL, Paris, France, 2005, pp. 55–64.

Suthiwarapirak, P.; Matsumoto, T.; and Kanda, T., “Multiple Cracking and Fiber Bridging Characteristics of Engineered Cementitious Composites under Fatigue Flexure,” Journal of Materials in Civil, V. 16, No. 5, 2004, pp. 433-443.

Yao, S. X.; and Gerwick B. C., “Development of Self-Compacting Lightweight Concrete for RFP Reinforced Floating Concrete Structures,” US Army Corps of Engineers Research and Development Center, San Francisco, CA, USA, Technical report, 2006.

Yuan, F.; Pan, J.; Xu, Z.; and Leung, C. K. Y., “A Comparison of Engineered Cementitious Composites Versus Normal Concrete In Beam–Column Joints Under Reversed Cyclic Loading,” Materials and Structures, V. 46, No. 1-2, 2012, pp. 145–159.

3. Development of lightweight composite beams with high shear capacity

3.1. Abstract

This investigation aimed to develop hybrid composite lightweight concrete beams with improved shear capacity and strength. A semi-lightweight high-performance engineered cementitious composite (ECC) layer was added to either the compression or tension side of the beam to improve the shear capacity while maintaining low average density of the composite beam. The ECC material was developed with two types of fibers, including polyvinyl alcohol fibers (PVA) with 8 mm (0.31 in.) length, and steel fibers (SFs) with 35 mm (1.38 in.) length. The study compared the theoretical predictions of ultimate shear capacity calculated by design code models and proposed a model to the experimental results. The results indicated that the strategy of using a high-performance ECC layer in lightweight concrete beams can successfully alleviate the reduction in the shear strength of lightweight concrete, with a slight increase of no more than 9% in the density. For example, using an ECC layer with PVA fibers in the compression side of the lightweight control beam increased the density from 1727 kg/m^3 (107.81 lb/ft^3) to 1843 kg/m^3 (115 lb/ft^3) while it significantly improved the normalized shear strength, reaching a value that exceeded the normalized shear strength of the normal-weight concrete beam with a density of 2276 kg/m^3 (142.1 lb/ft^3). Using an ECC layer in the compression side of the lightweight control beam also showed a noticeably higher post diagonal cracking shear resistance and post cracking shear ductility compared to the control lightweight beam, full-cast ECC beams, and normal-weight concrete beam.

3.2. Introduction

The production of lightweight concrete is typically accomplished by partially or totally replacing the normal- weight aggregate with lightweight aggregate. Several types of lightweight aggregate with variable strength are commercially available in the construction market, such as expanded shales, expanded clay, expanded slag, sintered fly ash aggregate, and expanded slate lightweight aggregate. Some types of lightweight aggregate such as expanded slate and expanded shales are characterized by a relatively high strength that can help to achieve more efficient strength-to-weight ratio (Sari and Pasamehmetoglu, 2005; Kılıç et al., 2003). Lightweight concrete proved to have high fire resistance and thermal insulation (Shafigh et al., 2011; Lotfy et al., 2016). Such advantages make lightweight concrete a good candidate for many structural applications such as precast units, post-tensioned concrete ceilings, and long-span bridges (Chai, 2016; Szydlowki and Mieszcak, 2017; Kayali, 2008). On the other hand, despite the advantages of lightweight concrete, the inclusion of lightweight aggregate in concrete negatively affects the compressive and tensile strength (Hossain et al., 2013; Abouhussien et al., 2015). Also, replacing normal-weight aggregate with lightweight aggregate appeared to reduce the ductility, energy absorption, and impact resistance of concrete (Dymond et al., 2010; Ismail and Hassan, 2014; Abouhussien et al., 2015). The cracks in lightweight concrete are generally propagated through the lightweight aggregate rather than the cement matrix, which makes the lightweight concrete more brittle than normal-weight concrete (Balaguru and Dipsia, 1993; Gao et al., 1997; Kayali et al., 2003).

Engineered cementitious composite (ECC) is characterized by high tensile strain that reaches up to 600 times higher than normal concrete (Şahmaran and Li, 2010; Kong et al., 2003). Moreover, ECC has high energy absorption capacity, fatigue life, impact resistance, and shattering resistance (Suthiwarapirak et al., 2004; Meng et al., 2019; Ismail and Hassan, 2021). The multiple microcracks with tiny widths (less than 100μm) developed in ECC under uniaxial tensile stresses allow the concrete to exhibit a strain-hardening behavior, and, in turn, exhibits higher ductility and deformability (Ranade et al., 2014). ECC also has high durability properties, including high resistance to freezing and thawing and chloride attack, compared to normal concrete (Şahmaran and Li, 2007; Şahmaran et al., 2009). Said and Razak (2015) studied the effect of using different volume fractions of synthetic fibers on the behavior of ECC slabs. Their results indicated that the ultimate load, deflection at ultimate loads, and deflection at failure increased as the fiber volume fraction increased up to 2%. Further increasing the volume fraction beyond 2% led to a reduction in the deformability and ductility of ECC slabs due to the poor dispersion of fibers. Ismail et al. (2018) also investigated the structural behavior of beam-column joints developed with ECC reinforced with different types of fibers. Their study reported that ECC reinforced with steel fibers (SFs) showed the highest improvement in the load carrying capacity, ductility, and energy dissipation compared to other ECC reinforced with polymeric fibers. On the other hand, the ECC joints reinforced with polymeric fibers showed better cracking behavior compared to those reinforced with SFs.

Shear strength of structural concrete elements mainly depends on the compressive strength of the uncracked compression zone (contributes to 20-40% of the concrete shear strength),

the dowel action of longitudinal reinforcement (contributes to 15-25% of shear resistance), and aggregate interlock mechanism (contributes to 35-50% of shear strength) (Taylor, 1974). Despite the higher contribution of the aggregate interlock in the shear transfer, ECC developed without coarse aggregate proved to have higher shear resistance compared to normal conventional concrete. The higher shear resistance of ECC is related to the higher volume fraction of fibers, which contributes to reducing the diagonal crack width and increasing the interparticle friction along the crack length (Ismail and Hassan, 2021; Kang et al., 2017; Hassan, 2020). Kang et al. (2017) conducted an experimental investigation to study the shear behavior of ECC specimens reinforced with polyvinyl alcohol fibers (PVA) and compared the results with conventional concrete specimens. They reported that ECC specimens showed higher normalized shear strength that reached up to 1.54 times higher than conventional concrete specimens. Their results also revealed that ECC matrix provided a higher clamping force to stirrups, which allowed for higher residual shear stresses compared to conventional concrete matrix.

The high volume of fly ash (with relatively low specific gravity) in ECC mixtures helped to develop ECC with a density as low as 2069 kg/m^3 (129.16 lb/ft^3), which can be considered as semi-lightweight concrete (as per CSA design code). Therefore, combining such superior properties of ECC with the favorable properties of lightweight concrete can result in developing a new composite with promising potential for structural applications that require low concrete density and high shear resistance. Adding an ECC layer to lightweight concrete beams can help to enhance the shear resistance and alleviate the brittle behavior of lightweight concrete without a significant increase in the unit weight of

concrete. However, the location, thickness, and type of ECC mixtures to be added to lightweight concrete are considered significant factors that need to be investigated in order to optimize hybrid composite lightweight beams with maximized shear capacity and reduced weight. This study aimed to investigate the shear behavior of hybrid composite concrete beams developed by adding a layer of ECC to lightweight concrete (LWC) beams at different cross-sectional locations (tension and compression zones). Two different types of fibers (PVA and SFs) were tested in ECC to evaluate the improvement in the shear capacity versus the unit weight of the composite beam. Full-depth lightweight concrete beam, two full-depth ECC beams, and one full-depth normal-weight concrete beam were also tested for comparison. The tested properties were cracking behavior, failure mode, deformability, ultimate shear resistance, first diagonal crack load, post diagonal crack shear resistance, post cracking shear ductility, and energy absorption. The experimental results of ultimate shear capacity were also compared to the theoretical predictions calculated by design code models and the proposed model.

3.3. Research Significance

Lightweight concrete (LWC) is a promising material with a high potential for use in structural applications. However, despite the advantages of using LWC in structural applications, LWC has a negative effect on the shear resistance, ductility, and strength of concrete. Previous studies have shown that ECC has a high shear resistance, ductility, cracking behavior, and energy absorption. This concrete can also be optimized with relatively low density and high strength. Therefore, adding an optimized low-density ECC layer to lightweight concrete in a composite beam section will not only compensate for

the reduced strength of lightweight concrete but will also maintain low average density of the composite structure. Unfortunately, no studies have been conducted to evaluate the structural behavior of lightweight-ECC composite beams. The authors believe that this study is essential for designers/engineers to understand the behavior of this composite beam, especially when different strategies concerning ECC type and location of layers are considered.

3.4. Experimental Program

3.4.1. Material Properties

The mixture compositions of lightweight concrete, ECC, and normal-weight concrete are shown in **Table 3-1**.

Table 3-1 Compositions of all developed mixtures

Mix. #	Mix. ID	BC	C/BC	SCM (type)	SCM/BC	S/BC	C.A./BC	w/BC	PVA (vol. %)	SFs (vol. %)	f'c (Mpa)	STS (MPa)
1	LWC	1	0.4	MK+FA	0.2+0.4	0.94	0.8	0.4	--	--	45	2.8
2	ECCP	1	0.45	MK+FA	0.2+0.35	0.36	--	0.27	2	--	70.4	9.4
3	ECCS	1	0.45	MK+FA	0.2+0.35	0.36	--	0.27	--	2	89.9	11.1
4	NWC	1	0.5	MK+FA	0.2+0.3	1.61	1.13	0.4	--	--	64.8	4.3

Note: BC = binder content; C = cement; SCMs = supplementary cementing materials; FA = fly ash; MK = Metakaolin; S = lightweight sand / silica sand; C.A. = lightweight coarse aggregate; w/BC = water-to-binder ratio (i.e., cement + SCMs); PVA = polyvinyl alcohol fiber; SFs = steel fibers; and 1 kg/m^3 = 0.06243 lb/ft^3

- The lightweight concrete (LWC) mixture was developed as self-consolidating concrete. The binder content in this mixture included 40% type GU Portland cement, similar to ASTM C150 Type I, 20% Metakaolin (MK) similar to ASTM (C618) class N, and 40% Fly Ash (FA) similar to ASTM(C618) Type F. The percentages of MK and FA were selected based on trial mixtures conducted by the authors to meet the requirements of the European Guideline for Self-consolidating Concrete (SCC) in terms of flowability, passing ability, and segregation resistance. MK was particularly used to enhance the mixture viscosity, particle suspension, and reduce the risk of lightweight aggregate segregation, while FA was used to enhance the mixture flowability and reduce the high-range water reducer admixture (HRWRA) content in the concrete mixture. Expanded slate coarse aggregate (ESCA) and expanded slate fine aggregate (ESFA) with a specific gravity of 1.53 and 1.8, respectively, were used as coarse and fine lightweight aggregates, respectively. The absorption ratios of ESCA and ESFA were 7.1% and 10%, respectively.
- The binder content of ECC mixtures included type GU Portland cement similar to ASTM C150 Type I, MK similar to ASTM C618 class N, and FA similar to ASTM C618 Type F. The fine aggregate used in these mixtures was silica sand with 0.4 mm maximum aggregate size and 2.65 specific gravity. Two types of fibers were used in ECC mixtures: (a) polyvinyl alcohol (PVA) fibers with 8 mm (0.31 in.) length, 1600 MPa (232 ksi) tensile strength, and 1.3 specific gravity; (b) single hook-ends steel fibers (SFs) with 35 mm (1.38 in.) length and 1150 MPa (166.8 ksi) tensile strength.

- The normal-weight concrete (NWC) mixture was developed as self-consolidating concrete. This mixture contained 50% type GU Portland cement, similar to ASTM C150 Type I, 20% Metakaolin (MK) similar to ASTM (C618) class N, and 30% Fly Ash (FA) similar to ASTM (C618) Type F. The percentages of MK and FA were selected based on previous research conducted by the authors (AbdelAleem et al., 2017) to meet the requirements of the European Guidelines for Self-consolidating Concrete (SCC) in terms of flowability, passing ability, and segregation resistance. Crushed granite and natural sand with a specific gravity of 2.6 and absorption ratio of 1% were used as coarse and fine aggregates, respectively.

The gradation curve for crushed granite, natural sand, ESCA, ESFA, and silica sand are shown in **Figure 3-1**. Also, the configuration and geometry of PVA and SFs are shown in **Figure 3-2**. The required flowability of NWC, LWC, and ECC mixtures was achieved by using polycarboxylate-based high-range water reducer admixture (HRWRA) similar to ASTM C494 Type F.

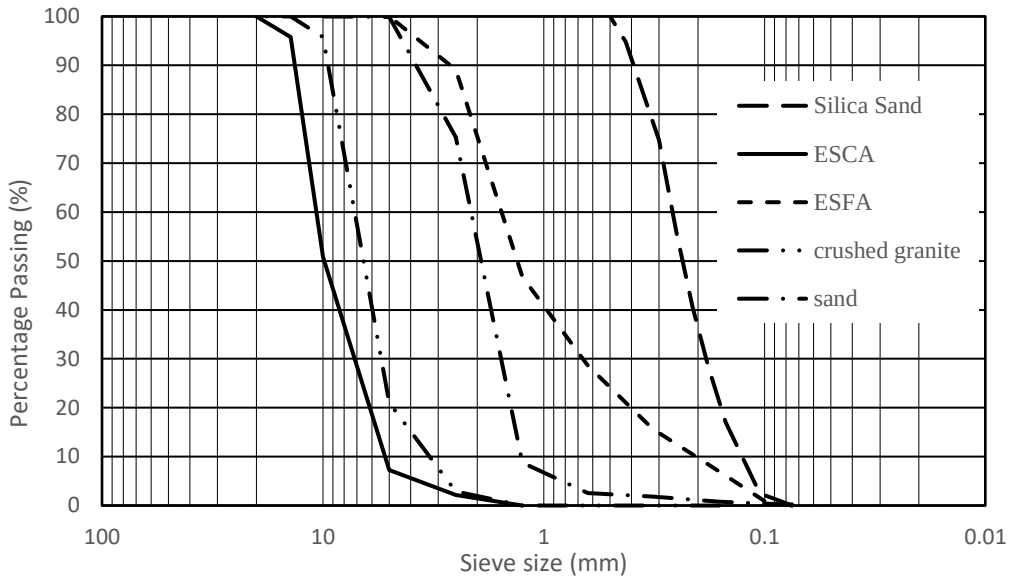

(1 mm = 0.039 in)

Figure 3-1 Grading curves for the aggregates used

(1 mm = 0.039 in)

Figure 3-2 Geometry and configuration of fibers used

3.4.2. Concrete Specimens

This investigation evaluated the shear behavior of hybrid composite beams comprised of two layers—LWC and ECC—reinforced with different fiber types. Two different locations were chosen for the ECC layer: the tension side and compression side of the beam. The study included a total of eight beams designed as follows (see **Figure 3-3**):

- One LWC beam (B1) poured with lightweight coarse and fine aggregate in full depth. This beam was used as a reference control beam for comparison.
- Two ECC beams (B2 and B3) poured in full depth with ECC and reinforced with two types of fibers. B2 was reinforced with PVA fibers and B3 with SFs. These beams were chosen to study the shear behavior of full-depth ECC beams compared to LWC (B1). These beams were also used to evaluate the behavior of SFs compared to PVA fibers in terms of the shear capacity and strength of full-depth ECC beams.
- Two hybrid composite beams, B4 and B5, had an ECC layer reinforced with two types of fibers in the compression side. B4 was poured with an ECC layer reinforced with PVA fibers, while B5 was poured with an ECC layer reinforced with SFs. The depth of LWC part in B4 and B5 was 165 mm (6.5 in.), while the depth of the ECC layer was 85 mm (3.3 in.). These beams were developed and tested to evaluate the effect of using a compression-side ECC layer (with different fiber types) on the shear performance and strength of the beam.

- Two hybrid composite beams, B6 and B7, had an ECC layer reinforced with two types of fibers in the tension side. B6 was poured with an ECC layer reinforced with PVA fibers, while B7 was poured with an ECC layer reinforced with SFs. B6 and B7 were poured with a layer of ECC in the tension side with a depth of 85 mm (3.3 in.), while the remaining depth was poured with LWC. These beams were tested to study the effect of using a tension-side ECC layer (with different fiber types) on the shear performance and strength of the beam.
- One NWC beam (B8) was poured with normal-weight aggregate in full depth. This beam was used as a reference NWC beam for comparison.

It should be noted that the depth of the ECC layer was selected as 85 mm (3.3 in.) in both tension and compression sides to meet two requirements: (a) to ensure an adequate concrete confinement around the longitudinal steel reinforcement bars in both tension and compression sides by adding a cover thickness above and below the bar diameter; (b) to provide sufficient depth for the compression concrete block in order to be entirely covered by the ECC layer. All tested beams were designated by the type of concrete (NWC, LWC, ECC), type of fibers (P for PVA and S for SFs), and location of ECC layer (tension (T) or compression (C)). For example, the composite beam with ECC layer reinforced with PVA fiber in the compression side would be labeled as ECCP-C.

3.4.3. Casting and Specimen Preparation

For the reference beams that were poured in full depth (LWC, ECCP, ECCS, and NWC), the concrete was gradually poured into the formwork for a 250 mm depth (9.8 in.) (full depth). For SCC beams (LWC and NWC), the concrete was compacted under its own

weight, while in vibrated-concrete beams (ECCP and ECCS) electrical vibrators were used to apply a mechanical compaction to ensure full compaction of the concrete in the formwork, and then a trowel was used to smooth the surface. For composite beams with ECC layer on either the top or the bottom side, as in B4, B5, B6, and B7, the LWC layer with a depth of 165 mm (6.5 in.) was poured first. After the initial setting, steel dowels were buried in the LWC concrete such that half the dowels protruded from the concrete surface. Moreover, a cubic cavity was dug up in the LWC to create an ECC concrete shear key in the LWC layer. The steel dowels and concrete shear keys were designed to carry the shear flow between the ECC layer and LWC layer, in order to provide a sufficient bond between the two layers. After reaching the final setting, the ECC layer was poured with a depth of 85 mm (3.3 in.) in either tension or compression sides (the beam was poured upside down in the case of the ECC layer in the tension side). It should be noted that the LWC surface was cleaned prior to pouring the ECC layer to remove any loose particles, and a good compaction was applied when pouring the ECC layer to make sure the cubic bore in the LWC layer was properly filled with ECC mixture to form the shear key precisely. For all beams, six cylinders with 100 mm (4 in.) diameter and 200 mm (8 in.) height were poured from each mixture to obtain the compressive and splitting tensile strengths according to ASTM C39 and ASTM C496, respectively. The formwork was demolded 24 hours after each beam was poured, and then the beam was air-cured with the cylinders for 28 days until the testing date.

3.4.4. Four-Point Loading Test Setup and Loading Procedure

The steel reinforcement details, dimensions, and test setup for all tested beams are shown in **Figure 3-3**. All beams had a 250 mm x 250 mm (9.8 in. x 9.8 in.) cross-section, a total

length of 1500 mm (59 in.), an effective load span of 1120 mm (44 in.), and an effective depth of 197.5 mm (7.8 in.). All beams were poured without shear reinforcement; only six 10M stirrups were used to hold the compression reinforcement in place in the compression zone. The six stirrups were distributed such that two stirrups were positioned under loading points, two stirrups at the supports, and the last two stirrups were attached to the ends of the longitudinal reinforcement. The tension and compression reinforcement were two 25M and two 10M, respectively.

All tested beams were subjected to a four-point loading pattern as shown in **Figure 3-3**. The shear span was kept constant at 495 mm (19.5 in.) for all tested beams, achieving a shear span to effective depth ratio of 2.5, which ensures shear failure before flexural failure (Kani et al., 1979; Cho and Kim et al., 2003). A single-point load was applied by an actuator with 500 KN (112.4 kips) capacity to a rigid steel plate, which distributed the load in two points spaced 130 mm (5.1 in.) apart acting on the concrete surface. The load was progressively applied until the first crack was noticed and then constant steps of 45 KN (10 kips) each were applied until failure. Cracks were marked and their widths were measured using a crack microscope (60X magnification with 0.02 mm least count) at each load step. During the test, two linear variable differential transformer (LVDT) was used to measure the midspan vertical deflection (**Figure 3-3**). Also, another two LVDTs were attached to the beam ends (one from each end) to ensure that there was no slippage between the two layers in the composite beams during the test (see **Figure 3-3**). First diagonal crack load, ultimate shear load, deflections, cracking patterns, and failure modes were recorded during the test. The experimental results for all tested beams are shown in **Table 3-2**.

Table 3-2 Results of all tested beams

Beam #	Beam ID	shear capacity (KN)			Deflection corresponding to ultimate load	Ductility coefficient (DC)	Post diagonal shear resistance (PDSR)	Energy absorption (kN.mm)	Failure mode	Cracking at failure stage		Density (kg/m^3)
		1st diagonal crack load	Shear load	Normalized shear						Number	Maximum width (mm)	
B1	LWC	111.2	93.1	13.9	3.9	1.85	0.4	425.6	Shear	9	3	1726.9
B2	ECCP	166.8	179.25	21.4	7.4	3.55	0.53	1684.4	Shear	20	1.95	2069
B3	ECCS	177.9	210.05	22.2	8.5	3.8	0.58	2433	Flexural	23	2	2200
B4	ECCP-C	66.7	133.45	15.9	6.6	5.11	0.75	1186.5	Shear	23	3	1843
B5	ECCS-C	88.9	152.25	16.1	6.2	4.1	0.7	974.3	Shear	18	2.4	1887.8
B6	ECCP-T	120.1	125.9	18.8	6.1	3.05	0.52	910.1	Shear	17	2.5	1843
B7	ECCS-T	124.6	112.3	16.7	5.4	2.74	0.45	766.4	Shear	15	1.4	1887.8
B8	NWC	129.2	122.15	15.2	3.8	2.24	0.47	626.2	shear	8	3	2276

1 mm = 0.039 in.; 1 KN = 0.224 Kips; 1 KN.m = 8.850 Kips.in.

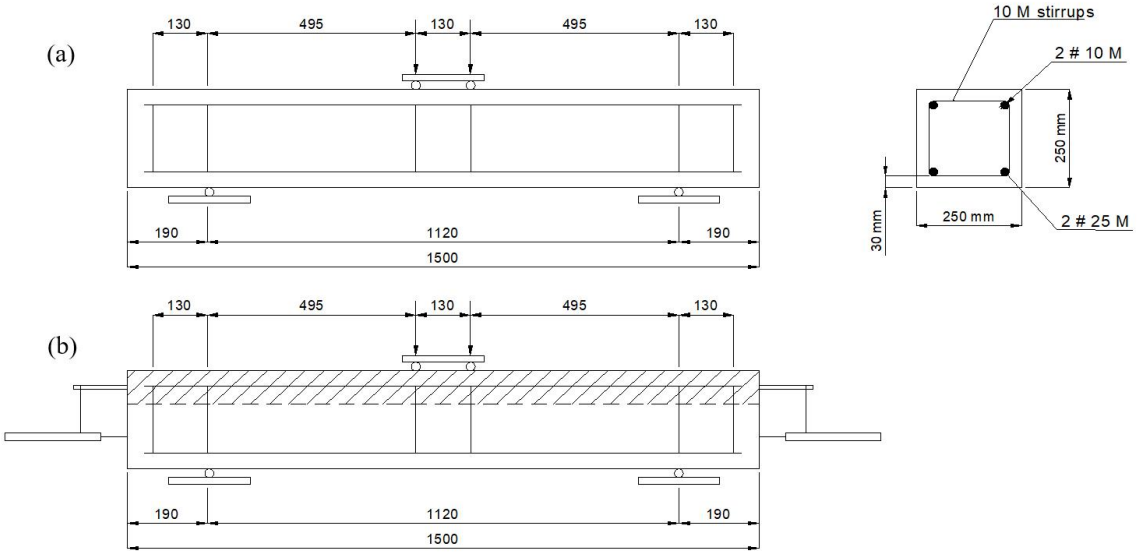

(1 mm = 0.039 in)

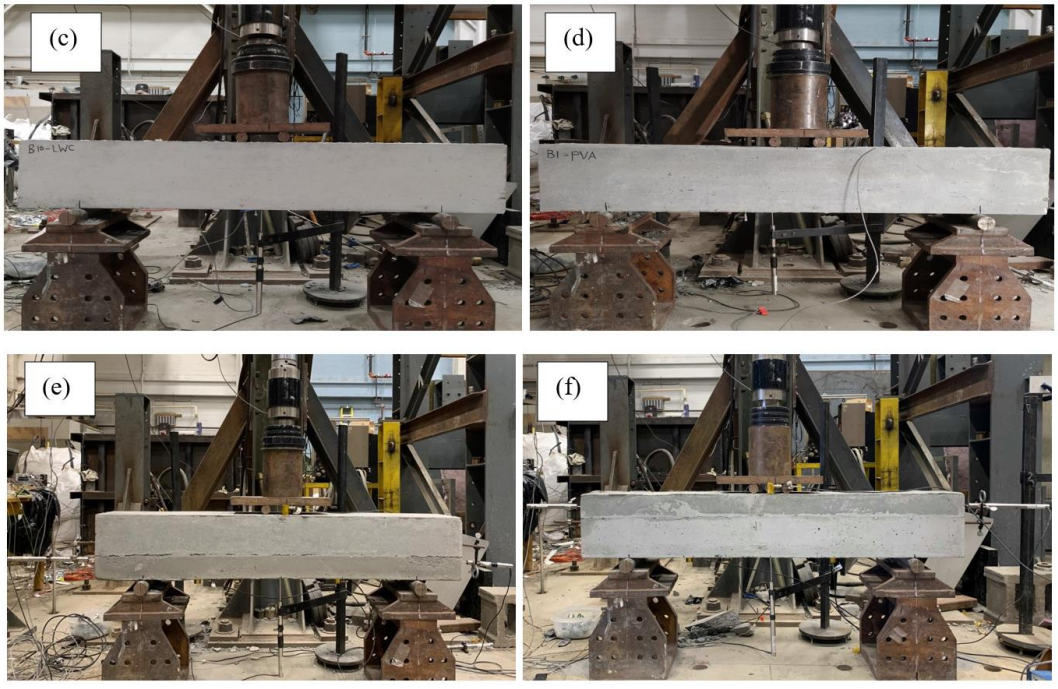

Figure 3-3 Beam dimensions, reinforcement details for (a) LWC/NWC/ ECC; (b) composite beams with ECC layer, Test setup for (c) LWC/NWC; (d) full depth ECC (ECCS, ECCP); (e) composite beams with ECC layer in tension side; (f) composite beams with ECC layer in compression side

3.5. Discussion of Test Results

3.5.1. Failure Mode and Cracking Behavior

The cracking behavior at failure stage, mode of failure, and maximum vertical and diagonal crack widths for all tested beams are shown in **Figure 3-4** and **Table 3-2**. For the reference LWC beam and NWC beam, at the early stage of loading, the first vertical crack was initiated at the midspan between the loading points at tension side of the beam. By increasing the applied load, more vertical cracks started to initiate in the shear span at both sides of the beam (i.e., the area between the support and point load). With further increase in the applied load, diagonal cracks started to initiate in the shear span at the mid-height of the beam, then propagated upward toward the point loads and downward toward the supports. Additional loading resulted in an increase in the number and widths of both vertical and diagonal cracks, followed by a sudden failure of the beam before the tensile reinforcement reached the yield. Such failure of LWC was characterized by the formation of a single major diagonal crack with a width of 3 mm (0.12 in.) and an angle of 30 degrees. The total number of cracks in the LWC beam reached up to nine. The ECCP reference beam showed a similar mode of failure but with a higher number of cracks and smaller crack widths compared to the LWC beam. For example, the number of cracks in the ECCP reference beam reached up to 20 cracks compared to nine cracks in the LWC beam. Also, the maximum diagonal crack width and angle of ECCP reached 1.95 mm (0.08 in.) and 42 degree compared to 3 mm (0.12 in.) and 30 degree in the LWC beam. The smaller crack widths of the ECCP reference beam compared to the LWC beam may be attributed to the effect of PVA fibers in arresting the cracks and limiting their widths. On the other hand,

the higher number of cracks in the ECCP beam compared to the LWC beam may be related to the higher deformation capacity of the ECCP beam (B2 compared to B1). Unlike ECCP and LWC beams, the ECCS reference beam showed a flexure mode of failure rather than shear mode of failure. With further load application the ECCS beam showed a propagation of the vertical flexure cracks until the longitudinal reinforcement reached yield, then the concrete crushed in the compression side. The hooked ends of SFs (compared to PVA fibers) helped to further increase the stitching mechanism of the fiber, which contributed to delaying the initiation and propagation of the diagonal crack and allowed the beam to fail in ductile flexural failure rather than brittle shear failure (Hassan, 2020; Ismail and Hassan, 2021).

For composite beams with ECC layer in the compression side (B4 and B5), it can be observed that shear failure was the dominant mode of failure for such beams. By looking at cracking pattern of the composite beam with ECCP layer in the compression side (B4), it can be seen that a higher number of cracks and larger crack widths were observed in the ECCP-C beam compared to the reference LWC beam (B4 compared to B1). This can be related to the higher compression strain of ECCP layer in the composite beam, which allowed for a higher deformation capacity and, in turn, increased the number of cracks with wider crack widths. Moreover, despite the ECCP-C composite beam and ECCP reference beam having the same concrete type in compression zone, ECCP-C showed a higher number of cracks and larger crack widths compared to the ECCP reference beam. This is due to the lower tensile strength of the LWC layer (placed in the tension side of ECCP-C composite beam) allowing more cracks to initiate and propagate in the tension side of the ECCP-C beam compared to the ECCP reference beam. The results also showed that the

ECCP-C composite beam (B4) exhibited a higher number of cracks and larger crack widths than the ECCS-C composite beam (B5). This can be related to the higher compression strain capacity of ECC with PVA fibers compared to ECC with SFs (Ismail and Hassan, 2021), which allowed ECCP-C to reach higher deformation before failure (associated with higher number of cracks) compared to the ECCS-C composite beam (B5).

Composite beams with ECC layer in the tension side (ECCP-T and ECCS-T) also exhibited shear mode of failure. By examining the cracking pattern of composite beams ECCP-T and ECCS-T (B6 and B7), it can be seen that both beams showed fewer cracks and with narrower maximum diagonal crack width compared to their counterpart composite beams with ECC layer in the compression side (ECCP-C and ECCS-C). This can be related to the lower deformation capacity of ECCP-T and ECCS-T beams compared to ECCP-C and ECCS-C beams. Moreover, the presence of an ECC layer reinforced with fibers in the tension side of the beam (as in ECCP-T and ECCS-T) contributed to arresting the cracks and reducing their widths.

LWC

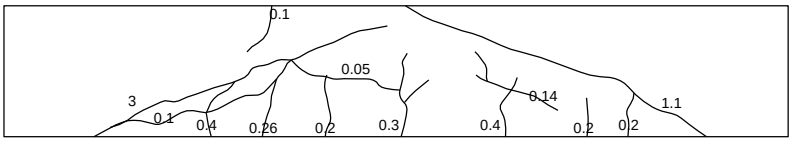

ECCP

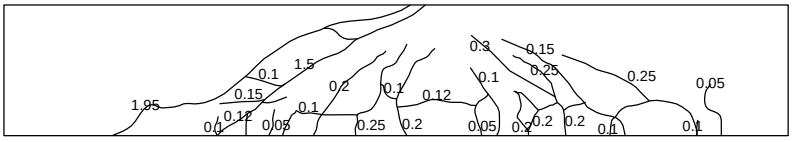

ECCS

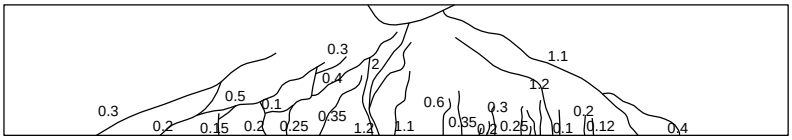

ECCP-C

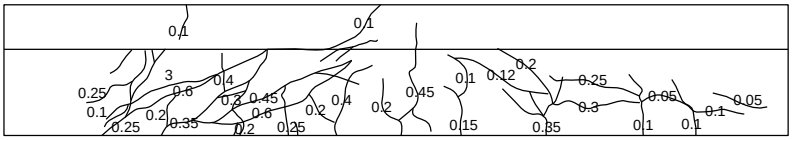

ECCS-C

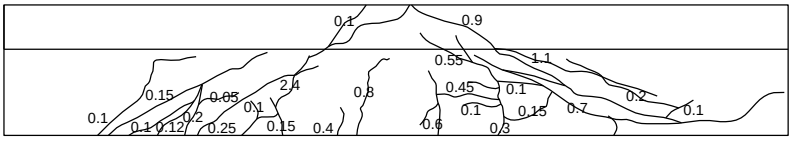

ECCP-T

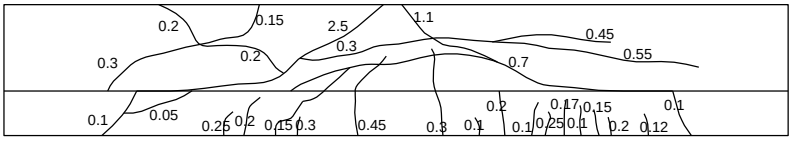

ECCS-T

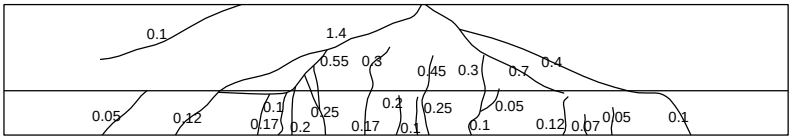

NWC

(1 mm = 0.039 in)

Figure 3-4 Cracking pattern of all tested beams

3.5.2. Load-Deflection Curves

Figure 3-5 shows the load-deflection curves for all tested beams. The load-deflection curve of the LWC beam had a relatively high initial stiffness up to the initiation of first flexural crack. With further increase in the applied load, more cracks started to initiate and propagate vertically until, at a certain level of loading, the first diagonal crack (detected by visual inspection) was initiated. After initiation of the first diagonal crack, the beam stiffness started to decrease, exhibiting a higher rate of deformation and further widening of the diagonal crack width until the ultimate load was reached. After reaching the ultimate load, the load-deflection curve suddenly dropped, indicating a significant brittle shear failure. The maximum deflection and ultimate shear capacity of the LWC beam reached up to 3.9 mm (0.15 in.) and 93.1 KN (20.9 kips), respectively.

For the ECC reference beam reinforced with PVA fibers (ECCP), the load-deflection curve indicated a higher beam stiffness, maximum deflection, and ultimate shear capacity compared to the LWC beam. This can be attributed to the fibers' bridging mechanism, which plays an important role in transferring stress across the cracked section and, in turn, allows the ECCP beam to sustain higher load and experience larger deformations. The results also showed that despite the absence of shear reinforcement in all tested beams, the ECCS reference beam exhibited a flexure mode of failure rather than shear failure (which was exhibited by all other tested beams). Moreover, the highest beam stiffness, maximum deflection, and ultimate load capacity were observed in the ECCS reference beam compared to other beams. This may be related to the same reasons discussed before in the failure mode section. Despite the comparable deflection at ultimate load for NWC and

LWC beams, the NWC beam showed higher initial stiffness and ultimate shear capacity than the LWC beam.

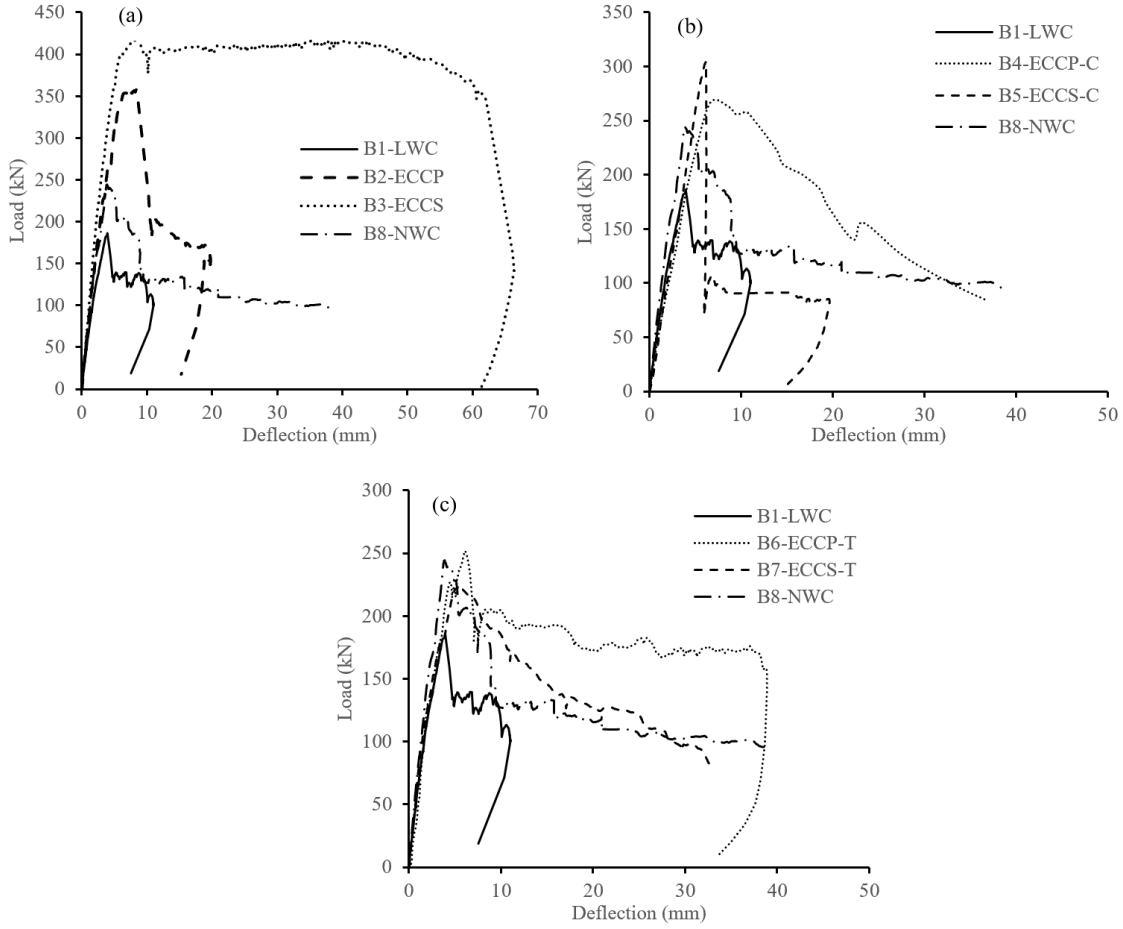

1 mm = 0.039 in.; 1 KN = 0.224 Kips

Figure 3-5 Experimental load-midspan deflection responses: (a) reference beams (LWC, NWC, ECCP, and ECCS); (b) reference beam and composite beams with ECC layer in the compression side (LWC, NWC, ECCP-C, and ECCS-C); (c) reference beam and composite beams with ECC layer in the tension side (LWC, NWC, ECCP-T, and ECCS-T)

By looking at the load-deflection curve of composite beams with ECC layer in the compression side (B4 and B5), it can be observed that ECCP-C and ECCS-C showed a higher deformation capacity (lower stiffness) compared to the LWC control beam. The

results also revealed that developing composite beams with ECC layer in the compression side (B4 and B5) significantly enhanced the ultimate shear capacity of lightweight concrete, with a slight increase in the concrete unit weight. For example, adding ECCP layer in the compression side (B4) increased the normalized shear capacity of the composite beam by 14.4%, compared to the LWC reference, with relatively small increase in the beam weight (1843 kg/m^3 (115 lb/ft^3) for ECCP-C compared to 1727 kg/m^3 (107.81 lb/ft^3) for LWC). Moreover, the normalized shear capacity of B4 (beam with ECCP layer in the compression side) exceeded the normalized shear capacity of NWC by 4.6%, despite the big difference in the two beams' density (2276 kg/m^3 (142.1 lb/ft^3) for NWC compared to 1843 kg/m^3 (115 lb/ft^3) for ECCP-C). **Table 3-2** also shows that despite the higher ultimate shear capacity of ECCS-C compared to ECCP-C, the deformation capacity of ECCP-C appeared to be higher than that of ECCS-C. This may be related to the higher compression strain capacity of the ECCP layer compared to the ECCS layer, as mentioned earlier.

Similar to composite beams with ECC layer in the compression side, ECCP-T and ECCS-T exhibited a higher shear capacity and maximum deflection compared to the LWC beam. For example, ECCP-T and ECCS-T composite beams showed a higher shear capacity of 1.35 and 1.2 times, respectively, higher than that of LWC beam. On the other hand, by comparing the composite beams with ECC layer in the tension side to their counterparts with ECC layer in the compression side (B6 and B7 compared to B4 and B5), it can be observed that composite beams with ECC layer in the compression side showed a better shear performance compared to composite beams with ECC layer in the tension side. This can be confirmed by examining the ultimate shear capacity, deformation capacity, and

cracking behavior of composite beams (B4 and B5 compared to B6 and B7). For example, ECCS-C composite beam with ECCS layer in the compression side exhibited a shear capacity and deformation capacity of1.36 and 1.15 times, respectively, higher than its counterpart composite beam with ECCS layer in tension side (ECCS-T). Using ECC layer with PVA fibers in the tension side of the composite beam showed higher shear capacity compared to using ECC layer with SFs. This may be related to the better dispersion of PVA fibers compared to SFs in ECC mixtures, in which, for the same fiber volume fraction, the PVA fiber with lower fiber density had a higher number of single fibers dispersed in the mixture. This, in turn, helped to maximize the effect of PVA fibers in stitching the cracks, leading to minimized crack widths, which increased the friction along the diagonal crack and hence improved the shear strength.

3.5.3. Post Diagonal Cracking Resistance

The post diagonal cracking shear resistance (PDSR) presents the shear resistance of the beam beyond the initiation of the first diagonal crack and up to failure. The calculated values of the PDSR for all tested beams are presented in **Table 3-2**. The PDSR can be calculated as per **Eq. 3-1** (Hassan et al., 2015) given below.

$$\text{PDSR} = \frac{(\text{ultimate load-first diagonal crack load})}{\text{ultimate load}} \quad (3\text{-}1)$$

From **Table 3-2** it can be observed that the LWC reference beam had a PDSR factor of 40%, which indicates that this beam was able to sustain 40% of the ultimate load beyond the initiation of first diagonal crack. On the other hand, by looking at ECC reference beams (B2 and B3), it can be indicated that these beams showed higher PDSR reaching up to 1.33 (for ECCP) and 1.45 (for ECCS) times that of the LWC beam. The higher PDSR of ECC

beams, despite the absence of coarse aggregate, may be related to the high volume of fibers in ECC mixture. These fibers contributed to restricting the cracks from widening, leading to narrower diagonal cracks and, hence, higher shear resistance after the PDSR. The results also showed that the NWC beam exhibited higher PDSR compared to the LWC beam, which was expected as NWC contains normal-weight coarse aggregate.

For composite beams with ECC layer in the compression side, the results showed that the PDSR factors of ECCP-C and ECCS-C (B4 and B5) appeared to be higher than NWC and ECC reference beams (B8, B2, and B3). The higher PDSR of ECCP-C and ECCS-C compared to their counterpart reference beams ECCP and ECCS may be related to the significantly lower first diagonal crack load of the composite beam with ECC layer in the compression side compared to ECC reference beams (B4 and B5 compared to B2 and B3). Since ECCP-C and ECCS-C had an LWC layer of 165 mm (6.5 in.) in the tension side, with significantly lower tensile strength (see **Table 3-1**), the initiation of first diagonal crack occurred at a lower load compared to ECC reference beams.

By examining the composite beams with ECC layer in the tension side (B6 and B7), it can be seen that ECCP-T and ECCS-T exhibited lower PDSR factors compared to their counterpart ECCP-C and ECCS-C composite beams. This can be attributed to the lower ultimate load capacity and higher first diagonal crack load of composite beams with ECC layer in the tension side (B6 and B7) compared with those with ECC layer in the compression side (B4 and B5). The first diagonal crack load of ECCP-T and ECCS-T was influenced by the ECC layer placed in the tension side (that has a high tensile strength), which in turn contributed to increasing the first diagonal crack load in ECCP-T and ECCS-T compared to ECCP-C and ECCS-C.

3.5.4. Post Cracking Shear Ductility and Energy Absorption

The post cracking shear ductility of tested beams was expressed in terms of ductility coefficient (DC), which can be calculated as the ratio between the deflection corresponding to ultimate load (Du) and the deflection corresponding to first diagonal crack load (Ddc) as shown in **Eq. 3-2** below (Hassan et al., 2010).

$$DC = Du/Ddc \quad (3\text{-}2)$$

The energy absorption capacity of tested beams was calculated by measuring the area under load-deflection curves up to the ultimate load. Consequently, the ability of beams to absorb energy mainly depends on the deformation capacity and ultimate load capacity of tested beams. **Table 3-2** shows the DC and energy absorption capacity of all tested beams. From the table it can be seen that among all tested beams, the lowest post cracking ductility and lowest energy absorption capacity were observed in the LWC beam, which reached up to 1.85 and 425.6 KN.mm (3.77 kips.in), respectively. On the other hand, a significant enhancement in both post cracking shear ductility and energy absorption capacity was noticed in ECC reference beams compared to the LWC beam. For example, ECCP reference beam showed a DC and energy absorption capacity that reached up to 1.92 and 3.96 times, respectively, higher than that of the LWC beam. Meanwhile, the increases in DC and energy absorption capacity reached up to 2.1 and 5.7 times, respectively, when comparing ECCS reference beam to the LWC beam. This can be related to the significant enhancement in the ultimate shear load and maximum deflection of ECC reference beams compared to the LWC beam, which helped to increase the area under load-deflection curve of ECC beams and, in turn, enhanced the energy absorption capacity. It can be observed

that the NWC beam exhibited a higher DC and energy absorption capacity compared to the LWC beam.

The results also showed that composite beams with ECC layer in the compression side (B4 and B5) exhibited further enhancement in the post cracking shear ductility compared to LWC, NWC, and ECC reference beams (B1, B8, B2, and B3). Meanwhile, the energy absorption capacity of B4 and B5 appeared to be less than that of ECC reference beams (B2 and B3) but still higher than the LWC beam and NWC beam (B1 and B8), see **Table 3-2**. Despite ECCP-C and ECCS-C (B4 and B5), which exhibited lower maximum deflection (Du) compared to ECCP and ECCS (B2 and B3), B4 and B5 showed significantly lower deflection corresponding to first diagonal crack load (Ddc) (due to the lower first diagonal crack load as mentioned earlier) compared to B2 and B3. This, in turn, contributed to enhancing the DC of ECCP-C and ECCS-C over ECCP and ECCS. In the meantime, the lower ultimate shear load and deflection corresponding to ultimate load of ECCP-C and ECCS-C led to a lower enhancement in the energy absorption capacity compared to ECCP and ECCS reference beams. It should be noted that adding ECC layer in the compression side of the LWC beam (as in B4 and B5) helped to develop relatively lightweight composite (1843-1888 kg/m^3 (115-117.9 lb/ft^3) density) with enhanced structural performance that exceeded the NWC beam with 2276 kg/m^3 (142 lb/ft^3) density. By looking at composite beams with ECC layer in the tension side, it can be noticed that a lower DC and energy absorption capacity were observed for ECCP-T and ECCS-T beams compared to their counterpart ECCP-C and ECCS-C beams. However, using ECC layer in the tension side of the LWC beam (as in B6 and B7) still showed an enhancement in the DC and energy absorption capacity over the control LWC beam and NWC beam (B1 and

B8). For instance, using ECCP as a tension layer of the LWC beam (B6) increased the DC and energy absorption capacity by 1.64 and 2.14 times, respectively, compared to the control LWC beam (B1), while these increases reached up to 1.36 and 1.45 times, respectively, when compared to the NWC beam (B8).

3.5.5. Theoretical Prediction of Shear Strength According to Design Codes

The theoretical shear capacities of LWC beam (B1), NWC beam (B8), and composite beams with ECC layer in the compression side (B4 and B5) were predicted by four design codes, namely CSA (2004), ACI 318 (2019), AASHTO-LRFD (2014), and EC2 (2005). These codes are most commonly used in designing structural members subjected to shear and flexural stresses. However, the shear stresses calculations of the aforementioned code models do not include the effect of fibers. Therefore, the shear capacities of ECC reference beams (B2 and B3) and composite beams with ECC layer in the tension side (B6 and B7) (which have a fiber contribution in shear stresses calculations) were not predicted using the design code models mentioned above.

The design code equations for the four codes are as follows:

CSA (2004):

$$V_u = \lambda\beta\sqrt{f_c'}bd_v \quad (3\text{-}3)$$

Where λ is a lightweight concrete modification factor (λ =1 for normal-weight concrete, 0.85 for semi-lightweight concrete (1850 kg/m^3 to 2150 kg/m^3 (115.5- 134.2 lb/ft^3)), and 0.75 for lightweight concrete (clause 8.6.5 of CSA A23.3); f_c' is the concrete compressive strength, $\sqrt{f_c'}$ shall not exceed 8 MPa (clause 11.3.4 of CSA A23.3); b is the width of concrete section; d_v is the effective shear depth which is taken as the greater of 0.9d or

0.72 of the member's height; and β is a factor calculated as $\beta = \frac{0.40}{(1+1500\varepsilon_x)}\frac{1300}{(1000+S_{ze})}$; and

$S_{ze} = \frac{35S_z}{15+a_g} \leq 0.85S_z$; and $\varepsilon_x = (M_f/d_v + V_f)/2(E_s A_s)$

Where ε_x is the longitudinal strain at mid-height of the member due to factored loads; E_s is the steel modulus of elasticity; S_z is the crack spacing parameter = d_v; and a_g is the maximum aggregate size in the concrete. For beams with an overall thickness not greater than 250 mm (9.8 in.), the value of β shall be taken as 0.21 (as mentioned in clause 11.3.6.2 of CSA A23.3).

ACI 318 (2019)

$$V_u = \left[0.158\lambda\sqrt{f_c'} + 17\rho_w \frac{d}{a}\right] bd \leq 0.29\sqrt{f_c'}bd \quad (3\text{-}4)$$

Where λ is a lightweight concrete reduction factor, taken as 0.85 for sand-lightweight concrete, 0.75 for all-lightweight concrete, and 1.0 for normal-weight concrete (section 8.6.1 of ACI 318-14); ρ_w is the longitudinal reinforcement ratio (A_s/bd); A_s is the area of longitudinal reinforcement; *a* is the shear span in mm; *d* is the effective depth of the beam in mm; and *b* is the width of the concrete section.

AASHTO-LRFD (2014)

$$V_u = 0.083\beta\sqrt{f_c'}b_v d_v \quad (3\text{-}5)$$

Where β is a factor indicating the ability of diagonally cracked concrete to transmit tension as specified in article 5.8.3.4; b_v is the effective web width; and d_v is the effective shear depth.

For lightweight concrete, the term $\sqrt{f_c'}$ shall be replaced by $0.85\sqrt{f_c'}$ for sand-lightweight concrete and $0.75\sqrt{f_c'}$ for all-lightweight concrete (article 5.8.2.2 of AASHTO-LRFD).

EC2 (2005)

$$V_{Rd,C} = \left[C_{Rd,c}\lambda K(100\rho_s f_c')^{1/3}\right]b_w d \geq k_2 K^{3/2}\sqrt{f_c'}\,b_w d \quad (3\text{-}6)$$

Where $C_{Rd,c}$= 0.18 for normal-weight concrete and 0.15 for lightweight concrete; $\lambda = 0.4 + 0.6\rho_c/2200$, where ρ_c is the dry density for the relevant class in kg/m^3; K is a factor that takes into account the size effect ($K = 1 + \sqrt{200/d} \leq 2.0$); ρ_s is the longitudinal reinforcement ratio; and k_2 is a factor that accounts for the minimum shear stress (k_2 = 0.03 for lightweight concrete and 0.035 for normal-weight concrete).

Figure 3-6 shows the ratio between V_{exp}/V_{theo} for LWC beam, NWC beam, and composite beams with ECC layer in the compression side (B1, B8, B4, and B5) based on all design code models (CSA, ACI, AASHTO-LRFD, and EC2).

From the figure it can be observed that all design codes were conservative in predicting the ultimate shear capacity of LWC, NWC, ECCP-C, and ECCS-C beams, showing a high margin of safety against the experimental shear capacity. The most conservative prediction of the ultimate shear capacity was obtained by ACI code, while EC2 showed the least conservative prediction. Unlike the other code predictions, EC2 takes into account the effect of the beam's depth (size effect) on the shear capacity of the beam. However, the depth of all tested beams in this investigation was relatively small, which unlikely to have contribution toward the shear resistance of the beam (Hassan et al., 2008). In the EC2 equation, the calculation of the value of K in all beams was higher than 2, but because of the equation limitation (K≤2), it was taken as 2. Perhaps a lower limitation of the K value should have been considered in the equation in order to account for small beam depths.

Therefore, the K value of the EC2 equation might have contributed to increasing the predicted value of the shear, moving toward a less conservative prediction. The results also revealed that the values of V_{exp}/V_{theo} of LWC tested in this investigation were relatively high compared to NWC. In addition, these values also appeared to be higher than other V_{exp}/V_{theo} values reported in the literature for different LWC mixtures (Alengaram et al., 2011; Hassan et al., 2015). This can be attributed to the fact that in this study ESCA was used in LWC mixture. And this aggregate has been reported to have relatively higher strength compared to most other types of lightweight aggregate available on the market Hassan et al., 2015; Mo et al., 2016). This, in turn, helped to enhance the experimental shear strength compared to the predicted one, providing higher margin of safety.

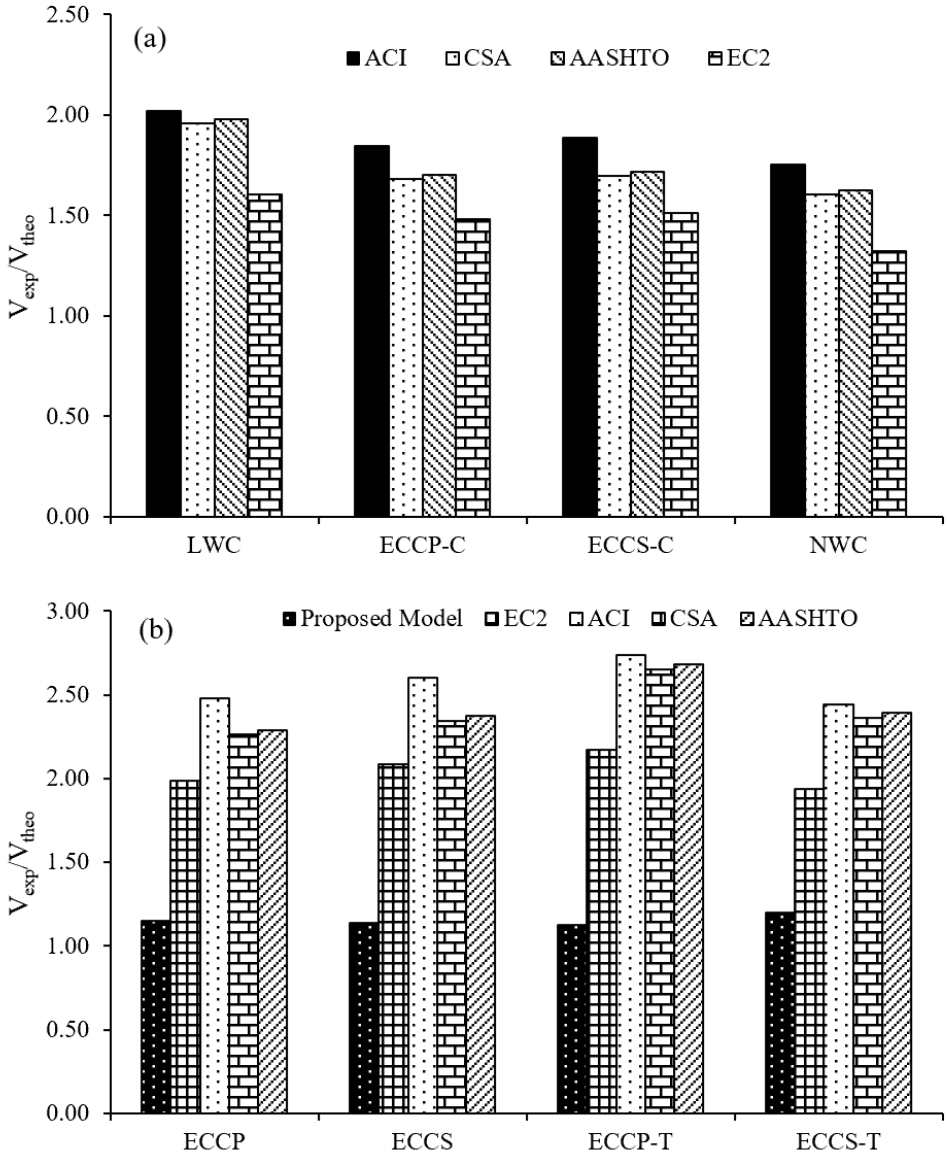

Figure 3-6 Experimental-to-theoretical ultimate shear ratios for all tested beams: (a) theoretical prediction of ultimate shear capacity for LWC, NWC, and composite beams with ECC layer in the compression side; (b) theoretical prediction of ultimate shear capacity for ECC reference beams and composite beams with ECC layer in the tension side

In this study, the proposed model used to predict the shear capacity of ECC reference beams and composite beams with ECC layer in the tension side (B2, B3, B6, and B7) was based

on the EC2 code model but with the addition of fiber contribution V_f to the code model. The proposed model equation can be expressed as follows:

$$Vu = V_{Rd,C}\ (EC2) + V_f \quad (3\text{-}7)$$

$$V_f = 0.41\tau\ F\ b\ h_o \quad (3\text{-}8)$$

Where V_f is the shear resistance provided by fibers proposed by Narayanan and Darwish (1987); τ is fiber matrix interfacial bond stress, taken as 4.15 MPa (0.6 ksi) for steel fibers (Swamy and Bahia, 1985) and 2.93 MPa (0.42 ksi) for PVA fibers (Yang and Li, 2010); F is a fiber factor = $(l_f/d_f)\ \nu_f\ D_f$; l_f is the fiber length; d_f is the fiber diameter; ν_f is the fiber volume fraction; D_f is a bond factor: 0.5 for smooth fiber, 0.75 for crimped and hooked-ends fiber, 1 for indented fiber; b is the beam cross-section width; h_o is the thickness of the tension side of the beam that has fibers (equal to thickness of ECC layer in composite beams B6 and B7), see **Figure 3-7**. It should be noted that in ECC reference beams the height h_o was calculated as (d-c), in which c is the compression zone height calculated using the measured strain recorded by strain gauges attached to the top of concrete (compression strain) and longitudinal tension reinforcement (tension strain).

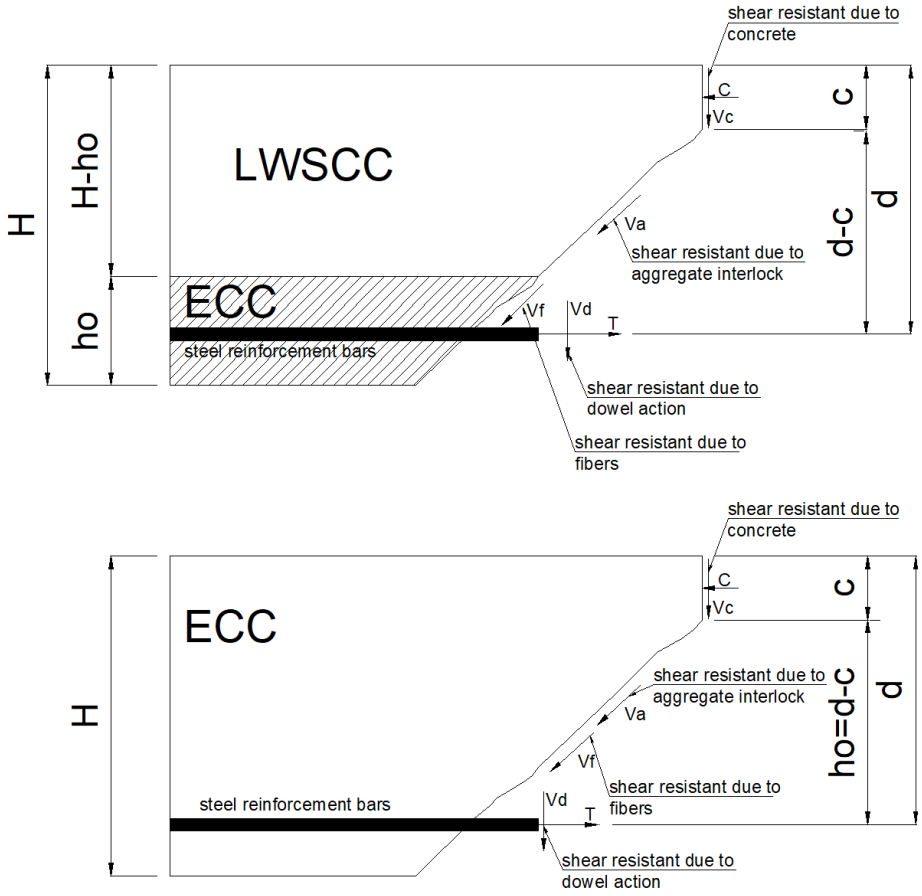

Figure 3-7 Shear force distribution mechanism for (a) composite beams with ECC layer in the tension side; (b) ECC reference beams

Figure 3-6 shows the V_{exp}/V_{theo} values of ECC reference beams (B2 and B3) and composite beams with ECC layer in the tension side (B6 and B7) for the proposed model and all design codes for comparison. From the figure, it can be observed that all design codes were conservative in estimating the ultimate shear capacity, showing high values of V_{exp}/V_{theo}. On the other hand, the proposed model more accurately predicted the ultimate shear capacity for ECCP, ECCS, ECCP-T, and ECCS-T beams compared to all design code models. For instance, the proposed model exhibited V_{exp}/V_{theo} values of 1.13 and 1.2 for ECCP-T and ECCS-T beams, respectively, while these values reached up to 2.17 and 1.94,

respectively, when EC2 code model was used. This can be related to the fact that the proposed model accounts for the effect of fibers on enhancing the ultimate shear capacity of tested beams.

3.6. Conclusions

This study presented the shear behavior of hybrid composite reinforced concrete beams comprised of two layers: LWC layer and ECC layer. The ECC layer was placed at different cross-sectional positions (in the tension side and compression side) to improve the shear capacity while maintaining low average unit weight of the composite beam. The effect of using different types of fibers in the ECC layer (PVA fiber and SFs) was also investigated. The study included several properties to evaluate the shear performance of the composite beams: deformability, failure mode, cracking behavior, first diagonal cracking load, ultimate shear capacity, post diagonal shear resistance, post diagonal cracking shear ductility, and energy absorption. From the experimental investigation conducted in this study, the following conclusions can be drawn:

1. Using ECC layer (either ECCP or ECCS) in the compression side of lightweight concrete beam compensated for the reduced shear capacity of the beam and enhanced the normalized shear strength to reach a value exceeded the normalized shear strength of the NWC beam. In the meantime, the increase in the concrete unit weight of such composite did not exceed 9% of the density of the LWC beam.
2. Using ECC layer in the compression side of LWC (as in ECCP-C and ECCS-C) showed a higher number of cracks with larger crack widths compared to LWC, NWC, and ECC reference beams. On the other hand, placing ECC layer in the

tension side of LWC (as in ECCP-T and ECCS-T) exhibited a reduced number of cracks and widths compared to ECC reference beams and their counterpart beams with ECC layer in the compression side (ECCP-C and ECCS-C).

3. For the composite beam with ECC layer in the compression side, despite the increase in the shear capacity when SFs were used compared to PVA fibers (14% increase), the enhancement in the deformation capacity of the beam was higher when PVA fibers were used compared to SFs.
4. Using ECC layer in the compression side of the LWC beam helped to develop relatively lightweight composite (1843-1888 kg/m^3 (115-117.9 lb/ft^3) density) with enhanced structural performance in terms of post cracking shear ductility, post diagonal shear resistance, ultimate shear capacity, and energy absorption, which exceeded the performance of NWC beam with 2276 kg/m^3 (142 lb/ft3) density.
5. Composite beams with ECC layer in the tension side appeared to have lower post diagonal cracking shear resistance, post cracking shear ductility, ultimate shear capacity, and energy absorption compared to composite beams with ECC layer in the compression side, but still higher than LWC and NWC beams.
6. All code model predictions were conservative in estimating the ultimate shear capacity for NWC beam and composite beams with ECC layer in the compression side, and they were more conservative with the LWC beam. Meanwhile, the proposed model (taking the fibers contribution into account in EC2 model) allowed for a closer prediction of the ultimate shear capacity compared to all code models.

3.7. References

AASHTO, “LRFD Bridge Design Specifications and Commentary, seventh edition,” American Association of State Highway and Transportation Officials, Washington, DC, 2014, 1264.

AbdelAleem, B.H.; Ismail, M.K.; and Hassan, A.A., “Properties of self-consolidating rubberised concrete reinforced with synthetic fibres,” Magazine of concrete research, V. 69, No. 10, 2017, pp. 526-540.

Abouhussien, A.A.; Hassan, A.A.; and Hussein, A.A., “Effect of expanded slate aggregate on fresh properties and shear behaviour of lightweight SCC beams,” Magazine of concrete research, V. 67, No. 9, 2015, pp. 433-442.

Abouhussien, A.A.; Hassan, A.A.; and Ismail, M.K., “Properties of semi-lightweight self-consolidating concrete containing lightweight slag aggregate,” Construction and building materials, V. 75, 2015, pp. 63-73.

ACI Committee, “Building code requirements for structural concrete (ACI 318-08) and commentary,” American Concrete Institute, 2019.

Alengaram, U.J.; Jumaat, M.Z.; Mahmud, H.; and Fayyadh, M.M., “Shear behaviour of reinforced palm kernel shell concrete beams,” Construction and building materials, V. 25, No. 6, 2011, pp. 2918-2927.

ASTM C39/C39M “Standard Test Method for Compressive Strength of Cylindrical Concrete Specimens,” ASTM International, West Conshohocken, PA, USA, 2021.

ASTM C150/C150M, “Standard Specification for Portland Cement,” ASTM International, West Conshohocken, PA, USA, 2020.

ASTM C494/C494M, “Standard Specification for Chemical Admixtures for Concrete,” ASTM International, West Conshohocken, PA, USA, 2019.

ASTM C496, “Standard Test Method for Splitting Tensile Strength of Cylindrical Concrete Specimens,” ASTM International, West Conshohocken, PA, USA, 2017.

ASTM C618, “Standard Specification for Coal Fly Ash and Raw or Calcined Natural Pozzolan for Use in Concrete,” ASTM International, West Conshohocken, PA, USA, 2019.

Balaguru, P.; and Dipsia, M.G., “Properties of fiber reinforced high-strength semi-lightweight concrete,” Materials Journal, V. 90, No. 5, 1993, pp. 399-405.

Canadian Standards Association Committee A23.3, “Design of concrete structures,” CSA A23.3-04. Rexdale, Ontario: Canadian Standards Association; 2004.

Chai, Y.H., “Service performance of long-span lightweight aggregate concrete box-girder bridges,” Journal of Performance of Constructed Facilities, V. 30, No. 1, 2016, pp. 04014196.

Cho, S.; and Kim, Y., “Effects of steel fibers on short beams loaded in shear,” ACI Structural Journal, V. 100, No. 6, 2003, pp.740–765.

Dymond, B.Z.; Roberts-Wollmann, C.L.; and Cousins, T.E., "Shear strength of a lightweight self-consolidating concrete bridge girder," Journal of Bridge Engineering, V.15, No. 5, 2010, pp. 615-618.

EN 1992-1-1. Eurocode 2, "Design of Concrete Structures – Part 1–1: General Rules and Rules for Buildings," Thomas Telford, London, UK, 2005.

Gao, J.; Sun, W.; and Morino, K., "Mechanical properties of steel fiber-reinforced, high-strength, lightweight concrete," cement and concrete composites, V. 19, No. 4, 1997, pp. 307-313.

Hassan, A.A., "Structural Performance of Self-Consolidating Engineered Cementitious Composite Beams Containing Crumb and Powder Rubber," ACI Material Journal, V. 117, No. 2, 2020.

Hassan, A.A.; Hossain, K.M.A.; and Lachemi, M., "Behavior of full-scale self-consolidating concrete beams in shear," cement and concrete composites, V. 30, No. 7, 2008, pp. 588-596.

Hassan, A.A.; Hossain, K.M.A.; and Lachemi, M., "Strength, cracking and deflection performance of large-scale self-consolidating concrete beams subjected to shear failure," Engineering structures, V. 32, No. 5, 2010, pp. 1262-1271.

Hassan, A.A.; Ismail, M.K.; and Mayo, J., "Shear behavior of SCC beams with different coarse-to-fine aggregate ratios and coarse aggregate types," Journal of materials in civil engineering, V. 27, No. 11, 2015, pp. 04015022.

Hossain, K.M.A.; Lachemi, M.; Sammour, M.; and Sonebi, M., "Strength and fracture energy characteristics of self-consolidating concrete incorporating polyvinyl alcohol, steel and hybrid fibres," Construction and building materials, V. 45, 2013, pp. 20-29.

Ismail, M.K.; Abdelaleem, B.H.; and Hassan, A.A., "Effect of fiber type on the behavior of cementitious composite beam-column joints under reversed cyclic loading," Construction and building materials, V.186, 2018, pp. 969-977.

Ismail, M.K.; and Hassan, A.A., "Fresh and Mechanical Properties of Semi-Lightweight Self-Consolidating Concrete Containing Lightweight Slag Aggregate," CSCE conference, 2014.

Ismail, M.K.; and Hassan, A.A. "Influence of fiber type on shear behavior of engineered cementitious composite," Magazine of concrete research, 2021, pp. 1-27.

Kang, S.B.; Tan, K.H.; Zhou, X.H.; and Yang, B., "Experimental investigation on shear strength of engineered cementitious composites," Engineering structures, V. 143, 2017, pp. 141-151.

Kani, G.N.J.; Huggins, M.W.; and Wittkopp, R.R., "Shear in reinforced concrete," Toronto: University of Toronto Press, 1979, pp. 1–225.

Kayali, O., "Fly ash lightweight aggregates in high performance concrete," Construction and building materials, V. 22, No. 12, 2008, pp. 2393-2399.

Kayali, O.; Haque, M.N.; and Zhu, B., "Some characteristics of high strength fiber reinforced lightweight aggregate concrete," Cement and concrete composites, V. 25, No. 2, 2003, pp. 207-213.

Kılıç, A.; Atiş, C. D.; Yaşar, E.; and Özcan F., "High-strength lightweight concrete made with scoria aggregate containing mineral admixtures," cement and concrete research, V. 33, No. 10, 2003, pp.1595-1599.

Kong, H.J.; Bike, S.G.; and Li, V.C., "Development of a self-consolidating engineered cementitious composite employing electrosteric dispersion/stabilization," Cement and Concrete Composites, V. 25, No. 3, 2003, pp. 301-309.

Lotfy, A.; Hossain, K.M.; and Lachemi, M., "Durability properties of lightweight self-consolidating concrete developed with three types of aggregates," Construction and building materials, V. 106, 2016, pp. 43-54.

Meng, D.; Lee, C.; and Zhang, Y., "Flexural fatigue properties of a polyvinyl alcohol-engineered cementitious composite," Magazine of concrete research, V. 71, No. 21, 2019, pp.1130-1141.

Mo, K.H.; Visintin, P.; Alengaram, U.J.; and Jumaat, M.Z., "Prediction of the structural behaviour of oil palm shell lightweight concrete beams," Construction and building materials, V. 102, 2016, pp. 722-732.

Narayanan, R.; and Darwish, I.Y.S., "Use of steel fibers as shear reinforcement," Structural Journal, V. 84, No. 3, 1987, pp. 216-227.

Ranade, R.; Zhang, J.; Lynch, J.P.; and Li, V.C., "Influence of micro-cracking on the composite resistivity of engineered cementitious composites," cement and concrete composites, V. 58, 2014, pp. 1-12.

Şahmaran, M.; and Li, V.C., "Engineered cementitious composites: Can composites be accepted as crack-free concrete?," Transportation Research Record, V. 2164, No.1, 2010, pp. 1-8.

Şahmaran, M.; Lachemi, M.; and Li, V.C., "Assessing the durability of engineered cementitious composites under freezing and thawing cycles," Journal of ASTM International, V. 6, No. 7, 2009, pp. 1-13.

Şahmaran, M.; and Li, V.C., "De-icing salt scaling resistance of mechanically loaded engineered cementitious composites," cement and concrete research, V. 37, No. 7, 2007, pp. 1035-1046.

Said, S.H.; and Razak, H.A., "The effect of synthetic polyethylene fiber on the strain hardening behavior of engineered cementitious composite (ECC)," Materials & Design, V. 86, 2015, pp. 447-457.

Sari, D.; and Pasamehmetoglu, A. G., "The effects of gradation and admixture on the pumice lightweight aggregate concrete," cement and concrete composites, V. 35, No. 5, 2005, pp. 936-942.

Shafigh, P.; Mahmud, H.; and Jumaat, M.Z., "Effect of steel fiber on the mechanical properties of oil palm shell lightweight concrete," Materials and design, V. 32, No. 7, 2011, pp. 3926-3932.

Suthiwarapirak, P.; Matsumoto, T.; and Kanda, T., "Multiple cracking and fiber bridging characteristics of engineered cementitious composites under fatigue flexure," Journal of Materials in Civil Engineering, V. 16, No. 5, 2004, pp. 433-443.

Swamy, R.N.; and Bahia, H.M., "The Effectiveness of Steel Fibers as Shear Reinforcement," In Proceedings of the Korea Concrete Institute Conference, V. 7, No. 3, 1985, pp. 35-40.

Szydlowki, R.; and Mieszcak, M., "Study of application of lightweight aggregate concrete to construct post-tensioned long-span slabs," Procedia Engineering, V. 172, 2017, pp. 1077-1085.

Taylor, H.P., "The fundamental behavior of reinforced concrete beams in bending and shear," Special Publication, V. 42, 1974, pp. 43-78.

Yang, E.H.; and Li, V.C., "Strain-hardening fiber cement optimization and component tailoring by means of a micromechanical model," Construction and building materials, V. 24, No. 2, 2010, pp. 130-139.

4. Behavior of novel hybrid lightweight concrete composites under drop-weight impact loading

4.1. Abstract

This investigation evaluated the feasibility of combining lightweight concrete (LWC) and engineered cementitious composite (ECC) in specific configurations to develop a lightweight hybrid composite with improved impact resistance. In this study, three mixtures were investigated: one LWC mixture fully produced with lightweight fine and coarse expanded slate aggregates; one ECC mixture developed with polyvinyl alcohol fibers (ECCP); and one ECC mixture developed with steel fibers (ECCS). For testing, cylindrical specimens and small-scale beams were constructed in a two-layer composite system having different configurations (i.e., different arrangements and depths). Additional specimens fully cast with LWC, ECCP, and ECCS were tested for comparison. The interface bond strength between LWC and either ECCP or ECCS was also evaluated. The performance of the developed composites was assessed under static flexural loading and drop-weight impact. The results showed that both ECCP and ECCS could achieve a good bonding with LWC substrate, i.e., above 90% of that measured for the monolithic LWC specimens, even with no surface preparations (i.e., roughening or using shear keys). Combining LWC with either ECCP or ECCS generated novel lightweight hybrid composites that can offer superior performance for different structural lightweight members exposed to high impact loading. For given arrangement and depth, the LWC-ECCS composite exhibited higher mechanical and impact performance whereas the LWC-

ECCP was distinguished by achieving an excellent impact resistance at a lighter self-weight.

4.2. Introduction

Lightweight concrete (LWC) is a special class of building materials that has received great attention from the construction industry. LWC surpassed other conventional concretes by its capability to construct structural elements with significantly lower self-weight. This capability reduces the great portion of deadload of structures and helps to reach more economically designed elements (i.e., less concrete volume and less reinforcement). The LWC could also be developed with high strengths, thus extending its suitability for multiple applications, including high-rise buildings, precast units, bridges, offshore structures, etc. (Shi and Yang, 2005; Yao and Gerwick et al., 2006; Hubertova and Hela, 2007; Papanicolaou and Kaffetzakis, 2011; Sadek et al., 2020a). In offshore structures, for example, achieving a low self-weight is a design requirement, but it is also necessary to maintain high endurance against the dynamic and impulsive loads that are expected from dropped objects and collisions due to waves, ships, and icebergs (Paik, 2017; Clauss, 2002; Sadek et al., 2020b). Such impulsive loads typically have a localized pattern that can induce significant damage to the body of structures, which in turn negatively affects the stability and service life of structures (Lok and Pei, 1996; Ismail and Hassan, 2017). The damage due to impulsive loads can be serious in concrete structures due to the high brittleness and low tensile strength of concrete. As such, the damage can be more significant in LWC structures as the porous structure and weakness of lightweight aggregates further worsen the brittleness and strength of LWC. Therefore, there is a need for improving the impact

resistance of LWC or finding a new alternative to construct high-performance lightweight structures against impulsive events. For this purpose, hybrid composites can be considered as a candidate solution, where two materials can be combined (e.g., LWC and another high-performance concrete) with relatively low density to achieve the desirable performance.

Engineered cementitious composite (ECC), invented by Victor Li based on micromechanics theory, is one of the high-performance cementitious materials (Li, 1993). ECC is typically developed with a high volume of cementitious materials (Portland cement + other supplementary cementitious materials), silica sand, and a moderate volume of fibers. Unlike conventional types of concrete, the ECC is known to have excellent strength and strain capabilities under both tensile and compressive loading while maintaining a relatively low density (Ismail et al., 2018; Ismail et al., 2019). Previous studies reported that under uniaxial tension, ECC could endure a stress up to 6 MPa and experience strain up to 600 times as much as conventional concretes can endure. The high tensile strain of ECC is typically accompanied by pseudo-strain-hardening behavior (Li et al., 2002; Kong et al., 2003) and the formation of closely spaced multiple micro-cracks with widths below 100 μm (Şahmaran and Li, 2010). Incorporating rich content of cementitious materials in ECC also helps to form a strong matrix that can carry high compressive stress of more than 70 MPa, which is associated with strain in the range of 0.4% to 0.65% (Ismail et al., 2019a; Said and Razak, 2015). Other studies evaluated the impact resistance of small-scale specimens that were fully cast with different ECC mixtures (i.e., ECCs developed with various compositions and different types of fibers) (Ismail et al, 2019b; Yildirim et al., 2019). The results obtained from these studies indicated that ECC showed high impact energy absorption capacity, which offers a superior construction material for multiple

structural applications where drastic impact loads are imposed. The high cracking resistance, ductility, and strengths of ECC also allow it to absorb high energy under fatigue loading (Meng et al., 2018; Suthiwarapirak et al., 2004). The ECC was also employed, on a structural level, to improve the ultimate capacity, ductility, and energy absorption capacity of beam-column joints (Ismail et al., 2018; Yuan et al., 2013; Said and Razak, 2016). In addition, the large-scale testing of reinforced concrete beams proved that the high shear strength of ECC could even replace the minimum shear stirrups (Ismail and Hassan, 2021).

The aforementioned properties of LWC and ECC make them strong candidates for developing new hybrid lightweight composite with improved impact resistance. Therefore, unlike any other studies, this study was conducted to investigate the performance of LWC-ECC composite under drop-weight loading. For this purpose, two-layer hybrid composites consisting of LWC and ECC, in the form of cylindrical specimens and small-scale beams, were cast with different configurations (i.e., different arrangements and layer depths). The interfacial bonding strength and static flexural strength of all developed composites were also examined. The ECC in this study was developed with two different types of fibers (PVA and SFs). The results of hybrid composites were compared to those that were fully cast with LWC.

4.3. Research Significance

Despite the advantages of using LWC in structural applications, LWC has low impact resistance, which limits its applicability for multiple applications. This highlights the need to improve the impact resistance of LWC or develop new high impact-resistant lightweight

composites that can be employed to construct high-performance lightweight structures against impact loads. Combining LWC with another high-performance cement-based material such as ECC can be an effective technique to merge the benefits of lightweight concrete, in addition to the high impact resistance, ductility, and energy absorption capacity of ECC, without much increase in the composite density. This composite, in turn, offers promising potentials for different structural applications that require both low self-weight and high impact resistance. Despite the superior performance expected by such composites, no sufficient information is available in the literature at both material and structural levels. Contributing to filling this gap of knowledge, the authors in this study carried out an experimental program to evaluate the impact resistance of LWC-ECC composites. The static flexural strength and interface bonding strength of all developed composites were also presented. The authors believe that the results obtained from this investigation are unique and can increase the understanding of the structural benefits that can be achieved from using hybrid LWC-ECC composite in certain applications such as protective and impact-resistant structures.

4.4. Experimental Program

4.4.1. Material Properties and Concrete Mixtures

The mixture proportions of LWC, ECCP, and ECCS are shown in **Table 4-1**. The LWC mixture was developed with fine and coarse expanded slate aggregates, which had a specific gravity of 1.53 and 1.8, respectively, and a water absorption of 7.1% and 10%, respectively. **Figure 4-1** shows the gradation curve for fine and coarse expanded slate aggregates used in this study. The mixture was produced with high self-compactability

properties satisfying the requirements of the European Guidelines for Self-compacting Concrete (2005). Therefore, the development process of the LWC mixture began with several trials until sufficient stability, segregation resistance, and strength were achieved. Based on the conducted trials, the most successful mixture was selected for use in this study. The optimized mixture was made from a ternary binder material system consisting of 40% type GU Portland cement, 40% fly ash (FA), and 20% metakaolin (MK), conforming to ASTM C150 type I (2020), ASTM C618 Type F (2019), and ASTM C618 class N (2019), respectively. The water-to-binder ratio was 0.4. It should be noted that prior to mixing, all aggregates were in a saturated surface dry condition. With such composition, a 28-day compressive strength of 43.8 MPa was achieved.

The ECCP and ECCS mixtures were also developed with a ternary binder material system consisting of 40% type GU Portland cement, 35% FA, and 20% MK, similar to ASTM C150 Type I (2020), ASTM C618 Type F (2019), and ASTM C618 class N (2019), respectively. In developing these mixtures, a silica sand gradation, similar to that presented in **Figure 4-1**, was used as a fine aggregate whereas no coarse aggregate was incorporated. The ECCP was reinforced with 8 mm polyvinyl alcohol (PVA) fibers having a specific gravity of 1.3, a tensile strength of 1600 MPa, and a modulus of elasticity of 40 GPa. Meanwhile, the ECCS was reinforced with 35 mm hooked-end steel fibers (SFs) having a specific gravity of 7.85, a tensile strength of 1150 MPa, and a modulus of elasticity of 210 GPa. Both PVA fibers and SFs used in this study are shown in **Figure 4-2**. It should be noted that with flexible PVA fibers, it was possible to develop ECCP with self-compactability properties. On the other hand, the stiff SFs caused a high amount of friction and blockage, which in turn did not allow ECCS to successfully meet the self-

compactability criterion, yet the ECCS was developed with a high slump of 200 mm (as per ASTM C143 (2020)). The fresh properties of all developed mixtures are presented in **Table 4-1**.

The workability of all mixtures was adjusted using a polycarboxylate-based high-range water-reducer admixture (HRWRA) similar to ASTM C494 Type F (2019).

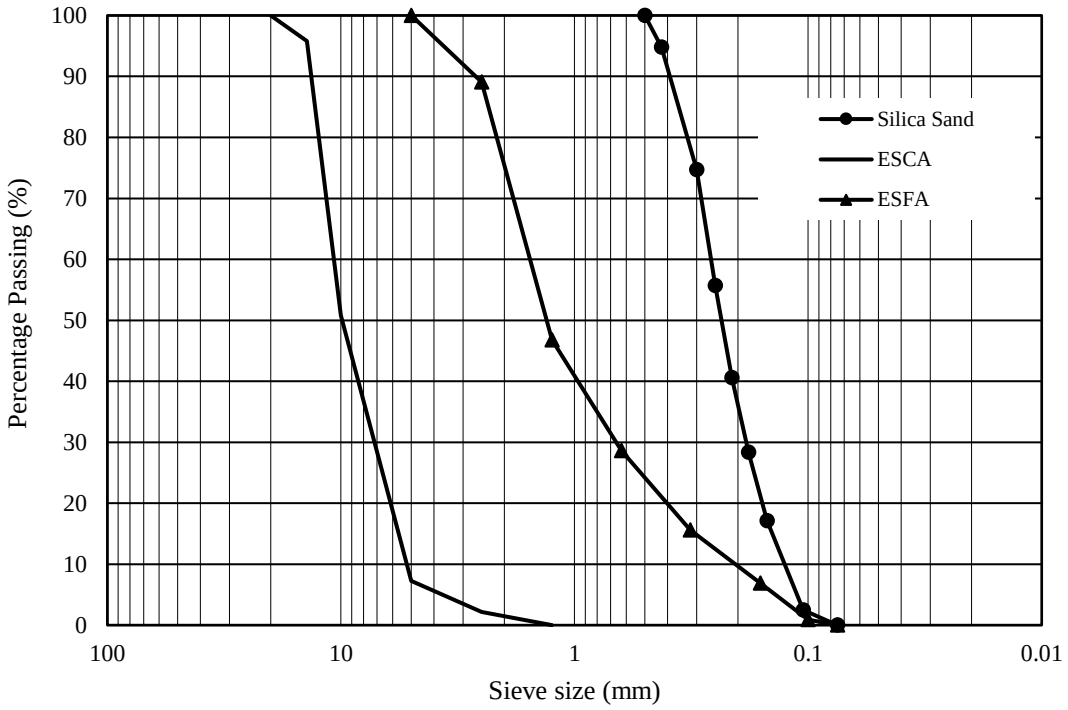

Figure 4-1 Gradation curves of the silica sand and lightweight aggregates used

Table 4-1 Mixtures used in this study

Compositions	LWC	ECCP	ECCS
Cement (kg/m^3)	220	576	576
FA (kg/m^3)	220	437.7	437.7
MK (kg/m^3)	110	253.4	253.4
ESCA (kg/m^3)	439.7	-	-
ESFA (kg/m^3)	517.3	-	-
SS (kg/m^3)	-	456.2	456.2
Water (kg/m^3)	220	342.1	342.1
Fibers (kg/m^3)	-	26	157
Fresh properties			
Slump flow (mm)	700	800	200
V-funnel time (sec)	11.51	9.88	-
L-box	0.82	0.94	-
Mechanical properties			
f'c (Mpa)	43.8	73.3	85.5
STS (MPa)	2.41	8.2	10.1

Note: FA = Fly Ash; MK = Metakaolin; ESCA = Expanded Slate Coarse Aggregate; ESFA = Expanded Slate Fine Aggregate; SS = Silica Sand.

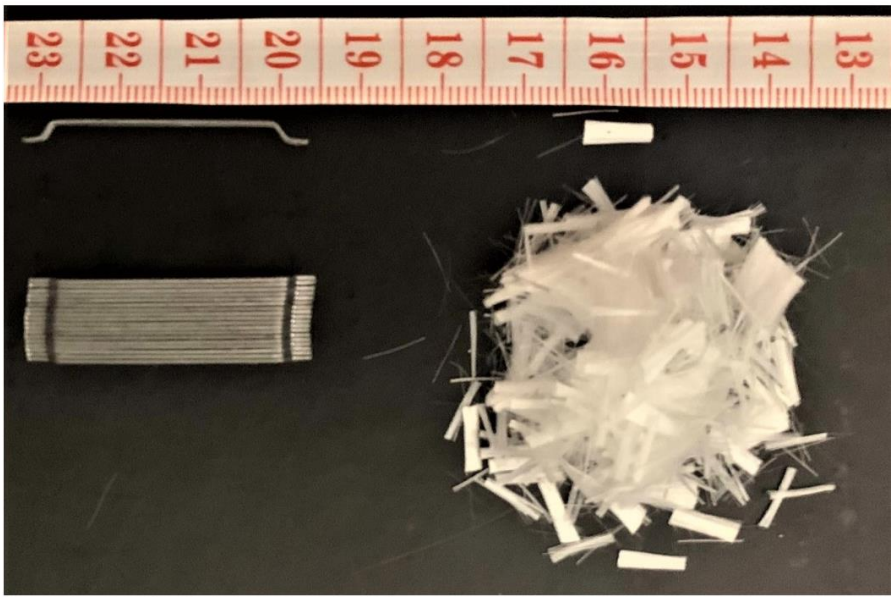

Figure 4-2 PVA and SFs fibers used

4.4.2. Mechanical Properties Tests For LWC, ECCP, and ECCS Mixtures

The compressive strength and splitting tensile strength (STS) of the developed mixtures were tested using 100 mm diameter x 200 mm high concrete cylinders, according to ASTM C39 (2021) and ASTM C496 (2017), respectively. Small-scale beams with dimensions of 100 mm x 100 mm x 400 mm were cast either in single- or two-layer hybrid composite and tested as per ASTM C78 (2021) to evaluate the static flexural strength. In all tests, each composite was tested using three identical specimens that had been moist-cured for 28 days.

4.4.3. Bond Strength Test For LWC-ECCP/ECCS Interface

The splitting tensile test (according to ASTM C496 (2017)) was used to evaluate the bond strength between the LWC and either the ECCP or the ECCS. To prepare specimens for this test, cylindrical molds with 100 mm diameter and 200 mm height were longitudinally cut into two halves. Then, all halves were horizontally positioned and filled with the LWC. After 24 hours, the cast LWC halves were taken and put in other full cylindrical molds. The second hollow-halves in the molds were cast with either the ECCP or the ECCS. It is worth noting that the ECCP or the ECCS were cast on the virgin surface of LWC, i.e., the cast surface was not roughened. After another 24 hours, the specimens were demolded and moist-cured for 28 days. After 28 days the composite cylinders were tested under the splitting tensile test with the interface surface between the two concretes aligned vertically under the two loading points (similar to procedures given in the ASTM C496 (2017)). The bond strength was calculated using **Eq. 4-1**.

$$\sigma_b = 2P/\pi A_i \quad (4\text{-}1)$$

Where P is the ultimate load, A_i is the area of interface taken as cylinder diameter (d) * cylinder length (l) (100*200 mm).

4.4.4. Impact Resistance Tests

4.4.4.1. Impact Test Procedures

After all specimens were moist-cured for 28 days, the drop-weight impact test was conducted using two procedures based on the specimens' type: cylindrical slices impact test and small-scale beams impact test.

- *For the cylindrical slices impact test:* three identical specimens with 150 mm diameter and 63.5 mm height were cast for each composite. The drop-weight test was carried out as per the procedures given by the ACI committee 544 (1999). In the test, a 4.45 kg hammer was dropped from a height of 457 mm onto a 63.5 mm steel ball that was located at the top surface.
- *For the small-scale beams impact test:* three identical beams with dimensions of 100 mm x 100 mm x 400 mm were tested for each composite under three-point flexural impact loading. The beams were simply supported with a loading span of 350 mm. And then a 4.45 kg hammer was dropped from a height of 150 mm onto a 63.5 mm steel ball located at the mid-span of the tested beams.

Figure 4-3 shows the motorized impact test used for both cylindrical slices and beams specimens. The impact device shown was equipped with a motor that performed the test by lifting and dropping the impact weight (4.45 kg) at a rate of 4 drops per minute. During the test, the drop-weight was designed to move through a vertical plastic cylinder to ensure a smooth repeated fall of the drop-weight perpendicular to the specimen being tested (see

Figure 4-3). The tests were run, and the number of blows needed to induce the first crack and failure crack (N_1 and N_2, respectively) in each specimen was determined to evaluate the ultimate impact resistance that could be sustained (according to **Eq. 4-2**):

$$IE = N_{1or2}\, mgh \qquad (4\text{-}2)$$

Since the mass of the drop hammer (m), the acceleration due to gravity (g), and the drop height (h) were constants for each test type, the N_1 and N_2 values were used in the discussion of results to express how the *IE* increased or decreased against the change of the variables studied.

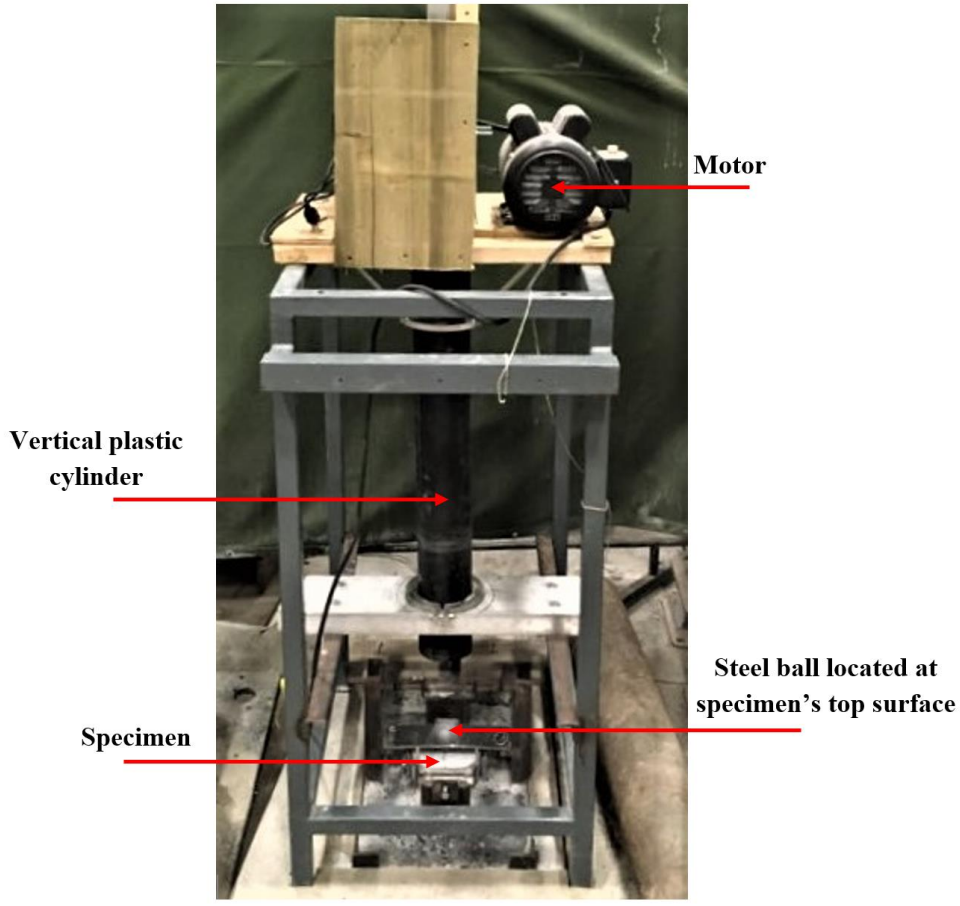

Figure 4-3 Configurations of the motorized-impact tests used

4.4.4.2. Impact Test Program

In this study, the impact resistance of different composites was tested using cylindrical specimens and small-scale beams.

For the 150 mm x 63.5 mm cylindrical slices, 11 composites were cast as follows (see **Figure 4-4**):

- Composites 1-3: they were fully cast with the LWC, ECCP, and ECCS, respectively.
- Composites 4-5: in these composites, the top layer was cast with ECCP and ECCS, respectively, with a depth of 0.25H (H = specimen height) and was designated as 0.25TPVA and 0.25TSF, respectively.
- Composites 6-7: the top layer was cast with ECCP and ECCS, respectively, with a depth of 0.5H and was designated as 0.5TPVA and 0.5TSF, respectively.
- Composites 8-9: the top layer was cast with ECCP and ECCS, respectively, with a depth of 0.75H and was designated as 0.75TPVA and 0.75TSF, respectively.
- Composites 10-11: the bottom layer was cast with ECCP and ECCS, respectively, with a depth of 0.5H and was designated as 0.5BPVA and 0.5BSF, respectively.

Composites 4-9 were cast so that the ECC was directly exposed to the impact loading in order to evaluate the performance of ECC as a protective layer for structural LWC members such as footings, slab on grade, and platforms. Whereas composites 10-11 were cast to assess how the ECC can dissipate the impact loading reaction that can be imposed by supporting base.

For the small-scale beams, nine composites were cast as follows (see **Figure 4-4**):

- Composites 12-14: they were fully cast with the LWC, ECCP, and ECCS, respectively.
- Composites 15-16: the bottom layer was cast with ECCP and ECCS, respectively, with a depth of 0.25H and was designated as 0.25BPVA and 0.25BSF, respectively.
- Composites 17-18: the bottom layer was cast with ECCP and ECCS, respectively, with a depth of 0.5H and was designated as 0.5BPVA and 0.5BSF, respectively.
- Composites 19-20: the top layer was cast with ECCP and ECCS, respectively, with a depth of 0.5H and was designated as 0.5TPVA and 0.5TSF, respectively.

Composites 12-18 were cast to assess the structural benefits of employing ECC in beam elements to carry tensile stress that result from impact loading, while composites 19-20 were cast to evaluate the role of ECC in dissipating the localized effect of impact loading on LWC. Composites 12-20 were also tested under static flexural load as per ASTM C78 (2021).

It should be noted that composites 4-20 were cast with different depth-combinations of ECC and LWC to evaluate the possible impact resistances that can be reached and the corresponding self-weight, as compared to those of LWC (composite 1). These parameters (i.e., impact resistance and self-weight) were evaluated when the depth of either ECCP or ECCS changed by a constant increment of 0.25H.

In all composites, the bottom layer was cast and left until the initial setting. In order to evaluate the impact resistance of the developed composites and avoid any unexpected debonding failure due to the aggressive effect of impact loading, random holes, scratches, and grooves were created on the surface of the bottom layer prior to casting the top layer,

as seen in **Figure 4-4**. After 24 hours, the surface was cleaned, wetted, and the top layer was poured.

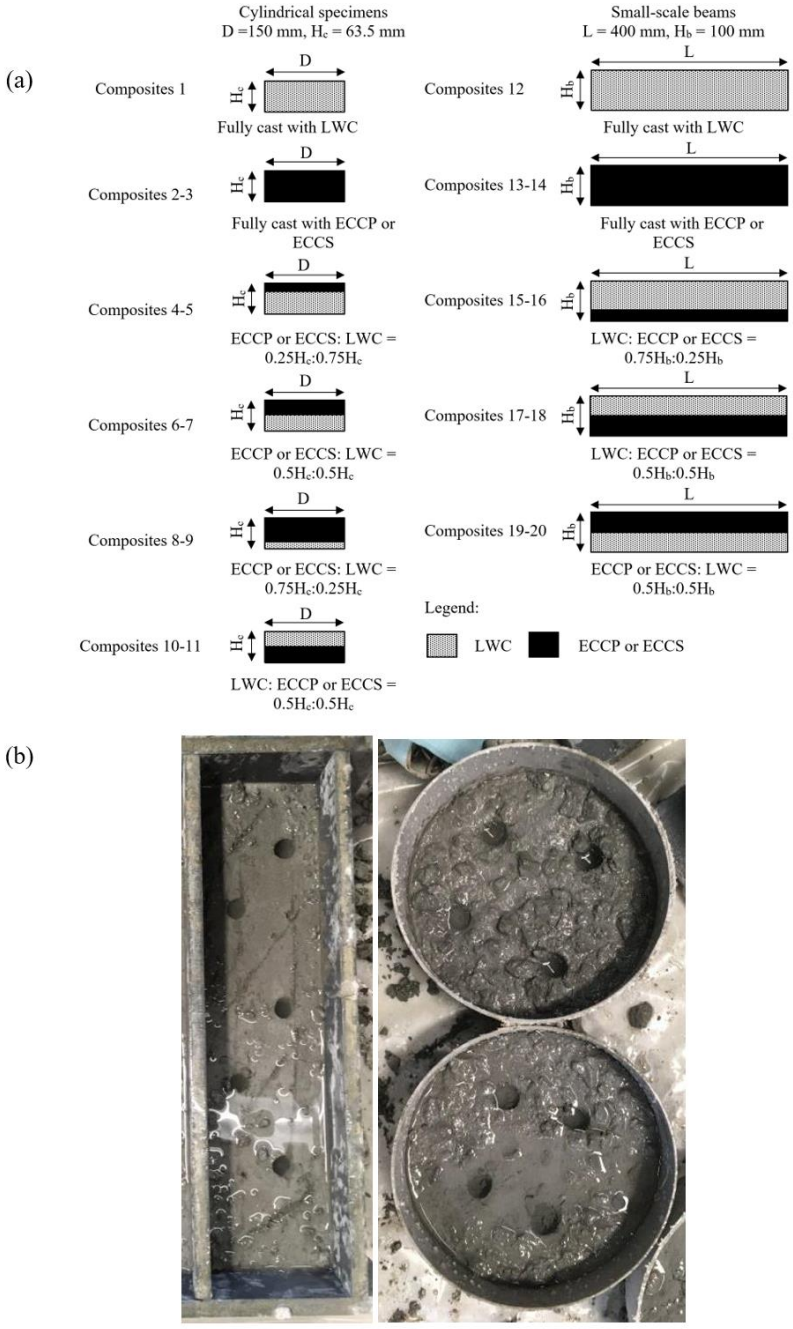

Figure 4-4 (a) Configurations of cast composites (b) preparation before casting the top layer

4.5. Discussion of Test Results

4.5.1. Mechanical Properties of LWC, ECCP And ECCS

The results in **Table 4-1** show that the LWC mixture developed in this investigation could achieve a maximum compressive strength of 43.8 MPa with a strength-to-weight (S/W) ratio of 2.53% (see **Figure 4-5**). Higher compressive strengths and S/W ratios were exhibited in the ECCP and ECCS; their compressive strengths reached up to 73.3 MPa and 85.5 MPa, respectively, with S/W ratios of 3.54% and 3.89%, respectively.

Figure 4-6 shows the STS/f_c' and SF/f_c' ratios for all developed mixtures. From the figure, it can be seen that the LWC mixture had STS/f_c' and SF/f_c' ratios of 5.5% and 8.2%, respectively. On the other hand, the presence of fibers in both ECCP and ECCS mixtures allowed the mixtures to sustain high tensile stress beyond the mortar cracking. This in turn yielded higher STS/f_c' and SF/f_c' ratios. The highest STS/f_c' and SF/f_c' ratios were exhibited by the ECCS compared to ECCP, thus indicating superior performance of SF fibers over PVA fibers. The STS/f_c' and SF/f_c' ratios were 11.2% and 11.5%, respectively, for the ECCP, while these values were 11.9% and 13.2%, respectively, for the ECCS.

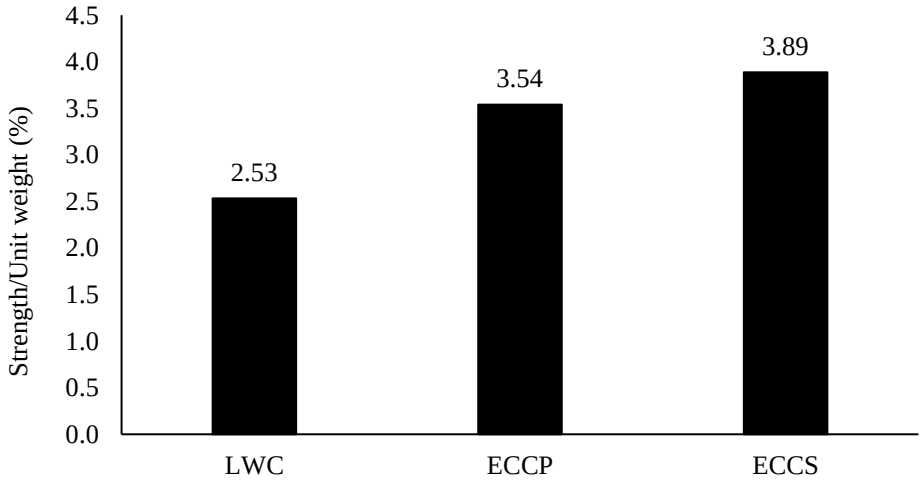

Figure 4-5 Strength-to-weight ratio of the developed mixtures

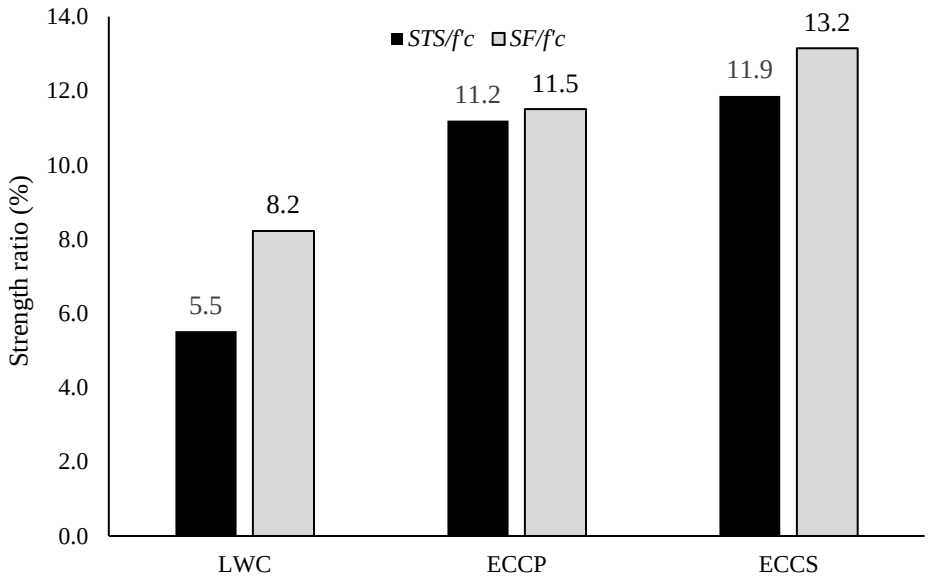

Figure 4-6 Splitting and flexural strength ratio of the developed mixtures

4.5.2. Bond Strength for LWC-ECCP/ECCS Interface

The results obtained from testing the hybrid cylindrical composites in the STS reflected a good interfacial bonding between ECCP/ECCS and LWC. As seen in **Figure 4-7**, the failure at the interface between LWC and either ECCP or ECCS occurred at a stress level of 2.26 MPa and 2.20 MPa, respectively. These values are more than 90% of what induced failure in the monolithic LWC cylinders (i.e., the ultimate STS of the LWC = 2.41 MPa). It is worth noting that in hybrid cylindrical composites, no surface preparations (i.e., surface roughening or shear keys) were implemented at the interface between the two layers; however, the rich contents of high reactive binders (i.e., cement and MK) in ECCP and ECCS apparently formed a high adhesion with LWC substrate.

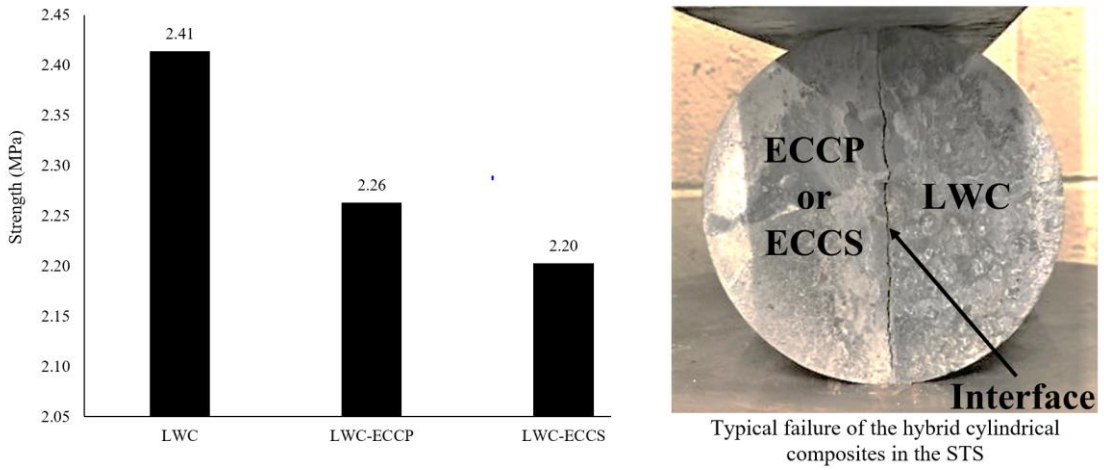

Figure 4-7 LWC-ECCP/ECCS interface bond strength

4.5.3. Static Flexural Strength

Figure 4-8 shows the load-midspan deflection curves of the fully cast and hybrid composite beams tested in flexure under four-point loading. As seen from the curves in **Figure 4-8a**, the LWC beam could sustain a load up to 12 kN corresponding to ultimate deflection of 1.14 mm. The failure occurred after the formation of a single vertical crack, which was associated with a sharp drop in the load-deflection curve. On the other hand, the inclusion of fibers in ECCP and ECCS beams helped them to sustain further loading beyond the formation of the first crack, and then exhibit higher loading and deformation capacity. The ECCP and ECCS had a capacity of 2.34 and 3.13 times as much as that exhibited by the LWC beam. The results of both ECCS and ECCP beams also proved that with the inclusion of SFs, ECC could be more efficient in developing composite with higher load-carrying capacity, while with the PVA fibers, the ECC could exhibit pseudo-strain-hardening behavior, saturated multiple cracking, and higher ductility. Since both SFs and PVA fibers had a high tensile strength, the fibers would be pulled out rather than

ruptured. Therefore, the superior performance of SFs over PVA, in terms of load carrying capacity, could be attributed to their longer anchorage length and hooked ends, which in turn transferred higher levels of stress. **Figure 4-9** shows the cracking pattern of ECCP and ECCS at failure.

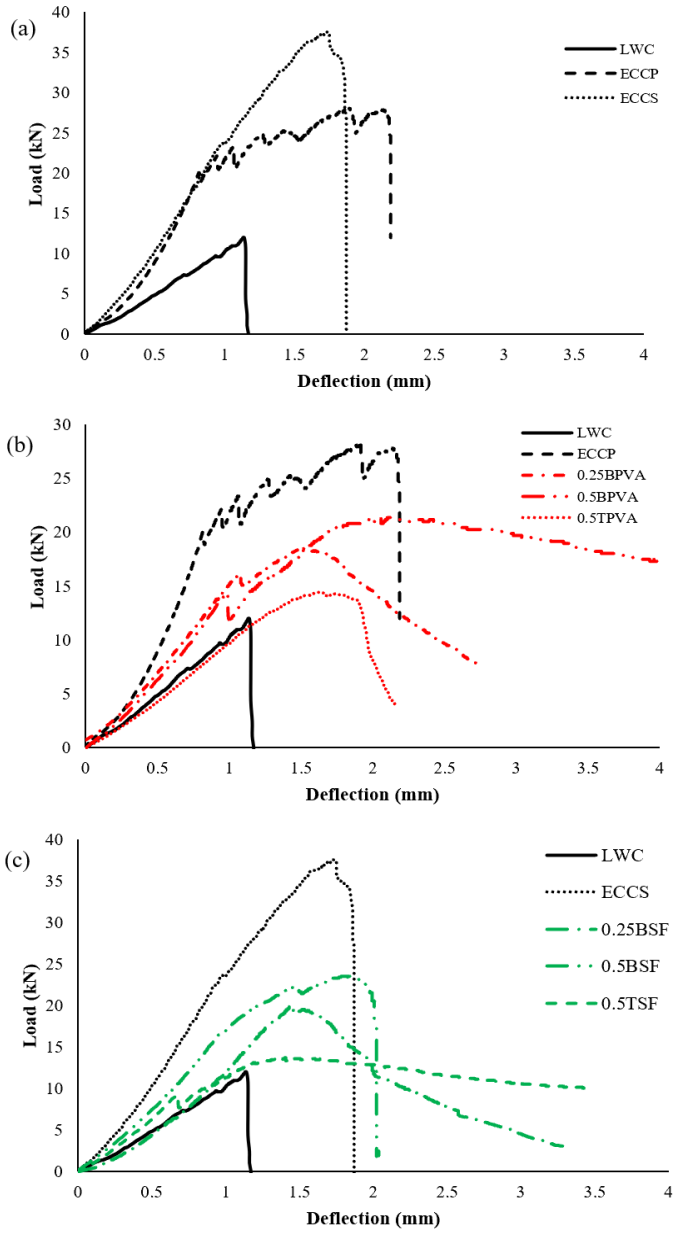

Figure 4-8 Load-midspan deflection of tested beams

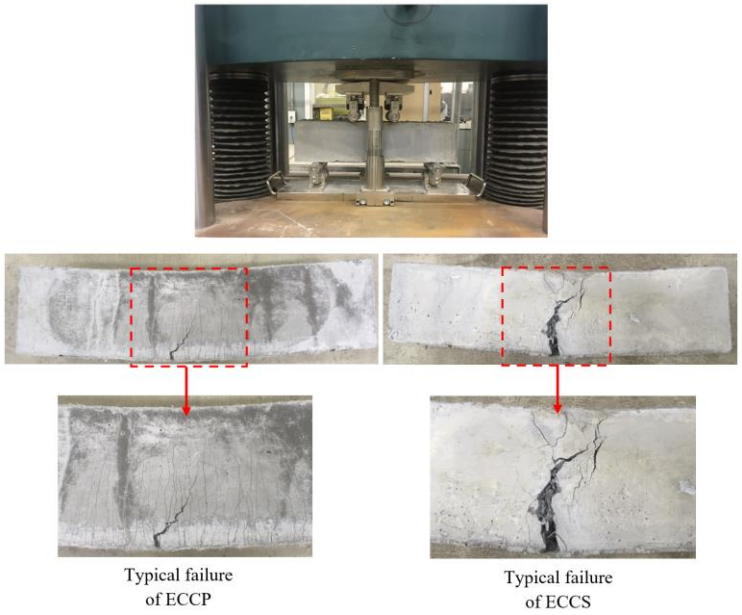

Figure 4-9 Typical cracking pattern of ECCP and ECCS at failure

Figures 4-8b and **4-8c** show the flexural performance of hybrid beams that were composed of LWC and either ECCP or ECCS in varied depths and arrangements. The first set of beams incorporated ECCP or ECCS as the bottom layer (i.e., tension side) with a depth of 0.25H and 0.5H (0.25BSF, 0.25BPVA, 0.5BSF, and 0.5BPVA). The results of this set indicated that despite the fact that the 0.25BPVA and 0.5BPVA beams had a self-weight of 5.3% and 10.5%, respectively, higher than that of the LWC beam, they could sustain ultimate loads of 55% and 78.3%, respectively, higher than that sustained by the LWC beams. Higher load carrying capacities were observed when SFs were used instead of PVA fibers in ECC. When the ECCS was placed at the bottom side with a depth of 0.25H and 0.5H (0.25BSF and 0.5BSF beams), the ultimate load carrying capacity increased over that of the LWC beams by 65.8% and 95.8%, respectively. However, the increase in the self-weight of ECC with SFs (0.25BSF and 0.5BSF), compared to the fully cast LWC, reached

up to 7.2% and 14.3%, respectively (compared to an increase of 5.3% and 10.5%, respectively, in ECC with PVA, as mentioned above).

The second set of beams incorporated either ECCP or ECCS at the top layer (i.e., compression side, 0.5TPVA and 0.5TSF) with a depth of 0.5H. Those beams showed higher deformability compared to the LWC beams, but because the low-tensile-strength LWC was located in the tension side, the cracks rapidly propagated to the interface and then to the ECCP/ECCS layer, eventually causing the failure. This in turn resulted in limited improvements in the load carrying capacity of the 0.5TPVA and 0.5TSF beams, which reached values of 20.8% and 14.2%, respectively, higher than that of the LWC beams.

In general, the results of the tested beams indicated that the ECCP and ECCS have promising potential for strengthening and repair applications, in particular for deteriorated LWC members, in which significant structural benefits can be obtained without causing a significant increase in the self-weight.

4.5.4. Impact Resistance of Cylindrical Slices

Table 4-2 and **Figure 4-10** show the average number of drops that induced the first crack (N_1) and failure crack (N_2) in three cylindrical specimens tested for each composite. As shown in the table, the specimens fully cast from the LWC showed a brittle behavior and very low energy absorption capacity, and the failure suddenly occurred after four drops with no prior cracks (i.e., $N_1 = N_2 = 4$). On the other hand, specimens made from either ECCP or ECCS exhibited a ductile failure and obviously greater energy absorption capacity, in which the specimens sustained a high number of drops until the formation of the first crack, and then a significant number of cracks were required to cause the failure.

The N_1 and N_2 were 275 and 595, respectively, for the ECCP, and 600 and 1250, respectively, for the ECCS.

Combining LWC with either ECCP or ECCS formed a lightweight hybrid composite with improved impact resistance. The ECCP or ECCS layer was used as a top layer, directly exposed to the drop-weight impacts, to simulate a protection layer to LWC, which was rested on a steel plate (i.e., representing strengthening LWC with ECC at the bottom layer). In these specimens (0.25TPVA, 0.5TPVA, 0.75TPVA, 0.25TSF, 0.5TSF, and 0.75TSF), the first crack was typically formed at the LWC layer (i.e., the weakest layer). When the ECCP was used with a depth of 0.25H, the first crack developed after four drops (on average), similar to the LWC specimens. As the depth of the ECCP layer increased from 0.25H to 0.75H (0.25TPVA and 0.75TPVA), the N_1 increased from 4 to 10. As the number of drops increased, the cracks propagated further, reaching to the interface after an average of 23 drops in 0.25TPVA specimens and 70 drops in 0.75TPVA. These results indicate that increasing the top ECCP layer's depth led to higher energy dissipation, and an increased number of drops were required to induce either the first crack, interface layer crack, or failure crack. By increasing the number of drops, the cracks continued propagating into the ECCP layer. However, the failure was finally governed by a significant crushing in the bottom LWC layer. A typical crack pattern for top and bottom layers is shown in **Figure 4-11**. The 0.25TPVA, 0.5TPVA, and 0.75TPVA specimens failed at an average of 43, 65, and 100 drops, respectively. Similar behavior was observed in ECC specimens that incorporated SFs (0.25TSF, 0.5TSF, and 0.75TSF), but higher energy dissipation and impact resistance were provided (see **Table 4-2** and **Figure 4-10**).

Table 4-2 Results of flexure and impact tests

Composite ID	Flexure test		Cylindrical specimens		Small-scale beams		Density (kg/m^3)
	Load (kN)	Deflection (mm)	N_1	N_2	N_1	N_2	
LWC	12.0	1.14	4	4	20	20	1727
ECCP	28.1	1.92	275	595	250	385	2091
ECCS	37.5	1.75	600	1250	2000	>2000	2222
0.25TPVA	-	-	4	43	-	-	1818
0.5TPVA	14.5	1.64	7	65	50	86	1909
0.75TPVA	-	-	10	100	-	-	2000
0.25TSF	-	-	4	100	-	-	1851
0.5TSF	13.7	1.49	10	140	90	216	1975
0.75TSF	-	-	22	200	-	-	2098
0.25BPVA	18.6	1.52	-	-	50	90	1818
0.5BPVA	21.4	2.12	5	40	130	167	1909
0.25BSF	19.9	1.45	-	-	70	135	1851
0.5BSF	23.5	1.86	7	95	734	1300	1975

To investigate the effect of placing the absorbent layer (ECCP or ECCS) underneath the LWC, 0.5BPVA and 0.5BSF specimens were tested. Compared to the 0.5TPVA and 0.5TSF specimens (which had ECC placed on the top layer), the 0.5BPVA and 0.5BSF specimens failed at a lower number of drops due to crushing of the top LWC layer under the localized pattern of impacts (see **Figure 4-11**). However, those composites still exhibited improved impact resistance compared to the fully cast LWC specimens. The 0.5BPVA and 0.5BSF specimens experienced their first crack at top layer after 8 and 10 drops, respectively, whereas the failure crack was induced at 40 and 95 drops, respectively.

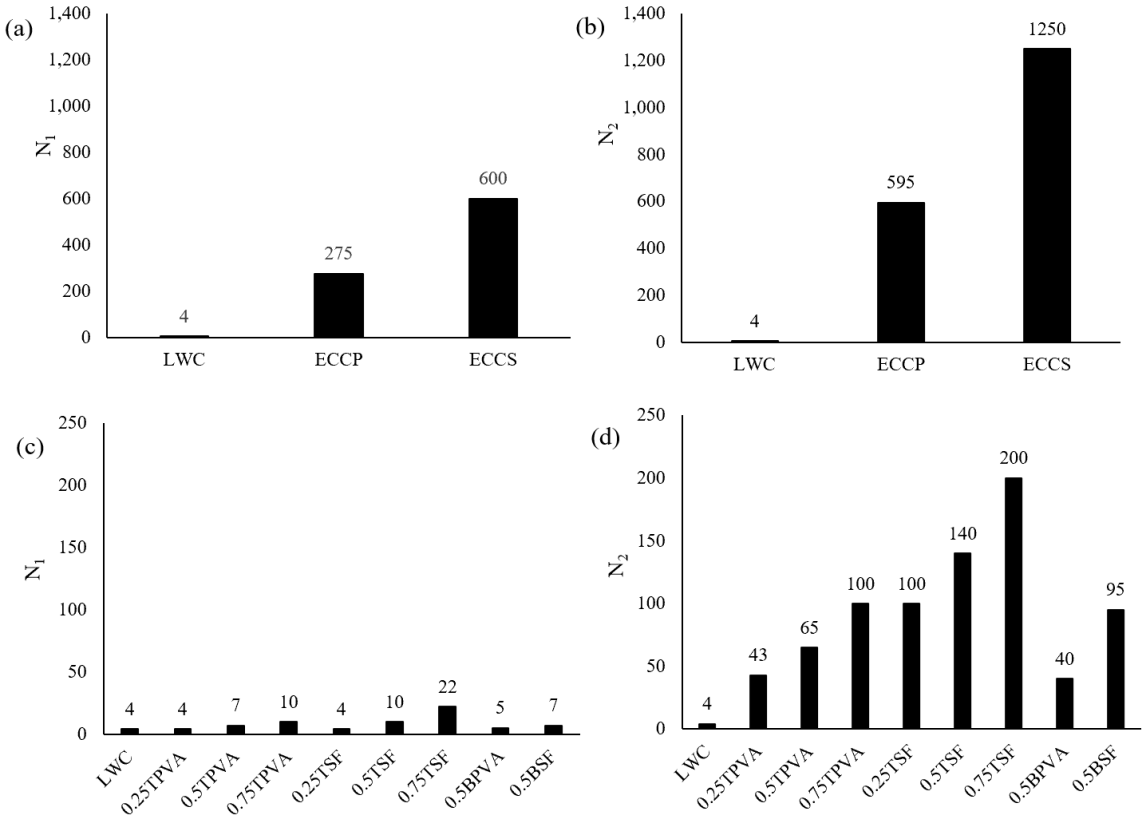

Figure 4-10 Results of impact resistance of cylindrical specimens (a) N1 of the single-layer specimens, (b) N2 of the single-layer specimens, (c) N1 of the two-layer hybrid composites, and (d) N2 of the two-layer hybrid composites

4.5.5. Impact Resistance of Small-Scale Beams

For each composite, the average values of N_1 and N_2 for small-scale beams are presented in **Table 4-2** and **Figure 4-12**. The results show that the LWC beams, similar to the cylindrical specimens, could not absorb high energy as only 20 drops suddenly caused the failure. On the contrary, significant energy absorption capacity was exhibited by the beams that were fully cast with ECCP and ECCS. The ECCP beams had N_1 and N_2 values of 250 and 385 (on average), respectively, whereas the ECCS beams exhibited the first crack after 650 drops but no final failure occurred even after 2000 drops. As mentioned earlier, the

superior performance of SFs could be attributed to their possible longer anchorage and hooked ends, thus providing high bonding and bridging action, which subsequently helped to transfer higher stress induced by drop impacts.

In hybrid composite beams (0.25BPVA, 0.5BPVA, 0.25BSF, and 0.5BSF), the presence of either ECCP or ECCS at the bottom helped to carry the tensile stress that resulted from impact loading, and then boosted the ability of beams to absorb high energy prior to failure. For example, in the 0.25BPVA and 0.25BSF, the beams endured 50 and 70 drops up to the first crack, respectively, and 90 and 135 drops, respectively, up to failure. It is worth noting that such higher impact absorption capacity (i.e., compared to the beams fully cast with LWC) was gained against slight increase in the self-weight, in which the self-weight of 0.25BPVA and 0.25BSF beams was only 5.3% and 7.2%, respectively, higher than that of the LWC beams. Further increase in the absorption capacity of beams was observed when the depth of either ECCP or ECCS increased. The 0.5BPVA and 0.5BSF beams sustained 130 and 734 drops, respectively, to produce the first crack, while the failure crack was observed after 167 drops and 1300 drops, respectively. Compared to the LWC beams, the 0.5BPVA and 0.5BSF beams had 10.5% and 14.3%, respectively, higher self-weight. The typical failure pattern, displayed in **Figure 4-11**, also showed that the failure of hybrid composites occurred due to the formation of a major vertical or inclined crack passing through both layers. It should be noted that no cracks were visually observed at the interface between the two concrete layers which indicates that the surface roughening and pitted holes that were formed on the LWC layer's surface were enough to achieve adequate bonding between layers, even under the effect of impact loading.

The results also indicated that beams with the ECCP or ECCS at the bottom half-height (0.5BPVA and 0.5BSF) also showed a good performance under the drop-weight loading but could not reach the high energy absorption capacity that was exhibited by 0.5TPVA and 0.5TSF. This was attributed to the fact that the failure was always governed by the brittle LWC placed at the bottom layer, which could not sustain high levels of tensile stress induced by drop-weight impacts.

The results of impact testing obtained from cylindrical specimens and small-scale beams indicated that LWC-ECC hybrid composite proved to have promising capabilities that can be employed to construct high impact resistant lightweight structural elements.

Figure 4-11 Typical failure crack patterns in the tested two-layer hybrid composites (cylindrical specimens and beams)

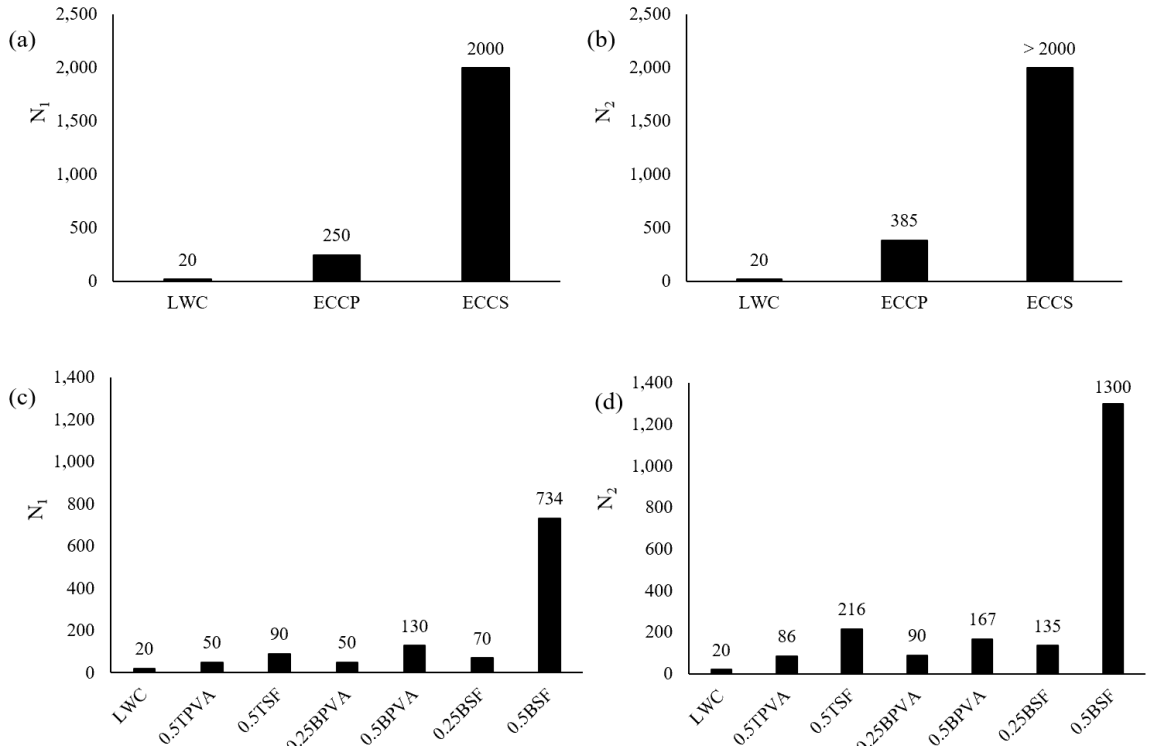

Figure 4-12 Results of impact resistance of beams (a) N1 of the single-layer specimens, (b) N2 of the single-layer specimens, (c) N1 of the two-layer hybrid composites, and (d) N2 of the two-layer hybrid composites

4.6. Conclusions

This study examined novel hybrid lightweight composites with high impact resistance. Each composite was developed with a two-layer system: LWC layer and ECC layer that were composed with varied depths and different arrangements. The performance of the developed composites was tested under static flexure, impact flexure, and axial impact loading. The interfacial bonding between LWC and either ECCP or ECCS was also evaluated. From the experimental results obtained in this study, the following conclusions can be drawn:

1. The splitting tensile test conducted on composite cylindrical specimens indicated evolution of an excellent interfacial bonding between LWC and either ECCP or ECCS. The LWC-ECCP/ECCS interfacial bonding strength reached to about 90% of that recorded by the monolithic LWC specimens, despite no surface preparation.
2. Combining LWC and ECCP or ECCS efficiently helped to develop novel composites with low density and improved impact resistance, thus presenting a promising candidate for strengthening lightweight structures exposed to high impact loading.
3. The best performance of LWC-ECCP and LWC-ECCS cylindrical specimens was achieved when ECCP and ECCS were used as a top layer (rather than the bottom layer), directly exposed to the impact loading. This is attributed to the higher resistance of fibrous layer (ECCP or ECCS) to the localized stress pattern of impact loading.
4. In the cylindrical slice impact test, whether LWC was at the top or bottom layer, the failure of the specimen was always governed by the low brittleness of LWC, whereas the ECCP/ECCS layer helped the composite to maintain a high stability.
5. The drop-weight test performed on small-scale beam specimens showed that the composites with ECCP or the ECCS as the bottom layer (located at the tension side) yielded higher impact energy absorption capacity than with LWC as the bottom layer. This is because of the better performance of fibrous layer (ECCP or ECCS) in carrying the tensile stress. Whereas in composites with LWC as the bottom layer, the failure was governed by the fracture of LWC.

6. Based on the results of all tested composites, as the depth of ECCP or ECCS layer increased the flexural strength and impact resistance of the composite were greatly improved and with only a slight increase in the self-weight. The increase in the self-weight ranged between 5.3% to 14.3% higher than that of the fully cast LWC specimens, when ECCP or ECCS were cast in a quarter to half the height of composites.
7. The results obtained from specimens fully or partially cast with ECCP or ECCS indicated that the SFs and PVA fibers proved to have high efficiency in developing composites with high performance under static and impact loading. Composites with SFs yielded higher impact energy absorption capacity whereas the PVA formed lighter composites.

4.7. References

ACI 544.2 R-89 “Measurement of properties of fiber reinforced concrete.”, West Conshohocken, PA, 1999.

ASTM C39 / C39M. “Standard Test Method for Compressive Strength of Cylindrical Concrete Specimens.” ASTM International, West Conshohocken, PA, USA, 2021.

ASTM C 78/C 78M. “Standard test method for flexural strength of concrete.” ASTM International, West Conshohocken, PA, USA, 2021.

ASTM C143 / C143M, “Standard Test Method for Slump of Hydraulic-Cement Concrete,” ASTM International, West Conshohocken, PA, USA, 2020, 4 pp.

ASTM C150/C150M. “Standard Specification for Portland Cement.” ASTM International, West Conshohocken, PA, USA, 2020.

ASTM C494/C494M, “Standard Specification for Chemical Admixtures for Concrete.” ASTM International, West Conshohocken, PA, USA, 2019.

ASTM C496. “Standard Test Method for Splitting Tensile Strength of Cylindrical Concrete Specimens.” ASTM International, West Conshohocken, PA, USA, 2017.

ASTM C618. “Standard Specification for Coal Fly Ash and Raw or Calcined Natural Pozzolan for Use in Concrete.” ASTM International, West Conshohocken, PA, USA, 2019.

EFNARC. “The European Guidelines for Self-Compacting Concrete Specification, Production and Use.” English ed. Norfolk, UK: European Federation for Specialist Construction Chemicals and Concrete Systems, 2005.

Clauss, G. F. “Dramas of The Sea: Episodic Waves and Their Impact on Offshore Structures.” Applied Ocean Research, V. 24, No. 3, 2002, pp. 147-161.

Hubertova, M.; and Hela R. “The Effect of Metakaolin and Silica Fume on The Properties of Lightweight Self-Consolidating Concrete.” ACI special publication, V. 243, 2007, pp. 35-48.

Ismail, M. K.; Abdelaleem B H and Hassan A. A. A. “Effect of Fiber Type on The Behavior of Cementitious Composite Beam-Column Joints Under Reversed Cyclic Loading.” Construction and Building Materials, V. 186, 2018,pp. 969-977.

Ismail, M. K.; and Hassan, A. A. A. “Impact Resistance and Mechanical Properties of Self-Consolidating Rubberized Concrete Reinforced with Steel Fibers.” Journal of Materials in Civil Engineering, V. 29, No. 1, 2017, 04016193.

Ismail, M. K.; and Hassan, A. A. A. “Influence of Fibre Type on The Shear Behaviour of Engineered Cementitious Composite Beams.” Magazine of Concrete Research, V. 73, No. 9, 2021, pp. 464-475.

Ismail, M. K.; Hassan, A. A. A.; and Lachemi, M. “Abrasion Resistance of Self-Consolidating Engineered Cementitious Composites Developed with Different Mixture Compositions.” ACI Materials Journal, V. 116, No. 1, 2019a, pp. 27-38.

Ismail, M. K.; Hassan, A. A. A.; and Lachemi, M. “Performance of Self-Consolidating Engineered Cementitious Composite under Drop-Weight Impact Loading.” Journal of Materials in Civil Engineering, V. 31, No. 3, 2019, https://doi.org/10.1061/(ASCE)MT.1943-5533.0002619.

Kong, H. J.; Bike, S. G.; and Li, V. C. “Development of A Self-Consolidating Engineered Cementitious Composite Employing Electrosteric

Dispersion/Stabilization.” Cement and Concrete Composites, V. 25, 2003, pp. 301–309.

Li, V. C. “From Micromechanics to Structural Engineering – The Design of Cementitious Composites for Civil Engineering Applications.” Journal of Structural Mechanics and Earthquake Engineering, JSCE, V. 10, No. 2, 1993, pp. 37-48.

Li, V. C.; Wu, C.; Wang, S.; Ogawa, A.; and Saito, T. “Interface Tailoring for Strain-Hardening Polyvinyl Alcohol-Engineered Cementitious Composites (PVA-ECC).” ACI Materials Journal, V. 99, No. 5, 2002, pp. 463–72.

Lok, T. S.; and Pei, J. S. “Impact Resistance and Ductility of Steel Fibre Reinforced Concrete Panels.” HKIE Trans, V. 3, No. 3, 1996, pp. 7-16.

Meng, D.; Lee, C.; and Zhang, Y. “Flexural Fatigue Properties of A Polyvinyl Alcohol-Engineered Cementitious Composite.” Magazine of Concrete Research, V. 71, No. 21, 2018, pp. 1130-1141.

Paik, J. K. “Recent Advances and Future Trends on Plasticity and Impact Mechanics of Ships and Offshore Structures.” Procedia Engineering, V. 173, 2017, pp. 17-24.

Papanicolaou, C. G.; and Kaffetzakis, M. I. “Lightweight Aggregate Self-Compacting: State-of-Pumice Application.” Journal of Advanced Concrete Technology, V. 9, No. 1, 2011, pp. 15-29.

Sadek, M. M.; Ismail, M. K.; and Hassan, A. A. A. “Stability of Lightweight Self-Consolidating Concrete Containing Coarse and Fine Expanded Slate Aggregates.” ACI Materials Journal, V. 117, No. 3, 2020a, pp. 133-143.

Sadek, M. M.; Ismail, M. K.; and Hassan, A. A. A. “Impact Resistance and Mechanical Properties of Optimized SCC Developed with Coarse and Fine Lightweight Expanded Slate Aggregate.” Journal of Materials in Civil Engineering, V. 32, No. 11, 2020, 04020324, 2020b.

Şahmaran, M.; and Li, V. C. “Engineered Cementitious Composites: Can Composites Be Accepted As Crack-Free Concrete?.” Transportation Research Record, V. 2164, No. 1, 2010, pp. 1–8.

Said, S. H.; and Razak, H. A. “The Effect of Synthetic Polyethylene Fiber on The Strain Hardening Behavior of Engineered Cementitious Composite (ECC).” Materials and Design, V. 86, 2015, pp. 447–457.

Said, S. H.; and Razak, H. A. “Structural Behavior Of RC Engineered Cementitious Composite (ECC) Exterior Beam–Column Joints Under Reversed Cyclic Loading.” Construction and Building Materials, V. 107, 2016,pp. 226-234

Shi, C.; and Yang, X. “Design and Application of Self-Consolidating Lightweight Concrete,” Proceedings of China 1st International Symposium on Design, Performance and Use of Self-Consolidating Concrete, RILEM Publication SARL, Paris, France, 2005, pp. 55-64.

Suthiwarapirak, P.; Matsumoto, T.; and Kanda, T. “Multiple Cracking and Fiber Bridging Characteristics of Engineered Cementitious Composites Under Fatigue Flexure.” Journal of Materials in Civil Engineering, V. 16, No. 5, 2004, pp. 433–443.

Yao, S. X.; and Gerwick, B. C. “Development of self-compacting lightweight concrete for rfp reinforced floating concrete structures.” US Army Corps of Engineers Research and Development Center, San Francisco, CA, USA, Technical report, 2006.

Yıldırım, G.; Khiavi, F.E.; Anıl, Ö.; Sahin, O.; Sahmaran, M.; Erdem, R. T. “Performance of Engineered Cementitious Composites Under Drop-Weight Impact: Effect of Different Mixture Parameters.” Structural Concrete, V. 21, No. 3, 2020, pp. 1051-1070.

Yuan, F.; Pan, J.; Xu, Z.; and Leung, C. K. Y. “A Comparison of Engineered Cementitious Composites Versus Normal Concrete in Beam–Column Joints Under Reversed Cyclic Loading.” Materials and Structures, V. 46, No. (1–2), 2013, pp. 145–159.

5. Summary and recommendation

5.1. Summary

The research program conducted in this thesis included three experimental studies, which investigated the use of ECC to strengthen LWC, aiming to reach high-performance lightweight structures. The ECC was developed with two types of fibers, namely polyvinyl alcohol fibers (ECCP) or steel fibers (ECCS). Chapter 2 investigated the flexure behavior of LWC beams strengthened with ECCP or ECCS. Chapter 3 evaluated the shear behavior of LWC beams strengthened with ECCP and ECCS. In chapters 2 and 3, the LWC beams were strengthened at either compression or tension zone. In these studies, the performance of all tested beams was evaluated by investigating their load-deflection response, cracking behavior, failure mode, first crack load, ultimate load, ductility, and energy absorption capacity. In addition, the flexure and shear capacity of the tested composites were successfully estimated using new model proposed based on a modification for existing standards' models. Chapter 4 focused on developing novel hybrid lightweight composites with high impact resistance. In this chapter, cylindrical specimens and small-scale beams were constructed with a two-layer system: LWC layer and ECCP or ECCS layer. The two layers in each composite were cast with varied depths and different arrangements. The performance of all developed composites was tested under drop-weight impact loading. The interfacial bonding strength between LWC and either ECCP or ECCS was also evaluated. From the experimental results obtained in the conducted studies, the following conclusions can be drawn:

The results of flexure tests indicate that:

- At material and structural levels, ECCS showed higher mechanical and flexural behaviour compared to ECCP. However, the ECCP was produced with lower density and self-compactability properties.
- Strengthening LWC beams with ECC (ECCP or ECCS) at either the compression or tension zone generally led to improving the flexural performance in terms of first crack load, ultimate load, ductility, and energy absorption capacity compared to the control LWC beam (non-strengthened beam). These results prove a superior performance for using ECC as a strengthening material.
- In strengthened beams, the increase in the first crack load and ultimate load was more pronounced when the ECC layer was placed at tension zone, while placing the ECC layer at the compression zone yielded higher ductility and energy absorption capacity.
- Compared to the control LWC beam, the use of ECCP or ECCS at the tension zone exhibited better cracking control, which can help to provide a higher protection for the tension steel reinforcement, even for exterior-exposed structures.

- When ECC layer was placed at the tension zone of the beam, the use of PVA fibers in the ECC showed more advantage over SFs in delaying the initiation of the first crack. However, using SFs in ECC at the tension zone yielded higher contribution to increasing the overall ultimate load-carrying capacity compared to using PVA fibers in ECC.
- In all strengthened beams, no sign of slip was observed at the LWC-ECC interface, which indicates that the shear reinforcement and the roughened interface surface could effectively ensure adequate bonding between the ECC and LWC layers.
- The ACI ultimate strength design method as well as the analysis developed by Henager and Doherty showed a conservative capability for estimating the flexural capacity of all tested beams. For beams with fibers, the accuracy of the estimations given by the Henager and Doherty model improved when the term of the tensile stress of fibrous concrete was obtained experimentally rather than by calculating it based on the model's equation.

The results of shear tests indicate that:

- The use of either ECCP or ECCS in strengthening the compression zone of LWC beam compensated for the reduced shear capacity of the beam and enhanced the normalized shear strength to reach a value exceeded the normalized shear strength of the NWC beam. In the meantime, the increase in the concrete unit weight of such composite did not exceed 9% of the density of the LWC beam.

- Using ECCP or ECCS layer at the compression zone of LWC beams (ECCP-C and ECCS-C) exhibited a higher number of cracks with larger crack widths compared to LWC, NWC, and ECC reference beams. On the other hand, placing ECCP or ECCS layer at the tension zone of LWC beams (ECCP-T and ECCS-T) yielded a reduced number of cracks and widths compared to ECC reference beams and their counterpart beams with ECC layer in the compression zone (ECCP-C and ECCS-C).
- In ECCP-C and ECCS-C beams, despite the higher increase in the shear capacity when SFs were used compared to PVA fibers (14% increase), the use of PVA fibers were more pronounced in improving the deformation capacity of the beam compared to SFs.
- The use of ECC layer in the compression zone of the LWC beam helped to develop relatively lightweight composite (1843-1888 kg/m^3 (115-117.9 lb/ft^3) density) with enhanced structural performance in terms of post cracking shear ductility, post diagonal shear resistance, ultimate shear capacity, and energy absorption, which exceeded the performance of NWC beam with 2276 kg/m^3 (142 lb/ft3) density.
- The ECCP-T and ECCS-T beams (LWC beams with ECC layer at the tension zone) appeared to have lower post diagonal cracking shear resistance, post cracking shear ductility, ultimate shear capacity, and energy absorption compared to the ECCP-C and ECCS-C beam (LWC beams with ECC layer at the compression zone), but still higher than LWC and NWC beams.

- For beams that were fully cast with ECC (ECCP and ECCS) or ECC layer was placed at the tension zone (ECCP-T and ECCS-T), among all investigated prediction models, the most accurate shear predictions were obtained by the model proposed in the present research which was adopted based on modifying the EC2 equation to take the fibers contribution into account.

The results of mechanical and impact tests indicate that:

- The results indicated that with no prior preparation at interface, ECCP or ECCS could achieve a good bonding with LWC. However, improving the bonding by shear key or surface roughening can be utilized to resist the aggressiveness of some loading conditions such as impulsive loads.
- Combining LWC and ECCP or ECCS together in one composite proved to be an effective approach to achieve high impact resistance at low density, which can contribute to constructing high-impact resistant lightweight structures.
- The results indicated that if loading conditions and supporting system are similar to that of tested cylindrical specimens (such as footings, slab on grade, and platforms), the use of ECCP or ECCS at the top layer (as a protective layer) is more efficient in resisting the localized stress pattern of impact loading.
- In beams exposed to impulsive loading, the use of ECCP or ECCS was more efficient when they were placed at the bottom layer due to the higher performance of fibrous layer (ECCP or ECCS) in carrying the tensile stress.

- In all tested configurations, increasing the depth of ECCP or ECCS layer led to an increase in the impact resistance of composite but accompanied with an increase in the self-weight. However, the increase in the self-weight reached up to a maximum of 14.3% higher than that of the fully cast LWC specimens, when ECCS was cast in half the height of composites.
- In all cylindrical specimens and small-scale beams, the ECCS always exhibited higher performance under static and impact loading compared to ECCP. On the other hand, ECCP had the advantage of achieving an excellent impact resistance (i.e., greatly higher than LWC) at lighter weight.

5.2. Limitations of Research

The results obtained from the conducted studies were influenced by various factors such as the properties of the materials, reinforcement, curing condition, size effect of specimens, application of load, and test setup. Any change in these factors may affect the outcomes. The impact test, in particular, was carried out using the available facilities at Memorial University, which facilitated to evaluate the impact resistance of the developed composites by only measuring the number of drops induced the first and failure crack. Therefore, using more advanced automated instruments can help to obtain better detailed measurements.

5.3. Recommendation For Future Research

1. Evaluating the effect of using ECC layer in varied depths on the flexure and shear behaviour of LWC beams.

2. Investigating the use of ECC in strengthening different LWC members (i.e. columns, walls, etc.) exposed to different load conditions (static, cyclic, impact, fatigue).

3. Conducting more comprehensive studies to evaluate the interface bonding strength between LWC and ECC with and without bonding agents or shear connectors.

4. Using more advanced technology (e.g., computerized impact testing machine) to accurately capture the response (e.g., ultimate force, energy, and strains) of the developed hybrid composites under impact loading.

5. Repeating studies 1, 2, and 3 using lightweight ECC that can be developed by partially or totally replacing silica sand with lightweight fine aggregates or rubber.

6. Repeating studies 1, 2, and 3 using another type of high-performance cement-based composites such as ultra-high strength cement-based composites and evaluating the results compared to that obtained the current studies.

Bibliography

AASHTO, “LRFD Bridge Design Specifications and Commentary, seventh edition,” American Association of State Highway and Transportation Officials, Washington, DC, 2014, 1264.

AbdelAleem, B.H.; Ismail, M.K.; and Hassan, A.A., “Properties of self-consolidating rubberised concrete reinforced with synthetic fibres,” Magazine of concrete research, V. 69, No. 10, 2017, pp. 526-540.

Abouhussien, A.A.; Hassan, A.A.; and Hussein, A.A., “Effect of expanded slate aggregate on fresh properties and shear behaviour of lightweight SCC beams,” Magazine of concrete research, V. 67, No. 9, 2015, pp. 433-442.

Abouhussien, A.A.; Hassan, A.A.; and Ismail, M.K., “Properties of semi-lightweight self-consolidating concrete containing lightweight slag aggregate,” Construction and building materials, V. 75, 2015, pp. 63-73.

ACI (American Concrete Institute), “Building Code Requirements for Structural Concrete (ACI 318-95) and Commentary (ACI 318 R-95),” Committee 318, Farmington Hills, MI, 2019.

ACI 544.2 R-89 “Measurement of properties of fiber reinforced concrete (544.2 R-89),”, West Conshohocken, PA, 1999.

ACI (American Concrete Institute), “Control of Cracking in Concrete Structures (224 R-90),” Committee 224, Farmington Hills, MI, 2001.

Alengaram, U.J.; Jumaat, M.Z.; Mahmud, H.; and Fayyadh, M.M., “Shear behaviour of reinforced palm kernel shell concrete beams,” Construction and building materials, V. 25, No. 6, 2011, pp. 2918-2927.

ASTM C39 / C39M. “Standard Test Method for Compressive Strength of Cylindrical Concrete Specimens.” ASTM International, West Conshohocken, PA, USA, 2021.

ASTM C 78/C 78M. “Standard test method for flexural strength of concrete.” ASTM International, West Conshohocken, PA, USA, 2021.

ASTM C143 / C143M, “Standard Test Method for Slump of Hydraulic-Cement Concrete,” ASTM International, West Conshohocken, PA, USA, 2020, 4 pp.

ASTM C150/C150M. “Standard Specification for Portland Cement.” ASTM International, West Conshohocken, PA, USA, 2020.

ASTM C494/C494M, “Standard Specification for Chemical Admixtures for Concrete.” ASTM International, West Conshohocken, PA, USA, 2019.

ASTM C496. “Standard Test Method for Splitting Tensile Strength of Cylindrical Concrete Specimens.” ASTM International, West Conshohocken, PA, USA, 2017.

ASTM C618. “Standard Specification for Coal Fly Ash and Raw or Calcined Natural Pozzolan for Use in Concrete.” ASTM International, West Conshohocken, PA, USA, 2019.

Atmaca, N.; Abbas, M. L.; and Atmaca, A., "Effects of Nano-Silica on the Gas Permeability, Durability and Mechanical Properties of High-Strength Lightweight Concrete," Construction and Building Materials, V. 147, 2017, pp. 17–26.

Balaguru, P.; and Dipsia, M.G., "Properties of fiber reinforced high-strength semi-lightweight concrete," Materials Journal, V. 90, No. 5, 1993, pp. 399-405.

British Standard Institute, "Structural Use of Concrete. Part 1: Code of Practice for Design and Construction," BS 8110, London, UK, 1997.

Canadian Standards Association Committee A23.3, "Design of Concrete Structures," CSA A23.3-04, Canadian Standards Association, Rexdale, Ontario, Canada, 2004.

CEB-FIP, "CEB-FIP Model Code 1990," Thomas Telford, London, UK, 1992.

Chai, Y.H., "Service performance of long-span lightweight aggregate concrete box-girder bridges," Journal of Performance of Constructed Facilities, V. 30, No. 1, 2016, pp. 04014196.

Cho, S.; and Kim, Y., "Effects of steel fibers on short beams loaded in shear," ACI Structural Journal, V. 100, No. 6, 2003, pp.740–765.

Clauss, G. F. "Dramas of The Sea: Episodic Waves and Their Impact on Offshore Structures." Applied Ocean Research, 2002, V. 24, No. 3, pp. 147-161.

Del Coz Díaz, J. J.; Alvarez Rabanal, F. P.; García Nieto, P. J.; and Serrano Lopez, M. A., "Sound Transmission Loss Analysis Through a Multilayer Lightweight Concrete Hollow Brick Wall by FEM And Experimental Validation," Building and Environment, V. 45, No. 11, 2010, pp. 2373-2386.

Deng, M.; Ma, F.; Ye, W.; and Li, F. "Flexural Behavior of Reinforced Concrete Beams Strengthened by HDC and RPC," Construction and Building Materials, V. 188, 2018, pp. 995–1006.

Dymond, B.Z.; Roberts-Wollmann, C.L.; and Cousins, T.E., "Shear strength of a lightweight self-consolidating concrete bridge girder," Journal of Bridge Engineering, V.15, No. 5, 2010, pp. 615-618.

EN 1992-1-1. Eurocode 2, "Design of Concrete Structures – Part 1–1: General Rules and Rules for Buildings," Thomas Telford, London, UK, 2005.

EFNARC. "The European Guidelines for Self-Compacting Concrete Specification, Production and Use," English ed. Norfolk, UK: European Federation for Specialist Construction Chemicals and Concrete Systems, 2005.

Gao, J.; Sun, W.; and Morino, K., "Mechanical properties of steel fiber-reinforced, high-strength, lightweight concrete," cement and concrete composites, V. 19, No. 4, 1997, pp. 307-313.

Go, C. G.; Tang, J. R.; Chi, J. H.; Chen, C. T.; and Huang Y. L., "Fire-Resistance Property Of Reinforced Lightweight Aggregate Concrete Wall," Construction and Building Materials, V. 30, 2012, pp. 725-733.

Hassan, A.A., "Structural Performance of Self-Consolidating Engineered Cementitious Composite Beams Containing Crumb and Powder Rubber," ACI Material Journal, V. 117, No. 2, 2020.

Hassan, A.A.; Hossain, K.M.A.; and Lachemi, M., "Behavior of full-scale self-consolidating concrete beams in shear," cement and concrete composites, V. 30, No. 7, 2008, pp. 588-596.

Hassan, A.A.; Hossain, K.M.A.; and Lachemi, M., "Strength, cracking and deflection performance of large-scale self-consolidating concrete beams subjected to shear failure," Engineering structures, V. 32, No. 5, 2010, pp. 1262-1271.

Hassan, A. A. A.; Ismail, M. K.; and Mayo J., "Mechanical Properties of Self-Consolidating Concrete Containing Lightweight Recycled Aggregate in Different Mixture Compositions," Journal of Building Engineering, V. 4, 2015, p. 113–126.

Hassan, A.A.; Ismail, M.K.; and Mayo, J., "Shear behavior of SCC beams with different coarse-to-fine aggregate ratios and coarse aggregate types," Journal of materials in civil engineering, V. 27, No. 11, 2015, pp. 04015022.

Henager, C. H.; and Doherty, T. J., "Analysis of Reinforced Fibrous Concrete Beams," Proceedings, ASCE, V. 12, ST-l, 1976, pp. 177-188.

Hossain, K.M.A.; Lachemi, M.; Sammour, M.; and Sonebi, M., "Strength and fracture energy characteristics of self-consolidating concrete incorporating polyvinyl

alcohol, steel and hybrid fibres," Construction and building materials, V. 45, 2013, pp. 20-29.

Hoff, G. C., "Fire Resistance of High-Strength Concretes for Offshore Concrete Platforms," Special Publication, V. 163, 1996, pp. 53-88.

Hubertova, M.; and Hela R., "The Effect of Metakaolin and Silica Fume on the Properties of Lightweight Self-Consolidating Concrete," ACI, Farmington Hills, MI, USA, ACI special publication 243, 2007, pp. 35–48.

Ismail, M. K.; Abdelaleem, B. H.; and Hassan, A. A. A., "Effect of Fiber Type on The Behavior of Cementitious Composite Beam-Column Joints Under Reversed Cyclic Loading," Construction and Building Materials, V. 186, 2018, pp. 969-977.

Ismail, M.K.; and Hassan, A.A., "Fresh and Mechanical Properties of Semi-Lightweight Self-Consolidating Concrete Containing Lightweight Slag Aggregate," CSCE conference, 2014.

Ismail, M. K.; and Hassan, A. A. A. "Impact Resistance and Mechanical Properties of Self-Consolidating Rubberized Concrete Reinforced with Steel Fibers." Journal of Materials in Civil Engineering, V. 29, No. 1, 2017, 04016193.

Ismail, M. K.; and Hassan A. A. A., "Influence of Fibre Type on the Shear Behaviour of Engineered Cementitious Composite Beams," Magazine of Concrete Research, V. 73, No. 9, 2021, pp. 464-475.

Ismail, M. K.; Hassan, A. A. A.; and Lachemi, M., "Performance of Self-Consolidating Engineered Cementitious Composite Under Drop-Weight Impact Loading," Journal of Materials in Civil Engineering, V. 31, No. 3, 2019, 04018400.

Ismail, M. K.; Hassan, A. A. A.; and Lachemi, M. "Abrasion Resistance of Self-Consolidating Engineered Cementitious Composites Developed with Different Mixture Compositions." ACI Materials Journal, 2019, V. 116, No. 1, pp. 27-38.

Ismail, M. K.; Sherir, M. A. A.; Siad, H.; Hassan, A. A. A.; and Lachemi, M., "Properties of Self-Consolidating Engineered Cementitious Composite Modified with Rubber," Journal of Materials in Civil Engineering, V. 30, No. 4, 2018b, https://ascelibrary.org/doi/abs/10.1061/%28ASCE%29MT.1943-5533.0002219.

Jafari, S.; and Mahini, S. S., "Lightweight concrete design using gene expression programing," Construction and Building Materials, V. 139, 2017, pp. 93–100.

Jun, P.; and Mechtcherine, V., "Behaviour of Strain-Hardening Cement-Based Composites (SHCC) Under Monotonic and Cyclic Tensile Loading: Part 1–Experimental Investigations," Cement Concrete Composites, V. 32, 2010, pp. 801–809.

Jovičić, V.; Šušteršič, J.; and Vukelič, Ž. "The Application of Fibre Reinforced Shotcrete as Primary Support for A Tunnel in Flysch," Tunnelling and Underground Space Technology, V. 24, No. 6, 2009, pp. 723-730.

Juradin, S.; Baloević, G.; and Harapin, A., “Experimental Testing of The Effects of Fine Particles on The Properties of The Self-Compacting Lightweight Concrete,” Advances in Materials Science and Engineering, V. 1, 2012.

Kang, S. B.; Tan, K. H.; Zhou, X. H.; and Yang, B., “Experimental Investigation on Shear Strength of Engineered Cementitious Composites,” Engineering Structures, V. 143, 2017, pp. 141-151.

Kani, G.N.J.; Huggins, M.W.; and Wittkopp, R.R., “Shear in reinforced concrete,” Toronto: University of Toronto Press, 1979, pp. 1–225.

Kayali, O., “Fly ash lightweight aggregates in high performance concrete,” Construction and building materials, V. 22, No. 12, 2008, pp. 2393-2399.

Kayali, O.; Haque, M.N.; and Zhu, B., “Some characteristics of high strength fiber reinforced lightweight aggregate concrete,” Cement and concrete composites, V. 25, No. 2, 2003, pp. 207-213.

Kılıç, A.; Atiş, C. D.; Yaşar, E.; and Özcan F., “High-strength lightweight concrete made with scoria aggregate containing mineral admixtures,” cement and concrete research, V. 33, No. 10, 2003, pp.1595-1599.

Kim, J. H. J.; Lim, Y. M.; Won, J. P.; Park, H. G.; and Lee K. M. “Shear capacity and failure behavior of DFRCC repaired RC beams at tensile region,” Engineering Structures, V. 29, 2007, pp. 121–131.

Kong, H. J.; Bike, S. G.; and Li, V. C. “Development of A Self-Consolidating Engineered Cementitious Composite Employing Electrosteric Dispersion/Stabilization.” Cement and Concrete Composites, 2003, V. 25, pp. 301–309.

Lachemi, M.; Bae, S.; Hossain, K. M. A.; and Sahmaran, M., “Steel-Concrete Bond Strength of Lightweight Self-Consolidating Concrete,” Materials and Structures, V. 42, 2009, pp. 1015-1023.

Li, V. C., “Advances in ECC research. Material Science to Application — A Tribute to Surendra P Shah,” ACI Bookstore, 2002, pp. 373–400.

Li, V. C., “Engineered Cementitious Composites (ECC) - Tailored Composites Through Micromechanical Modeling,” in Fiber Reinforced Concrete: Present and the Future, N. Banthia, A. Bentur, and A. Mufti, Eds., Canadian Society of Civil Engineers, Montreal, 1998, pp. 64-97.

Li, V. C. “From Micromechanics to Structural Engineering – The Design of Cementitious Composites for Civil Engineering Applications.” Journal of Structural Mechanics and Earthquake Engineering, JSCE, 1993, V. 10, No. 2, pp. 37-48.

Li, V. C.; Wu, C.; Wang, S.; Ogawa, A.; and Saito, T., “Interface Tailoring for Strain-Hardening Polyvinyl Alcohol-Engineered Cementitious Composites (PVA-ECC),” ACI Materials Journal, V. 99, No. 5, 2002, pp. 463–72.

Liu, H.; Zhang, Q.; Li, V.; Su, H.; and Gu, C. “Durability Study on Engineered Cementitious Composites (ECC) Under Sulfate And Chloride Environment,” Construction and Building Materials, Volume 133, 2017, pp. 171-181.

Lok, T. S.; and Pei, J. S. “Impact Resistance and Ductility of Steel Fibre Reinforced Concrete Panels.” HKIE Trans, 1996, V. 3, No. 3, pp. 7-16.

Lotfy, A.; Hossain, K.M.; and Lachemi, M., “Durability properties of lightweight self-consolidating concrete developed with three types of aggregates,” Construction and building materials, V. 106, 2016, pp. 43-54.

Meng, D.; Lee, C.; and Zhang, Y., “Flexural fatigue properties of a polyvinyl alcohol-engineered cementitious composite,” Magazine of concrete research, V. 71, No. 21, 2019, pp.1130-1141.

Mo, K.H.; Visintin, P.; Alengaram, U.J.; and Jumaat, M.Z., “Prediction of the structural behaviour of oil palm shell lightweight concrete beams,” Construction and building materials, V. 102, 2016, pp. 722-732.

Murthya, A. R.; Karihaloob, B. L.; Ranic, P. V.; and Priyad, D. S. “Fatigue Behaviour of Damaged RC Beams Strengthened with Ultra-High Performance Fibre Reinforced Concrete,” International Journal of Fatigue, V. 116, 2018, pp. 659-668.

Narayanan, R.; and Darwish, I.Y.S., “Use of steel fibers as shear reinforcement,” Structural Journal, V. 84, No. 3, 1987, pp. 216-227.

Okamura, H.; and Ouchi, M., "Self-Compacting Concrete," Journal of Advanced Concrete Technology, V. 1, No. 1, 2003, pp. 5–15.

Omar, A. T.; Ismail, M. K.; and Hassan, A. A. A., "Use of Polymeric Fibers in the Development of Semilightweight Self-Consolidating Concrete Containing Expanded Slate," Journal of Materials in Civil Engineering, V. 32, No. 5, 2020, 04020067.

Paik, J. K. "Recent Advances and Future Trends on Plasticity and Impact Mechanics of Ships and Offshore Structures." Procedia Engineering, 2017, V. 173, pp. 17-24.

Papanicolaou, C. G.; and Kaffetzakis, M. I., "Lightweight Aggregate Self-Compacting: State-of-Pumice Application," Journal of Advanced Concrete Technology, V. 9, No. 1, 2011, pp. 15–29.

Ranade, R.; Zhang, J.; Lynch, J. P.; and Li, V. C. "Influence of Micro-Cracking on The Composite Resistivity of Engineered Cementitious Composites," Cement and Concrete Research, V. 58, 2014, pp. 1-12.

Real, S.; Bogas, J. A.; Gomes, M. D. G.; and Ferrer, B., "Thermal Conductivity of Structural Lightweight Aggregate Concrete," Magazine of Concrete Research, V. 68, No. 15, 2016a, pp. 798–808.

Real, S.; Gomes, M. G.; Rodrigues, A. M.; and Bogas, J. A., "Contribution of Structural Lightweight Aggregate Concrete to The Reduction of Thermal Bridging Effect

in Buildings," Construction and Building Materials, V. 121, 2016b, pp. 460-470.

Sadek, M. M.; Ismail, M. K.; and Hassan, A. A. A. "Stability of Lightweight Self-Consolidating Concrete Containing Coarse and Fine Expanded Slate Aggregates." ACI Materials Journal, 2020, V. 117, No. 3, pp. 133-143.

Sadek, M. M.; Ismail, M. K.; and Hassan, A. A. A. "Impact Resistance and Mechanical Properties of Optimized SCC Developed with Coarse and Fine Lightweight Expanded Slate Aggregate." Journal of Materials in Civil Engineering, V. 32, No. 11, 2020, 04020324, 2020.

Sadek, M. M. "Properties of Self-Consolidating Concrete Containing Expanded Slate Lightweight Aggregate," Master Thesis, Memorial University of Newfoundland, Canada, October 2020.

Şahmaran, M.; Lachemi, M.; and Li, V.C., "Assessing the durability of engineered cementitious composites under freezing and thawing cycles," Journal of ASTM International, V. 6, No. 7, 2009, pp. 1-13.

Şahmaran, M.; and Li, V.C., "De-icing salt scaling resistance of mechanically loaded engineered cementitious composites," cement and concrete research, V. 37, No. 7, 2007, pp. 1035-1046.

Şahmaran, M.; and Li, V.C., "Engineered cementitious composites: Can composites be accepted as crack-free concrete?," Transportation Research Record, V. 2164, No.1, 2010, pp. 1-8.

Şahmaran, M.; Li, V. C.; and Li, M., "Transport properties of engineered cementitious composites under chloride exposure," ACI Materials Journal, V. 104, No. 6, 2007, pp. 604-611.

Said, S. H.; and Razak, H. A. "Structural Behavior of RC Engineered Cementitious Composite (ECC) Exterior Beam–Column Joints Under Reversed Cyclic Loading." Construction and Building Materials, 2016,V. 107, pp. 226-234

Said, S. H.; and Razak, H. A. "The Effect of Synthetic Polyethylene Fiber on The Strain Hardening Behavior of Engineered Cementitious Composite (ECC)." Materials and Design, 2015, V. 86, pp. 447–457.

Sari, D.; and Pasamehmetoglu, A. G., "The effects of gradation and admixture on the pumice lightweight aggregate concrete," cement and concrete composites, V. 35, No. 5, 2005, pp. 936-942.

Shafigh, P.; Mahmud, H.; and Jumaat, M.Z., "Effect of steel fiber on the mechanical properties of oil palm shell lightweight concrete," Materials and design, V. 32, No. 7, 2011, pp. 3926-3932.

Shi, C.; and Yang, X. "Design and Application of Self-Consolidating Lightweight Concrete," Proceedings of China 1st International Symposium on Design, Performance and Use of Self-Consolidating Concrete, RILEM Publication SARL, Paris, France, 2005, pp. 55-64.

Suthiwarapirak, P.; Matsumoto, T.; and Kanda, T., "Multiple Cracking and Fiber Bridging Characteristics of Engineered Cementitious Composites under

Fatigue Flexure," Journal of Materials in Civil, V. 16, No. 5, 2004, pp. 433-443.

Swamy, R.N.; and Bahia, H.M., "The Effectiveness of Steel Fibers as Shear Reinforcement," In Proceedings of the Korea Concrete Institute Conference, V. 7, No. 3, 1985, pp. 35-40.

Szydlowki, R.; and Mieszcak, M., "Study of application of lightweight aggregate concrete to construct post-tensioned long-span slabs," Procedia Engineering, V. 172, 2017, pp. 1077-1085.

Taylor, H.P., "The fundamental behavior of reinforced concrete beams in bending and shear," Special Publication, V. 42, 1974, pp. 43-78.

Ünal, O.; Uygunoğlu, T.; and Yildiz, A., "Investigation of Properties of Low-Strength Lightweight Concrete for Thermal Insulation," Building and Environment, V. 42, No. 2, 2007, pp. 584- 590.

Vandanapu, S. N.; and Krishnamurthy, M., "Seismic performance of lightweight concrete structures." Advances in Civil Engineering, V. 2018, 2018, pp. 1-6.

Yang, E.H.; and Li, V.C., "Strain-hardening fiber cement optimization and component tailoring by means of a micromechanical model," Construction and building materials, V. 24, No. 2, 2010, pp. 130-139.

Yao, S. X.; and Gerwick B. C., "Development of Self-Compacting Lightweight Concrete for RFP Reinforced Floating Concrete Structures," US Army Corps

of Engineers Research and Development Center, San Francisco, CA, USA, Technical report, 2006.

Yıldırım, G.; Khiavi, F.E.; Anıl, Ö.; Sahin, O.; Sahmaran, M.; Erdem, R. T. "Performance of Engineered Cementitious Composites Under Drop-Weight Impact: Effect of Different Mixture Parameters." Structural Concrete, V. 21, No. 3, 2020, pp. 1051-1070.

Yuan, F.; Pan, J.; Xu, Z.; and Leung, C. K. Y., "A Comparison of Engineered Cementitious Composites Versus Normal Concrete In Beam–Column Joints Under Reversed Cyclic Loading," Materials and Structures, V. 46, No. 1-2, 2013, pp. 145–159.

Zhang, J.; and Li, V. C. "Monotonic and Fatigue Performance in Bending of Fiber-Reinforced Engineered Cementitious Composite in Overlay System," Cement Concrete Research, V. 32, 2002, pp. 415–423.